INTRANUCLEAR TRAFFICKING OF FLUORESCENT HIV-1 PARTICLES

Alberto Albanese

Ph.D. Thesis in Molecular Biology

Supervisor: Dott.ssa Anna Cereseto

Scuola Normale Superiore

2009

TABLE OF CONTENTS

CHAPTER 1

INTRODUCTION

THE RETROVIRIDAE FAMILY OF RETROVIRUSES

The human immunodeficiency virus type 1 is an enveloped virus, characterized by an icosahedral capsid, containing the viral genome, which consists of two copies of positive single strand RNA. HIV-1 is classified as retrovirus and, like all the retroviruses, belongs to the Retroviridae family (International Committee on Taxonomy of Viruses (6th) et al., 1995). The peculiarity of retroviruses, as suggested by the term "retro", relies on the specific capability to perform the reverse transcription of their genome from RNA into DNA, which can then be integrated into the host cellular genome.

The Retroviridae family is the only viral family possessing this feature, which characterizes the Group VI of viruses of Baltimore classification. This classification is based on the genetic system of the viruses and describes the obligatory relationship between the viral genome and its mRNA. By convention, mRNA is defined as positive strand, because it contains the immediately translatable information. In the Baltimore classification, a strand of DNA that is of equivalent polarity is also designated as positive strand. The RNA and DNA complements of positive strands are designated as negative strands. According to Baltimore classification, viruses are divided into the following seven classes: (I) dsDNA viruses, (II) ssDNA viruses, (III) dsRNA viruses, (IV) (+)-sense ssRNA viruses, (V) (-)-sense ssRNA viruses, (VI) RNA reverse transcribing viruses, and (VII) DNA reverse transcribing viruses.

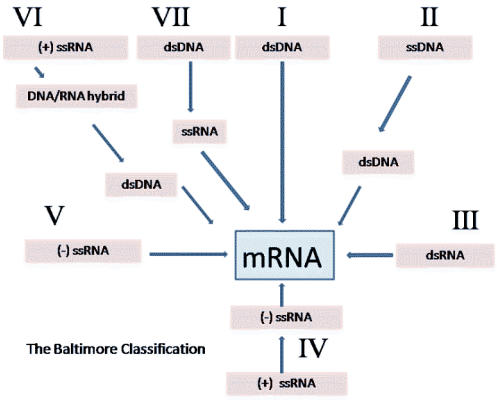

Figure 1-1. The Baltimore classification.

Retroviruses used to be taxonomically divided into three subfamilies: the Oncovirinae, which includes those with oncogenic potential; the Lentivirinae or slow

viruses, including HIV; and the Spumavirinae or foamy viruses, which have not been shown to be pathogenic (Coffin et al., 1997).

This taxonomic classification is no longer used and Retroviridae family has been reclassified into seven distinct genera largely on the basis of the sequence similarity within the *pol* gene (Coffin et al., 1997): mammalian C-type viruses (prototype MLV), avian C-type viruses (the ASLV, prototype RSV), B-type viruses (prototype MMTV), D-type viruses (prototype M-PMV), viruses of the HTLV/BLV group (prototype HTLV-1), lentiviruses (prototype HIV-1), and spumaviruses (prototype HFV) (Coffin et al., 1997; Zuckerman et al., 2004).

	Genus	Example	Virion morphology
1.	Avian sarcoma and leukosis viral group	Rous Sarcoma Virus	central, spherical core "C particles"
2.	Mammalian B-type viral group	Mouse Mammary Tumor Virus	eccentric, spherical core "B particles"
3.	Murine leukemia-related viral group	Moloney Murine Leukemia Virus	central, spherical core "C particles"
4.	Human T-cell leukemia–bovine leukemia viral	Human T-Cell Leukemia Virus	central, spherical core
5.	D-type viral group	Mason-Pfizer Monkey Virus	cylindrical core "D particles"
6.	Lentiviruses	Human Immunodeficiency Virus	cone-shaped core
7.	Spumaviruses	Human Foamy Virus	central, spherical core

Table 1-1. Classification of Retroviruses. (Coffin et al., 1997).

HIV-1 STRUCTURE

The HIV-1 virus is about 120 nm in diameter and roughly spherical. It is surrounded by an envelope composed by the plasma membrane of host-cell origin and the viral proteins gp120 and gp41. Immediately in the interior, matrix protein lines the inner surface of the viral particle. Deeper inside there is a cone-shaped viral core, which contains two molecules of positive RNA, the viral proteins involved in the essential enzymatic functions (protease, integrase

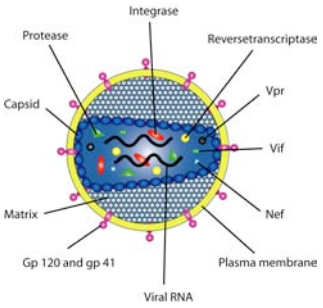

Figure 1-2. Schematic representation of HIV-1 structure.

and reverse transcriptase), and three of the viral accessory proteins (Vif, Vpr, and Nef) (Coffin et al., 1997; Frankel and Young, 1998).

VIRAL GENOME

Retroviral genomic RNA is a product of the host RNA synthesis machinery, and as such, the viral RNA genome has the structural features of a cellular messenger RNA, including a methylated cap ribonucleotide at the 5' end and a polyadenylated 3' end. Two direct repeats, termed R for repeated sequences, lie at the 5' and 3' end of the genomic viral RNA flanking the 5' cap and the 3' Poly(A) tail, respectively. Immediately adjacent and internal to the R sequences, there are two unique sequences, known as U5 at the 5' end and U3 at the 3' end of the viral RNA genome. Following U5 there is the primer binding site (PBS), a region annealed by a tRNA, that functions as the primer for reverse transcriptase to initiate synthesis of the minus strand of DNA. Adjacent to PBS there is the Ψ sequence, which is involved in the packaging of the genomic RNA into the assembling virions. Next, there are genes encoding structural, functional and accessory proteins. Finally, just upstream of U3, there is the polypurine tract, a purine-rich sequence, which is cleaved during reverse transcription to produce the RNA primer for the synthesis of the plus strand of viral DNA.

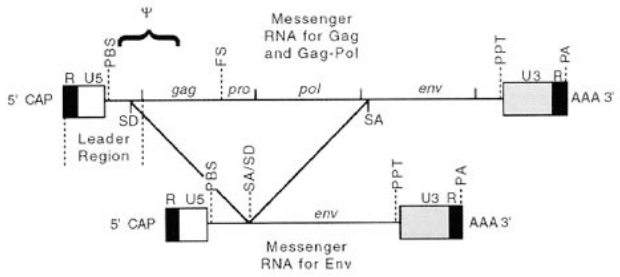

Figure 1-3. RNA viral genome. (Coffin et al., 1997).

HIV-1 PROTEINS

The retroviral genome is about 9-kb of RNA, and encodes nine open reading frames. Three of these encode the Gag, Pol, and Env polyproteins, which are subsequently proteolyzed into individual proteins common to all retroviruses. The four Gag

proteins, matrix (MA or p17), capsid (CA or p24), nucleocapsid (NC or p7), and p6, and the two Env proteins, gp120 and gp41, are structural components that make up the core of the virion and outer membrane envelope, respectively. The three Pol proteins, protease (PR), reverse transcriptase (RT), and integrase (IN), provide essential enzymatic functions and are also encapsulated within the viral particle, as mentioned above. HIV-1 encodes six additional proteins, often called accessory proteins, three of which (Vif, Vpr, and Nef) are found in the viral particle (Coffin et al., 1997; Frankel and Young, 1998).

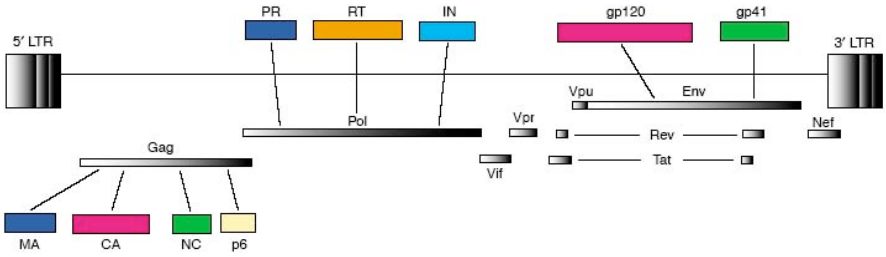

Figure 1-4. Organization of the HIV-1 genome. The location of the long terminal repeats (LTRs) and the genes encoded by HIV-1 are indicated. Gag, Pol and Env proteins are initially synthesized as polyprotein precursors. The Gag precursor is cleaved by the viral protease (PR) into the mature Gag proteins: matrix (MA), capsid (CA), nucleocapsid (NC) and p6. The GagPol precursor undergoes PR-mediated processing to generate the Gag proteins and the Pol enzymes: PR, reverse transcriptase (RT) and integrase (IN). The Env glycoprotein precursor gp160 is cleaved by a cellular protease during transport to the cell surface to generate the mature surface glycoprotein gp120 and the trans-membrane glycoprotein gp41. The sizes of the genes and encoded proteins are not to scale. (Freed, 2004).

The core and matrix proteins are encoded by Gag. The Gag proteins of the mature virus are p17, p24, p7 and p6, and are processed by cleavage of the p55 precursor protein by the viral protease (Coffin et al., 1997; Zuckerman et al., 2004). MA is the N-terminal component of the Gag polyprotein and is important for targeting Gag and Gag-Pol precursor polyproteins to the plasma membrane prior to viral assembly. Indeed, MA protein contains a bipartite membrane-binding signal: one is the 14-carbon, saturated fatty acid myristate covalently linked to N-terminal glycine residue, the other is the largely basic sequence located a short distance downstream. The two signals mediate high-affinity binding of MA and of Gag polyprotein to the lipid bilayer by hydrophobic interactions with membrane lipids and ionic bonds with negatively charged head groups of membrane phospholipids, respectively (Flint et al., 2004). As a consequence of this interaction, MA lines the inner surface of the mature viral particle. In addition, this protein appears to help incorporate Env

glycoproteins into viral particles (Mammano et al., 1995). Furthermore, MA is part of the pre-integration complexes (PICs) (Bukrinsky et al., 1993b) and the two nuclear localization signals (NLS) (Haffar et al., 2000) may facilitate the nuclear import (Gallay et al., 1995).

CA is the second component of the Gag polyprotein and forms the core shell of the HIV-1 viral particle with about 2000 molecules per virion (Scarlata and Carter, 2003). This protein is often used in Enzyme-Linked ImmunoSorbent Assay (ELISA) for quantifying the amount of virus. The C-terminal domain functions primarily in assembly and is important for CA dimerization and Gag oligomerization. Capsid is important for infectivity, by participating in viral uncoating through its interaction with cyclophilin A (cypA) (Kootstra et al., 2003; Saphire et al., 2002; Towers et al., 2002; Towers, 2007) and it is the major determinant of infection in growth-arrested cells (Yamashita and Emerman, 2004). Cyclophilin A is a cytosolic cellular protein that belongs to the peptidyl prolyl isomerases family and performs the cis-trans isomerization of proline peptide bonds in sensitive proteins (Towers, 2007). By interacting with Gag in infected cells, CypA is incorporated into nascent HIV-1 virions (Franke et al., 1994; Thali et al., 1994). CypA performs cis-trans isomerization at CA Gly89-Pro90 on the outer surface of the capsid (Bosco et al., 2002; Bosco and Kern, 2004) leading to an increased infectivity. The research group lead by Luban (Sayah et al., 2004) showed that cypA is an important cellular factor, since it is the target for the recently discovered old world monkey TRIM5α restriction factor (Song et al., 2005; Stremlau et al., 2004; Yap et al., 2004), which has been demonstrated to greatly decrease HIV-1 infectivity (Berthoux et al., 2005; Keckesova et al., 2006; Stremlau et al., 2006).

Nucleocapsid protein is the third component of the Gag polyprotein and coats the genomic RNA inside the virion core. The primary function of NC is to bind specifically, through its two zinc finger domains, to the packaging signal (Ψ) and deliver full-length viral RNAs into the assembling virion. The packaging signal is composed of three RNA hairpins located around the major splice donor site, the first of which contains the kissing loop involved in RNA dimerization. NC is a basic protein that also binds single-stranded nucleic acids nonspecifically, leading to

coating of the genomic RNA that presumably protects it from nucleases and compacts it within the core (Frankel and Young, 1998).

Protein p6 comprises the C-terminal 51 amino acids of Gag and is important for incorporation of Vpr during viral assembly (Cohen et al., 1990). In addition, p6 is required for efficient viral particle release (Demirov et al., 2002; Huang et al., 1995).

The *pol* gene encodes the enzymes protease, reverse transcriptase and integrase. When the virus buds from the membrane surface, it is released as immature noninfectious particle. PR mediates the cleavage of Gag and Pol polyproteins (Coffin et al., 1997).

RT protein catalyzes both RNA-dependent and DNA-dependent DNA polymerization reactions and contains an RNase H domain that cleaves the RNA portion of RNA-DNA hybrids generated during the reaction (Coffin et al., 1997). RT is a heterodimer containing a 560-residue subunit (p66) and a 440-residue subunit (p51), both derived from the Pol polyprotein (Flint et al., 2004), each of which contains a polymerase domain composed of four subdomains called fingers, palm, thumb and connection, and p66 contains an additional RNase H domain (Frankel and Young, 1998). Even though their amino acid sequences are identical, the polymerase subdomains are arranged differently in the two subdomains, with p66 forming a large active-site cleft and p51 forming an inactive closed structure. RT is characterized by an high error rate when transcribing RNA into DNA, since it lacks a proofreading function (Coffin et al., 1997).

Following reverse transcription, IN catalyzes a series of reactions to integrate the viral genome into a host chromosome. IN together with other viral and cellular proteins forms the pre-integration complex (PIC) and binds specific sequences located at the ends of the viral cDNA (att sites) (Coffin et al., 1997). This protein will be described in more detail in the subsequent sections.

The *env* gene encodes the gp41 and gp120 envelope glycoproteins, cleaved by cellular enzymes (furins) from the gp160 precursor (Zuckerman et al., 2004). The proteins gp120 and gp41 are located on the viral membrane surface and their

function is to bind the CD4 receptor of the target cells and mediate fusion between viral and cellular membranes, respectively (Frankel and Young, 1998).

In addition to *gag*, *pol* and *env*, HIV-1 carries six regulatory and accessory genes. The *tat* gene encodes a small protein, which is essential for efficient transcription of viral genes and for viral replication (Kessler and Mathews, 1992; Marcello et al., 2001), resulting in a remarkable increase of viral gene expression (Ratnasabapathy et al., 1990; Zhou and Sharp, 1995). Tat binds to a structured RNA element (TAR, transactivation-responsive region) present at the 5'-end of viral leader mRNA via cyclin T bridging between the activation domain of Tat and the TAR loop (Wei et al., 1998). Through this interaction, Tat recruits a series of transcriptional complexes, including histone acetyl transferases, which modify chromatin at the proviral integration site and make it more suitable to transcription, and P-TEFb (Positive Transcription Elongation Factor b), which stimulates RNA polymerase II phosphorylation by Cdk9, increasing the processivity of the enzyme complex (Bieniasz et al., 1998; Shilatifard et al., 2003; Wei et al., 1998).

Rev is a sequence-specific RNA binding phosphoprotein that is expressed during the early stages of HIV-1 replication (Malim et al., 1989). Rev transports to the cytoplasm single-spliced and un-spliced viral mRNA that are required for expression of HIV structural proteins and production of genomic RNA. Eukaryotes have evolved a special mechanism to retain the incompletely spliced RNAs in the nucleus. Since HIV-1 only has one LTR promoter, it encodes a single genome-length primary transcript. In order to express the various incompletely spliced viral transcripts, some HIV-1 transcripts must be transported out of the nucleus without splicing. Rev fulfill this function (Malim et al., 1989).

Nef is a 27 KDa myristoylated protein that is abundantly produced during the early phase of viral replication cycle. It is highly conserved in all primate lentiviruses, suggesting that its function is essential for survival of these pathogens. Nef has different roles in HIV-1 replication and disease pathogenesis. It down-regulates CD4 (Garcia and Miller, 1991), which limits the adhesion of a Nef-expressing T cell to the antigen-presenting cell, thus promoting the movement of HIV-infected cells into circulation and spread of the virus. Nef down-modulates MHC I (Schwartz et al.,

1996) cell surface expression, protecting HIV-infected cells from host CTL response. In addition, it interferes with cellular signal transduction pathways and it enhances virion infectivity and viral replication, since it induces actin remodeling and facilitates the movement of the viral core past a potentially obstructive cortical actin barrier (Campbell et al., 2004; Chowers et al., 1994).

Vpr is a 96 aa small basic protein. Despite its small size, Vpr has been shown to have multiple activities during viral replication. Vpr appears to participate in the anchoring the PICs to the nuclear envelope and to be involved in the nuclear translocation of the viral DNA (Heinzinger et al., 1994). In addition, Vpr induces cell cycle G2 phase arrest (Bartz et al., 1996; Di Marzio et al., 1995). The biological significance of Vpr-induced arrest during viral infection is not well understood. However, HIV-1 LTR seems to be more active in the G2 phase, implying that Vpr-induced G2 arrest may confer a favorable cellular environment for efficient transcription of HIV-1 (Goh et al., 1998).

Vpu is a 9 KDa membrane protein that induces the degradation of the CD4 receptor. Vpu interacts with a membrane-proximal domain of the cytoplasmic tail of CD4 and links it to h-βTrCP (Margottin et al., 1998). The CD4-Vpu-h-βTrCP ternary complex then recruits SKP1, a member of the ubiquitination machinery (West, 2003). As a result, CD4 is ubiquitylated and targeted to proteasomes for degradation. In addition, Vpu increases progeny virus secretion from infected cells. This function is related to the ability of Vpu to self-assemble into homooligomeric complexes that in vitro function as ion-conductive membrane pores (Bour and Strebel, 2003). The requirement of Vpu for efficient virus release is host cell-dependent (Varthakavi et al., 2003), suggesting that Vpu may counteract an inhibitory cellular factor that, in the absence of Vpu, inhibits virus release. Recent report showed that this factor is TASK-1, an acid-sensitive K^+ channel (Hsu et al., 2004). TASK-1 is structurally homologous to Vpu, suggesting oligomerization as a possible mechanism of inactivation of ion channel activity of these proteins (Hsu et al., 2004). However, the mechanism by which TASK-1 inhibits virion release is still unclear (Li et al., 2005).

Vif is a 192 aa protein that is expressed at high levels in the cytoplasm of infected cells. Vif was thought to be important because it is essential for the replication of HIV-1 in the peripheral blood lymphocytes, macrophages, and certain cell lines known as "nonpermissive" cells (Strebel et al., 1987). The molecular nature of the permissivity is related to a host cellular protein known as APOBEC3G (apolipoprotein B mRNA-editing enzyme catalytic polypeptide-like 3G), a potent inhibitor of HIV infection in the nonpermissive cells (Harris et al., 2002; Jarmuz et al., 2002). APOBEC3G is a member of the cytidine deaminase family, which prevents viral cDNA synthesis via deaminating deoxycytidines in the minus-strand retroviral cDNA replication intermediate (Harris et al., 2003; Yu et al., 2004). As a result, it creates stop codons or G to A transitions in the newly synthesized viral cDNA, which is then subjected to elimination by host DNA repair machinery (Zhang et al., 2003). Thus, APOBEC3G represents an innate host defense mechanism against HIV infection. However, the virus has also developed an offensive strategy to suppress the antiviral effect of APOBEC3G through Vif. Vif binds directly to APOBEC3G and counteracts its anti-HIV activity by promoting its degradation (Li et al., 2005). In addition, Vif is specifically packaged into virions, where it is processed by protease (Khan et al., 2002). Vif also stabilizes viral nucleoprotein complex through direct interaction with 5' region of HIV-1 genomic RNA (Simon and Malim, 1996).

HIV-1 REPLICATION CYCLE

Viral Entry

The tropism of HIV-1 for the target cells is governed by the presence of both the cellular receptor CD4 and a coreceptor on the plasma membrane of target cells (Dalgleish et al., 1984). Two types of coreceptor were identified: the chemokine receptors CCR5 [chemokine (C-C motif) receptor 5] and CXCR4 [chemokine (CXC motif) receptor 4] (Choe et al., 1996; Deng et al., 1996). The distribution of these coreceptors permits infection not only of $CD4^+$ T cells, but also macrophages and dendritic cells (DCs).

In order to enter the target cell, HIV-1 gp120 protein binds the CD4 receptor, inducing a conformational change and promoting the binding of the chemokine receptor CCR5 or CXCR4. It is noteworthy that individuals homozygous for a defective CCR5 allele are highly resistant to HIV-1 infection. The interaction between gp120, CD4 and the coreceptor induce a conformational change in gp41 that expose a hydrophobic glycine-rich "fusion" peptide, which initiate the fusion of the viral envelope with the plasma membrane in specific membrane microdomains rich in cholesterol, known as lipid rafts (Manes et al., 2000).

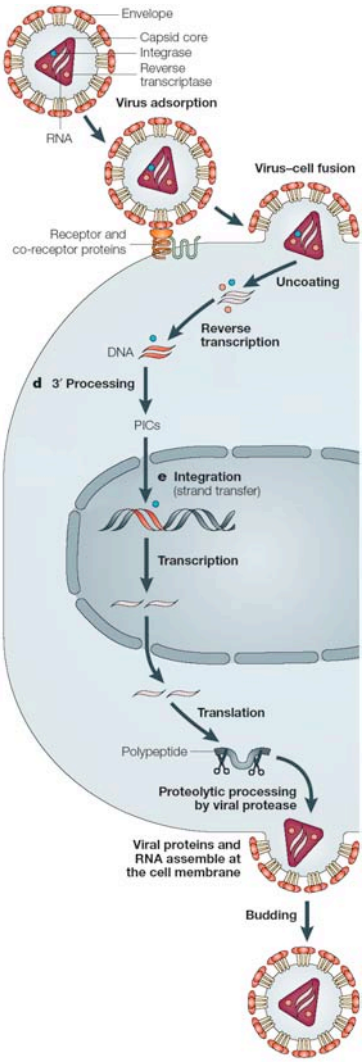

Figure 1-5.The HIV-1 replication cycle. (Pommier et al., 2005).

Retrotranscription

Following entry, the viral RNA genome is in the cell cytoplasm as part of a nucleoprotein complex, which associates with microtubules before the loss of the capsid structure (McDonald et al., 2002). The function of the microtubule-based mobility is to transport the HIV-1 viral complex from the cell periphery to the nucleus. The next step of viral infection is the synthesis of a DNA copy of the RNA viral genome, through the viral enzyme RT, and this process has been shown to start in the intact capsid structure (McDonald et al., 2002).

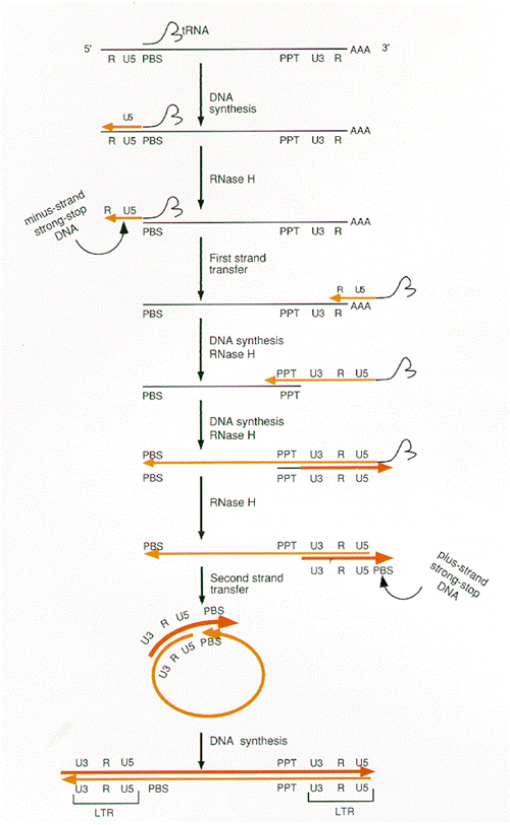

Figure 1-6. Schematic representation of HIV-1 reverse transcription. (Coffin *et al.*, 1997).

Reverse transcription is an essential step in HIV-1 life cycle, since it is a process that converts the genomic RNA into DNA. It has been proposed that retroviruses copackage two copies of positive single-stranded RNA to increase the probability of successful DNA synthesis (Coffin, 1979). During initiation of reverse transcription, a cellular tRNA primer ($tRNA^{Lys}$) is placed onto a complementary sequence in the viral genome, called the primer binding site (PBS). The reverse transcriptase recognizes this RNA-RNA complex and catalyzes the synthesis of minus-strand DNA starting from the 3' end of the tRNA primer, with the viral RNA acting as template. The synthesis of minus-strand DNA (-sssDNA) extends up to the 5' cap of the genomic RNA template and the RNase domain of RT cleaves the RNA portion of RNA-DNA hybrid. Continued minus-strand DNA synthesis requires a strand-transfer reaction that allows the 3'end of the genomic RNA to serve as a template. Once the first jump has occurred, the 3'end of the minus strand is extended up to the PBS of the RNA viral genome. The site where DNA plus-strand is initiated is the polypurine tract, where RNase H domain of RT cleaves the RNA to generate an RNA primer. RT catalyzes the synthesis of the plus-strand DNA (+sssDNA) up to a portion of the tRNA. The 3'end of the +sssDNA is complementary to the PBS of the –sssDNA and it is required as complementary region for the second strand transfer. Once the second jump has occurred, elongation of the plus and minus

strands can be completed. The final product is a blunt-ended linear duplex DNA (Coffin et al., 1997).

Compared to other DNA polymerases, RT lacks a 3' exonuclease activity capable to excise mispaired nucleotides, resulting in a more error-prone enzyme. This feature allows the HIV-1 to adapt to environment changes, helping it to escape immune system defensive mechanisms and even drugs treatment (Coffin et al., 1997).

Nuclear translocation

Once the reverse transcription process is completed, the newly synthesized viral DNA remains associated with a high molecular weight complex composed of both viral and cellular proteins, known as preintegration complex (PIC), that will be explained in more detail in the subsequent sections.

Whereas most retroviruses need the nuclear membrane disassembly during mitosis to allow the retrotranscribed viral complexes to access the host genome, lentiviruses have evolved a mechanism whereby the PIC is actively transported across the nuclear envelope through the nuclear pores. Several viral determinants for nuclear import have been proposed, including MA (Bukrinsky et al., 1993a), Vpr (Heinzinger et al., 1994), the IN enzyme (Gallay et al., 1997) and an unusual triple-stranded fragment of lentiviral DNA referred to as the DNA 'flap' (De Rijck and Debyser, 2006). Although a consensus has not emerged so far regarding the mechanism by which the PIC is imported to the nucleus, this unique property enables lentiviruses to infect non-dividing cells.

Integration

Once inside the nucleus, IN catalyzes the integration of the viral DNA into the host cell chromosome, which will be discussed in more detail in the subsequent sections. IN together with other viral and cellular proteins that forms the PICs bind specific sequences located at the end of the viral cDNA (*att* sites) (Coffin et al., 1997). So far no primary sequence in the cellular genome has been identified as the preferential binding site for IN and integration seems to occur at random on DNA molecules (Carteau et al., 1998; Stevens and Griffith, 1996). Only recently it has been showed that transcriptionally active genes are strongly favored as integration target sites

(Barr et al., 2006; Barr et al., 2005; Carteau et al., 1998; Ciuffi et al., 2005; Lewinski et al., 2005; Lewinski et al., 2006; Mitchell et al., 2004; Schroder et al., 2002; Wu et al., 2003).

Alternatively, the viral DNA may follow three different fates, all of which do not lead to the formation of a functional provirus. The ends of viral DNA may join to form a 2-LTR ring or the viral genome may undergo homologous recombination producing a single LTR ring. Finally, the viral DNA may integrate into itself (autointegration) leading to the formation of a rearranged circular structure (Coffin et al., 1997). None of these circular forms serve as precursor to integrated provirus, and none appear to contribute significantly to viral replication. Rather, they all appear to be dead-end by-products of aborted infections (Coffin et al., 1997).

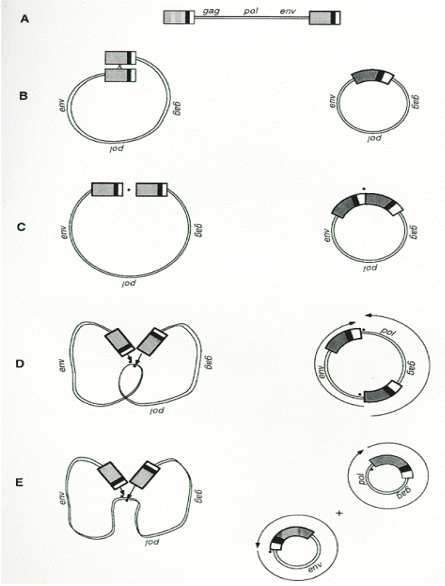

Figure 1-7. Unintegrated viral DNA structures. (A) The linear product of viral DNA synthesis is the precursor to the integrated provirus. (B) 1-LTR circle. This structure is consistent with one that could be formed by homologous recombination between the LTRs of the linear DNA molecule. (C) 2-LTR circle. This structure is consistent with one that could be formed by simply joining the ends of the linear DNA molecule, although there are often bases inserted or deleted at the "circle junction". (D and E) Autointegration products. These circular molecules are apparently formed by the suicidal integration of the viral DNA ends using the viral DNA itself as the target, instead of cellular DNA. Their structures depend on the site of integration (which determines the spacing between the two LTRs in the full- length circular products or the sizes of the two subgenomic circular products), and on the path of the DNA between the ends and the target site (which determines whether the product is a single full-length circle [D] or two smaller circles [E]). Dots indicate the sites of joining; arrows show orientation of the DNA sequence relative to the RNA genome. (Coffin et al., 1997).

Viral Transcription

In the integrated provirus, the 5' LTR acts as the viral promoter; it contains several positive transcription factor binding sites even if, in the absence of the viral Tat protein, the binding of these factors is not sufficient to activate the transcription of viral genes. However, the presence of these promoter elements results in the correct

positioning of RNA polymerase II at the site of initiation of transcription and to the assembly of the pre-initiation complex. At this point transcription starts but the polymerase produces predominantly short, non-polyadenylated RNA that include a hairpin structure at the 5' end of the nascent viral RNA, named trans-activation-responsive region (TAR) (Peterlin and Trono, 2003). Tat acts as a very powerful transcriptional activator of the integrated provirus by interacting with TAR and promoting the production of polyadenylated full-length RNA viral genomes.

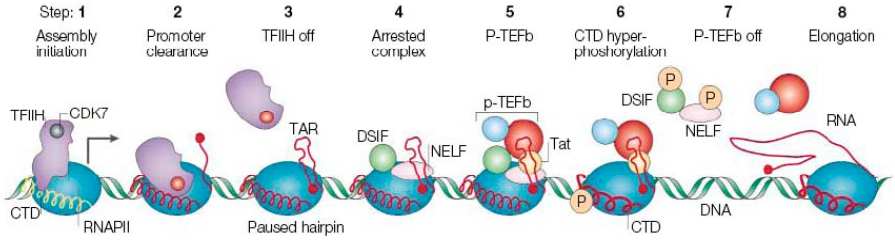

Figure 1-8. Mechanism of Tat transactivation. Activators that bind the promoter recruit RNA polymerase II (RNAPII) to the long terminal repeat (LTR). In the pre-initiation complex, the unphosphorylated carboxy-terminal domain (CTD) of RNAPII, which is shown as a yellow coil, binds mediators. Together with the general transcription factor TFIIH, which contains DNA-helicase and CTD-kinase activities, RNAPII clears the promoter and starts copying the viral genome. Cyclin-dependent kinase 7 (CDK7) in TFIIH is shown as a grey changing to red ball, indicating its activation as a kinase. The partially phosphorylated RNAPII arrests at or near the transactivation response element (TAR), synthesizing TAR and/or an alternative paused hairpin. 5,6-dichloro-1-β-D-ribofuranosylbenzimidazole (DRB)-sensitivity-inducing factor (DSIF) and negative elongation factor (NELF) then ensure that RNAPII does not elongate. RD — so named for its many repeats of arginine and glutamate residues — in NELF contains an RNA-recognition motif that binds the stem in TAR. For formation of the tripartite complex with transcriptional transactivator (Tat) and TAR, positive transcription elongation factor b (P-TEFb), which contains cyclin T1 (CYCT1) and CDK9, must be free of 7SK RNA, and CDK9 must be autophosphorylated. After its recruitment to TAR, P-TEFb phosphorylates suppressor of Ty 5 (SPT5) in DSIF and RD in NELF, and completes the phosphorylation of the CTD of RNAPII, thereby modifying RNAPII for efficient elongation. The phosphorylated CTD now binds elongators, which consist of capping enzymes, splicing apparatus and polyadenylation factors. Efficient elongation of transcription and viral replication ensue. The change in color of the CTD from yellow to red and its increased thickness indicate increased levels of phosphorylation. (Peterlin and Trono, 2003).

Tat-activated transcription originates different transcripts derived by the splicing of the full-length viral genome. The first viral transcripts that appear after infection are completely spliced and are rapidly transported into the cytoplasm following the same pathway as cellular mRNA (Cullen, 1998).

Incompletely spliced RNAs are blocked in the nucleus by the cellular machinery that control the integrity of the splicing process; the single spliced and unspliced transcripts persist in the nucleus due to defective donor and acceptor splice sites and to the inhibitory effect of Rev on splicing (Luo et al., 1994; Powell et al., 1997). The translocation of these transcripts into the cytoplasm depends on the expression of the Rev protein (Pomerantz et al., 1992). Rev is able to shuttle between the nucleus and the cytoplasm and binds the viral transcripts through the interaction with an RNA stem-loop structure named Rev responsive element (RRE), located in the env gene (Malim et al., 1990).

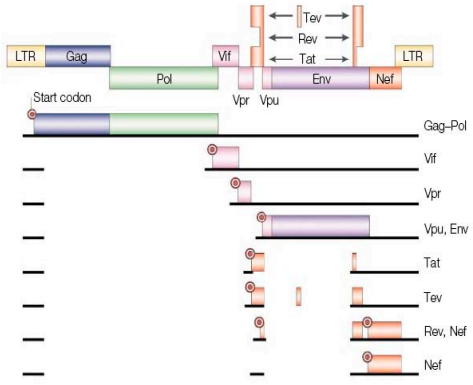

Figure 1-9. The HIV genome, transcripts and proteins. HIV transcripts. Integrated into the host chromosome, the 10-kb viral genome contains open reading frames for 16 proteins that are synthesized from at least ten transcripts. Black lines denote unspliced and spliced transcripts, above which coding sequences are given, with the start codons indicated. Of these transcripts, all singly spliced and unspliced transcripts shown above those encoding the transcriptional transactivator (Tat) require regulator of virion gene expression (Rev) for their export from the nucleus to the cytoplasm. The RNA target for Rev, the Rev response element (RRE), is contained in the gene encoding envelope protein (Env). (Peterlin and Trono, 2003).

Viral Assembly

Once translated, all the viral proteins necessary for the virion assembly and RNA genomes are transported to the plasma membrane, in cholesterol-rich lipid domains known as lipid rafts, where the building of new virions begins. The gp120/gp41 complex is transported via the Endoplasmic reticulum-Golgi pathway, whereas the Gag-Pol polyproteins are targeted to the plasma membrane after the myristoylation of Gag (Gottlinger et al., 1989). The resulting virions bud from the plasma membrane as immature virions. Their maturation is accomplished by viral protease activity that first cleaves Gag-Pol and then, starting from the Gag and Pol separated precursors, originates the single core proteins, matrix and the viral enzymes. The proteolytic activity ends when the virion is already detached from the host plasma membrane and results in the formation of mature infectious viruses (Coffin et al., 1997).

INTEGRASE

The name of the key enzyme mediating retroviral integration has evolved through several stages in the past 25 years, reflecting incremental progress in our understanding of its role and activities. Indeed, this enzyme was initially identified by its apparent molecular weight, then labeled "endonuclease", in recognition of the relatively non specific endonuclease activity observed in assays using unnatural DNA substrates, and finally "integrase" (IN), when it became clear that it was the enzyme that actually catalyzed the key chemical steps in integration (Coffin et al., 1997).

The integrase protein is encoded by sequences at the 3'end of the *pol* gene, immediately downstream from the sequences encoding reverse transcriptase. Once viral protease has cleaved the polyprotein, the stoichiometry of integrase protomers in the virion is 1:1 with reverse transcriptase protomers, or approximately 50-100 protomers per viral particle (Coffin et al., 1997).

Integrase catalyzes the integration of the viral DNA into the host cell genome, via a two-step process: the 3'-end processing and the 3'-end joining (Coffin et al., 1997).

Integrase Structure

HIV-1 integrase is a protein of 288 amino acids (about 32 kDa) and it shares similar structural domains with the other retroviral integrases. The domains consist of an N-terminal domain of 50 amino acids, a central domain of 160 amino acids, and a less conserved C-terminal domain of 80 amino acids.

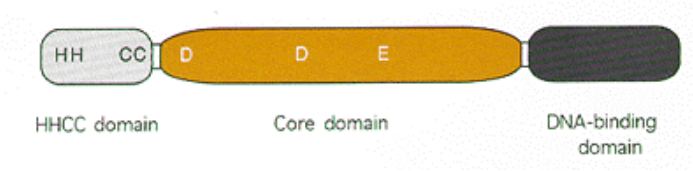

Figure 1-10. Schematic of the domain structure of retroviral integrases. The three domains appear to be stably folded when prepared separately. The amino-terminal-most (HHCC) domain is characterized by pairs of histidine and cysteine residues that are universally conserved among retroviral integrases. The central domain contains the catalytic site. It is characterized by a triad of universally conserved and essential residues, an aspartate, followed at some distance by an aspartate and glutamic acid that are always separated by 35 amino acids. The carboxy-terminal domain is sometimes called the DNA-binding domain, a bit of a misnomer since the core domain also binds DNA, but nevertheless an accurate reflection of its one known activity. (Coffin et al., 1997).

Within the N-terminal domain of IN is a putative zinc finger of the HHCC type. Using a zinc binding assay, Bushman *et al*. (Bushman et al., 1993) reported that wild-type HIV IN binds zinc. Recently, a solution structure of the N-terminal domain was determined and revealed a dimeric structure having an HHCC zinc binding motif that coordinates zinc. The folds of the N termini are similar to those of other DNA binding proteins in having a helix-turn-helix structural motif (Hindmarsh and Leis, 1999). The N terminus influences the catalytic activity of IN but does not contain its catalytic core and seems not to be involved in the multimerization (Hindmarsh and Leis, 1999).

The central core domain comprises residues 50 to 212 and has been shown to coordinate divalent cations. The crystal structures of the catalytic core domains for HIV-1 have been solved. The central core is the catalytic domain of the enzyme. The core domain is characterized by the catalytic triad of three highly conserved residues, D,D(35)E. Substitutions of any of these residues abolish end-processing and/or joining reactions. Crystal structures of the catalytic core, coordinating a divalent cation, have been determined for HIV by using Mg^{++}. The divalent cations were found to be coordinated by the two conserved aspartic acid residues of the catalytic triad (Hindmarsh and Leis, 1999).

The C terminus of IN is required both for 3'end processing and integration activity (Coffin et al., 1997). An HIV-1 IN fragment representing residues 235 to 288 binds nonspecifically to DNA (Hindmarsh and Leis, 1999). Interpretation of the DNA binding activity of the carboxy-terminal region is complicated by the fact that integration involves two different DNA substrates, which have different structural requirements: the viral cDNA and the host genomic DNA. The isolated carboxy-terminal region binds well to simple linear double-stranded DNA oligonucleotides (Engelman et al., 1994; Lutzke et al., 1994; Vink et al., 1993), suggesting that it may contribute to binding the viral cDNA ends (*att* sites) (Coffin et al., 1997). In addition, the C-terminus seems to be involved in the multimerization of IN (Hindmarsh and Leis, 1999) (Asante-Appiah and Skalka, 1999; Engelman, 1999).

Enzymatic Activity

Integration occurs in two well-characterized catalytic steps, referred to as end processing and end joining (Coffin et al., 1997; Hindmarsh and Leis, 1999).

End processing involves removal of a dinucleotide, adjacent to a highly conserved CA dinucleotide, from the 3' strand of the U3 and U5 viral DNA LTRs in a reaction involving a water molecule or other nucleophile (Engelman et al., 1991). This exposes a 3' hydroxyl group, whose oxygen is used as an attacking nucleophile on the target DNA during the joining reaction, in which the viral DNA is inserted into the cellular DNA. It is believed that a Mg^{++} atom coordinated in the active site of IN facilitates the deprotonation of the water to activate it as a nucleophile.

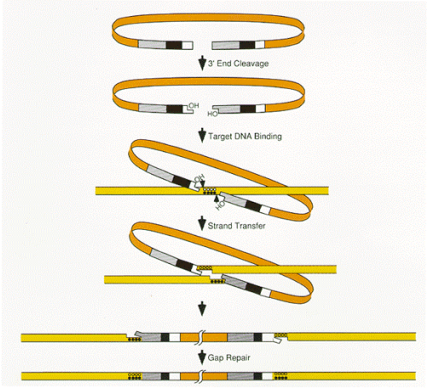

Figure 1-11. Schematic outline of the principal steps in retroviral DNA integration. (Coffin et al., 1997).

The DNA-joining step of integration, which involves the formation of new phosphodiester bonds joining the viral and host DNAs, proceeds without an extrinsic source of chemical energy. This suggests that the energy from the target DNA bonds that need to be broken in this step is used to form the new bonds that join the viral and target DNAs. This cleavage-ligation reaction proceed via a transesterification reaction and not via a covalent intermediate between IN and DNA (Engelman et al., 1991), as it happens, for example, between topoisomerases and DNA (Champoux, 1977).

Integration is accompanied by duplication of a short sequence from the target site, which flanks the integrated provirus as a direct repeat of 4-6 bp (Coffin et al., 1997).

The 5' ends of the viral DNA and the 3' ends of the host DNA remain unjoined. It is thought that repair of this integration intermediate is carried out by cellular enzymes, generating the integrated provirus (Coffin et al., 1997; Hindmarsh and Leis, 1999).

NUCLEAR STRUCTURE

The DNA of eukaryotic cells is sequestered from the cytoplasm in the nucleus and it is complexed with cellular proteins. The result is a very complex structure, with different levels of organization. Since retroviral integration takes place in the cellular genome, it is important to understand the organization of the host genome.

The Nucleus

The nuclear compartment is delimited from the cytoplasm by the nuclear envelope, constituted by two concentric lipid bilayer membranes. The inner membrane contacts the nuclear lamina, which forms a thin sheetlike meshwork giving

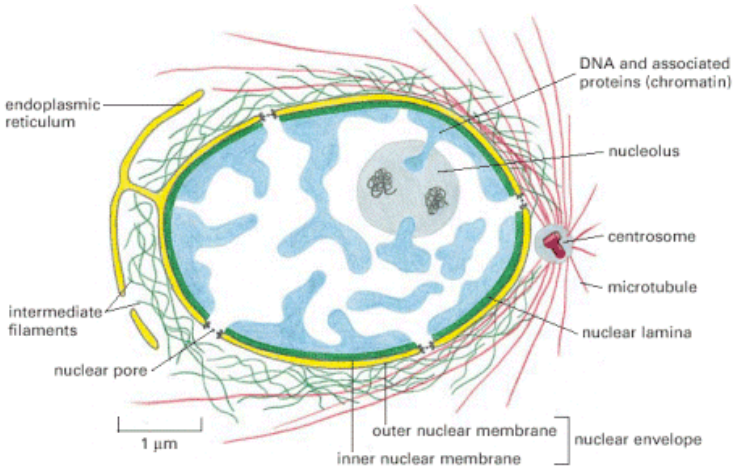

Figure 1-12. A cross-sectional view of a typical cell nucleus. The nuclear envelope consists of two membranes, the outer one being continuous with the endoplasmic reticulum membrane. The space inside the endoplasmic reticulum (the ER lumen) is colored yellow; it is continuous with the space between the two nuclear membranes. The lipid bilayers of the inner and outer nuclear membranes are connected at each nuclear pore. Two networks of intermediate filaments (green) provide mechanical support for the nuclear envelope; the intermediate filaments inside the nucleus form a special supporting structure called the nuclear lamina. (Alberts et al., 2002).

mechanical support to the nuclear envelope. The nuclear lamina is a layer of intermediate filament proteins. The α-helical heptad repeats of lamins form coiled-coil dimers, which associate head-to-tail in filaments that span from pore to pore

(Akhtar and Gasser, 2007). The outer membrane is directly connected to the endoplasmic reticulum of the cytosol. The space between these two membranes is continuous with the lumen of the endoplasmic reticulum (Alberts et al., 2002).

In order to allow the trafficking of molecules between the nuclear compartment and the cytosol the two membranes come into contact at openings called nuclear pore complexes. There are more than 3,000 pore complexes on the nuclear envelope of an animal cell. Each complex is composed of more than 50 different proteins, the nucleoporins, which are arranged with a striking octagonal symmetry. The nuclear pores are used for both import of molecules, like proteins synthesized in the cytosol, and export, like mRNAs transcribed in the nucleus.

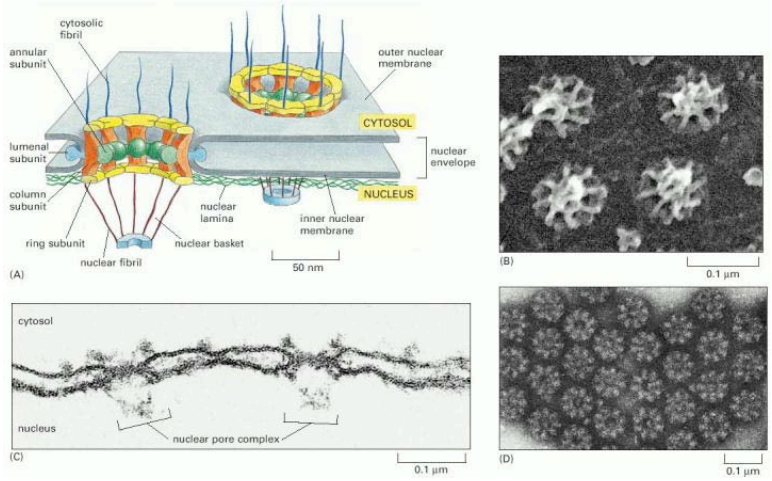

Figure 1-13. The arrangement of nuclear pore complexes in the nuclear envelope. (A) A small region of the nuclear envelope. In cross section, a nuclear pore complex seems to have four structural building blocks; column subunits, which form the bulk of the pore wall; annular subunits, which extend "spokes" (not shown) toward the center of the pore; luminal subunits, which contain transmembrane proteins that anchor the complex to the nuclear membrane; and ring subunits, which form the cytosolic and nuclear faces of the complex. In addition, fibrils protrude from both the cytosolic and the nuclear sides of the complex. On the nuclear side, the fibrils converge to form basketlike structures. Localization studies using immunoelectron microscopy techniques showed that the proteins that make up the core of the nuclear pore complex are symmetrically distributed across the nuclear envelope so that the nuclear and cytosolic sides look identical. This is in contrast to proteins that make up the fibrils, which are different on each side of the cytosolic or the nuclear side. (B) A scanning electron micrograph of the nuclear side of the nuclear envelope of an oocyte. (C) The continuity of the inner and outer nuclear membrane at the pore is apparent in this thin section electron micrograph, showing a side view of two nuclear pore complexes (brackets). (D) This electron micrograph shows face-on views of negatively stained nuclear pore complexes from which the membrane has been removed by detergent extraction. (Alberts et al., 2002).

Chromatin Organization

The DNA of human cells is made up of approximately $7x10^9$ nucleotides, divided between a set of 46 chromosomes, 22 pairs common to both males and females, plus two so-called sex chromosomes (X and Y in males and two Xs in females). Stretched out end to end, the human DNA would extend for a total length of about 1.8 meters.

Since the average diameter of a nucleus is around 6 μm, it comes out that the DNA must be tightly packaged to fit in it. This packaging is performed by proteins, which successively coil and fold the DNA into higher level of organization until the highest one that is the mitotic chromosome. The high overall packing ratio of the genetic material suggests that DNA cannot be directly packaged into the final structure of chromatin. Indeed there are hierarchies of organization.

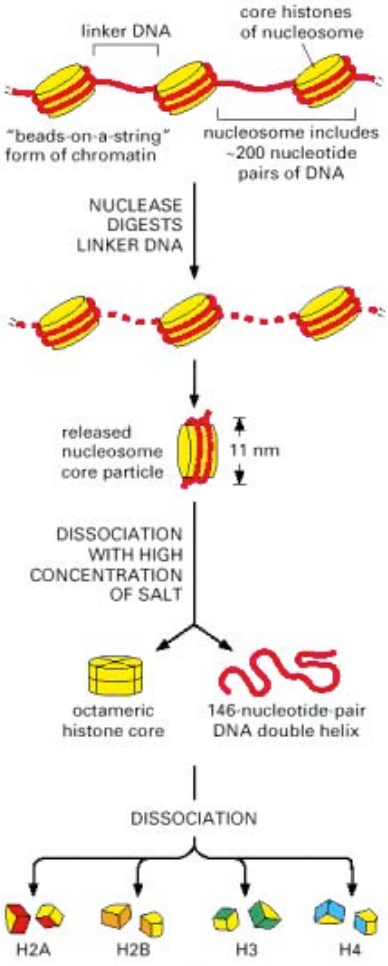

Figure 1-14. Structural organization of the nucleosome. A nucleosome contains a protein core made of eight histone molecules. As indicated, the nucleosome core particle is released from chromatin by digestion of the linker DNA with a nuclease, an enzyme that breaks DNA. (The nuclease can degrade the exposed linker DNA but cannot attack the DNA wound tightly around the nucleosome core.) After dissociation of the isolated nucleosome into its protein core and DNA, the length of the DNA that was wound around the core can be determined. This length of 146 nucleotide pairs is sufficient to wrap 1.65 times around the histone core. (Alberts et al., 2002).

The proteins that bind the DNA to form the eukaryotic chromosome are divided into two classes: the *histones* and the *nonhistone chromosomal proteins*. The complex resulting from both classes of proteins and the nuclear DNA is called *chromatin*.

The first and most basic level of chromatin organization is the *nucleosome*. At this level the double strand DNA is wrapped around a complex of eight histone proteins, called the histone core. This histone octamer consists of two copies each of H2A,

H2B, H3 and H4. The organization of DNA with proteins to form nucleosomes leads to a chromatin length that is one-third of the initial one. At this stage the chromatin is a continuous of nucleosomes and resembles a series of beads on a string. This structure, called 10 nm fiber, is not still clear whether exists *in vivo* or is only an artifact, as a consequence of unfolding during extraction *in vitro*.

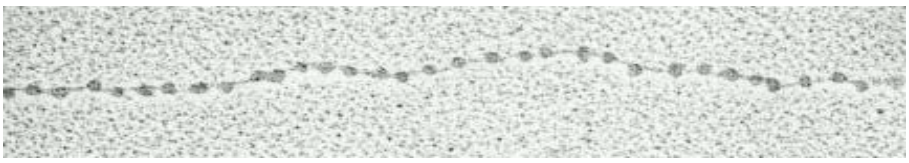

Figure 1-15. Nucleosomes as seen in the electron microscope. This electron micrograph shows a length of chromatin that has been experimentally unpacked, or decondensed, after isolation to show the nucleosomes (Alberts et al., 2002).

The 10 nm fiber condenses into a more packed form, named 30 nm fiber. The presence of histone H1 is required to form the 30 nm fiber. Histone H1 condense the 10 nm fiber through its interaction with nucleosomes, changing the path of the DNA and leading to a fiber resembling a solenoid (Schalch et al., 2005). It has about 6 nucleosomes per turn, which correspond to a packing ratio of 40 (1 μm of this fiber contains 40 μm of DNA).

These still extended structures present in the interphase chromosomes condense more and more during mitosis to form highly condensed structures called mitotic chromosomes. At this stage each chromosome consist of two daughter DNA molecules produced by DNA replication and they are folded separately to produce two sister chromosomes, called sister chromatids, held together at their centromers. Several mechanisms of chromatin condensation that lead to the formation of the highly condensed chromosome structure have been proposed (Belmont, 2002; Belmont and Bruce, 1994; Poirier and Marko, 2002; Strukov et al., 2003; Swedlow and Hirano, 2003), but the most known is the “radial loop model” (Coelho et al., 2004; Maeshima and Laemmli, 2003; Swedlow and Hirano, 2003). In this model the 30 nm fiber forms loops, which in turn coil to form the mitotic chromosome.

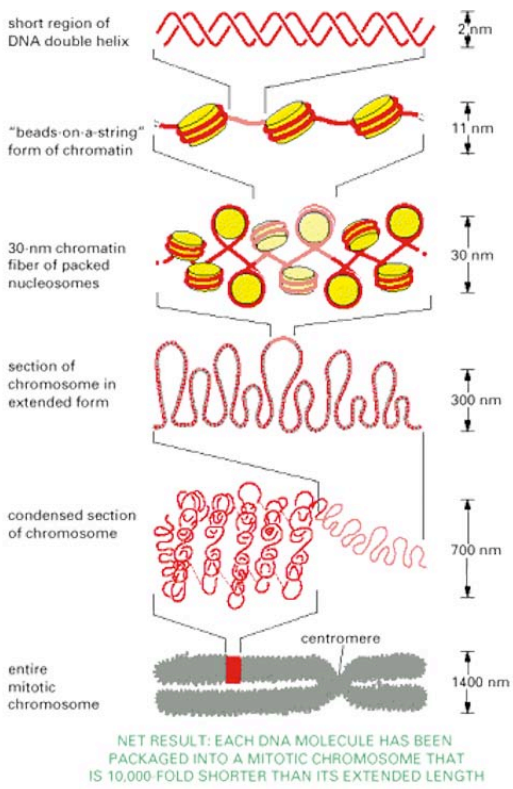

Figure 1-16. Chromatin packing. This model shows some of the many levels of chromatin packing postulated to give rise to the highly condensed mitotic chromosome. (Alberts et al., 2002).

Interphase chromatin

Highly condensed chromosomes are present in the eukaryotic cell for a brief period, during the act of cell division. During most of the life cycle of the cell, however, its genetic material occupies an area of the nucleus in which individual chromosomes can't be distinguished. The structure of interphase chromatin doesn't change visibly between one division and the following. The characteristics of chromatin in interphase nuclei have been studied at light microscope since the 1930s, distinguishing two types of material: a highly condensed and a less condensed form, called *heterochromatin* and *euchromatin*, respectively.

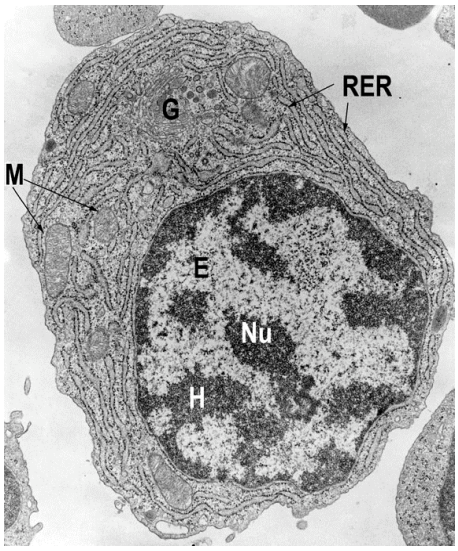

Figure 1-17. Electron micrograph of a cell nucleus. A thin section through a nucleus stained with Feulgen shows heterochromatin (H) as compact regions clustered near the nucleolus (Nu) and the nuclear membrane. Euchromatin (E) appears as less condensed regions. (Lewin, 2004).

Euchromatin is composed of the types of chromosomal structures such 30 nm fiber and looped domains. It has relatively dispersed appearance in the nucleus and occupies most of the nuclear region. Heterochromatin, in contrast, is characterized by regions very densely packed with fibers, displaying a condition comparable to that of the chromosome at mitosis. It includes additional proteins and although present in many locations along chromosomes, it is concentrated in specific regions, including the centromeres and the telomeres (Alberts et al., 2002; Lewin, 2004). The amount and distribution of condensed chromatin is similar in terminally differentiated cells of the same lineage, but it varies in the nuclei of different cell types, indicating that nuclear organization may be cell-type specific (Francastel et al., 2000).

The same fibers run continuously between euchromatin and heterochromatin, which implies that these states represent different degrees of condensation of the genetic material. In the same way, euchromatic regions exist in different states of condensation during interphase and during mitosis. So the genetic material is organized in a manner that permits alternative states to be maintained side by side in chromatin, and allows cyclical changes to occur in the packaging of euchromatin between interphase and division (Lewin, 2004).

The structural condition of the genetic material is correlated with its activity. Indeed, active genes are contained within euchromatin, but only a small minority of the sequences in the euchromatin is transcribed at any time. So location in euchromatin is necessary for gene expression, but is not sufficient for it. Heterochromatin is not transcribed and replicates late in the S phase of cell cycle (Lewin, 2004; Wu et al.,

2005). This suggests that condensation of the genetic material is associated with (perhaps is responsible for) its inactivity. Heterochromatin can be distinguished in facultative or constitutive heterochromatin. The former is the fraction of chromatin that is condensed and inactive in a given cell lineage, which may be decondensed and active in another. The latter is the fraction of heterochromatin that stays compact through the cell cycle. It is mainly composed of repetitive sequences (e.g. satellite DNA), and is concentrated as mentioned above in centromeres and telomeres (Francastel et al., 2000).

Epigenetic

Historically, the word "epigenetics" was used to describe events that could not be explained by genetic principles. Conrad Waddington, who is given credit for coining the term, defined epigenetics as "the branch of biology which studies the causal interactions between genes and their products, which bring the phenotype into being" (Goldberg et al., 2007).

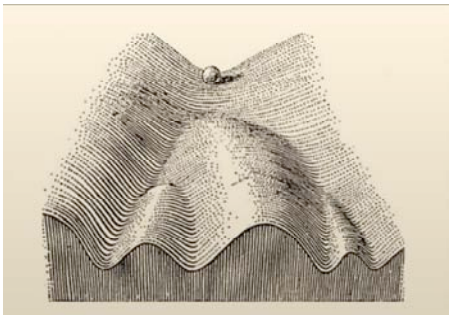

Figure 1-18. Epigenetic. In 1957, Conrad Waddington proposed the concept of an epigenetic landscape to represent the process of cellular decision-making during development. At various points in this dynamic visual metaphor, the cell (represented by a ball) can take specific permitted trajectories, leading to different outcomes or cell fates. Figure reprinted from Waddington, 1957. (Goldberg et al., 2007).

Epigenetics, in a broad sense, is a bridge between genotype and phenotype; it's a phenomenon that changes the final outcome of a locus or chromosome without changing the underlying DNA sequence. More specifically, epigenetics may be defined as the study of any potentially stable and, ideally, heritable change in gene expression or cellular phenotype that occurs without changes in Watson-Crick base pairing of DNA.

Much of today's epigenetic research is converging on the study of covalent and noncovalent modifications of histone proteins and DNA and the mechanisms by which such modifications influence overall chromatin structure (Goldberg et al., 2007). The efforts in studying these chromatin modifications have clearly showed that epigenetic contributes to regulate chromatin structure and DNA accessibility;

nevertheless, it's part of the core mechanism for regulating the transcriptional status of a genetic locus, whether a small element within an individual gene, a chromosomal domain, or even an entire chromosome (Bernstein et al., 2007).

Among the epigenetic modifications there are mainly two categories: histone posttranslational modifications and DNA methylation. All these chromatin modifications influence how the genome is made manifest across a different array of developmental stages, tissue types and even disease states (Margueron et al., 2005).

Histone Post-Translational Modifications

The binding of a chemical group to one or more aminoacidic residue of histones is known as histone posttranslational modification (HPTM). There are a large number of HPTMs, and they divide into two groups (Allis et al., 2007): (1) small chemical groups, including acetylation, phosphorylation and methylation; (2) the much larger peptides, including ubiquitylation and sumoylation.

The mechanism through which HPTMs may affect chromatin structure and/or gene transcription is still poorly understood. Three mechanisms are commonly considered (Allis et al., 2007). In the first one, the binding of chemical compounds may change the charge of the aminoacids, altering the organization of the chromatin, leading it to a more or less condensed structure. The other two mechanisms propose that a structural change of the aminoacids, as a consequence of the HPTMs, may favor or block the binding of specific proteins, such as chromatin remodeling proteins, chromatin modifying complexes, and transcriptional factors.

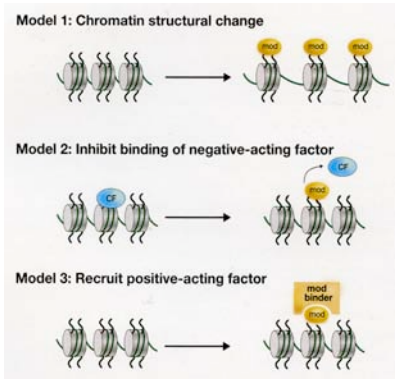

Figure 1-18. Models showing how histone posttranslational modifications affect the chromain template. Model 1 proposes that changes to chromatin structure are mediated by the *cis* effects of covalent histone modifications, such as histone acetylation or phosphorylation. Model 2 illustrates the inhibitory effect of an HPTM for the binding of a chromatin-associated factor (CF). In model 3, an HPTM may provide binding specificità for a chromatin-associated factor. (Allis et al., 2007).

Histones may be modified at many sites. To date, more than 60 different residues have been identified, either by specific antibodies or by mass spectrometry

(Kouzarides, 2007; Macek et al., 2006). This large number of histone posttranslational modifications and their various combinations have led to the idea that they regulate via combinatorial patterns, in temporal sequences, and can be established over short- and long-range distances.

Acetylation

Less condensed chromatin regions are transcriptionally active (Felsenfeld and Groudine, 2003; Weintraub and Groudine, 1976). Indeed, these regions are characterized by an "open" chromatin configuration, which is more accessible to enzymes involved in DNA regulatory processes, such as transcription (Allis et al., 2007). In addition, these regions showed to be closely correlated with acetylated histones (Hebbes et al., 1994), revealing a role for acetylation in chromatin condensation and gene regulation.

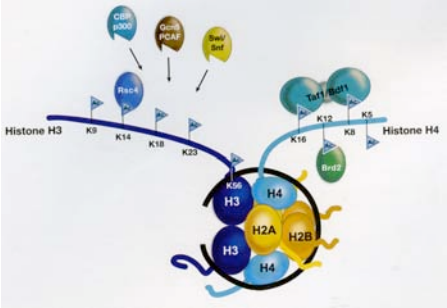

Figure 1-19. Characterized sites of histone acetylation. Histones are mostly acetylated at lysine residues located in the amino termini of H3 and H4, with the exeption of H3K5 localized in the globular domain. The proteins that express binding specificity to acetylated histones are shown. (Allis et al., 2007).

Acetylation is a histone posttranslational modification mediated by a family of proteins called histone acetyl transferases (HAT). These enzymes transfer an acetyl group from acetyl-coenzyme A (acetyl-CoA) to the ε-amino group of specific lysine residues within the histone basic N-terminal tail region (Roth et al., 2001). HAT proteins can acetylate lysine on all four core histones, but different enzymes possess distinct specificities in their substrate of choice.

To date three families of HAT have been described. One major HAT family, GNAT (for GCN5 related acetyltransferase), targets histone H3 as its major substrate. A second family, the MYST, targets histone H4 as its main substrate. A third major family, CBP/p300, targets both H3 and H4, and is the most promiscuous. Each of these acetyltransferase families is also able to acetylate non-histone substrates (Allis et al., 2007; Glozak et al., 2005).

The acetylation of histones may regulate chromatin structure through different mechanisms. It neutralizes the positively charged lysines, reducing the strength of binding of the strongly basic histones or histone tails to negatively charged DNA, opening chromatin for gene activation (Vettese-Dadey et al., 1996). But another mechanism exploited is the involvement of a specialized protein domain called bromodomain that specifically binds to acetylated lysines. Bromodomain is commonly found in many HATs, such as GCN5 and CBP/p300, and other chromatin-associated proteins (Allis et al., 2007; Dhalluin et al., 1999). Proteins containing this motif bind to acetylated histones and, thus, associate with chromatin (Hassan et al., 2002).

Histone Acetylated site	Role in transcription
H3K9	Activation
H3K14	Activation
H3K18	Activation
H3K56	Activation
H4K5	Activation
H4K8	Activation
H4K12	Activation
H4K16	Activation
H2A	Activation
H2BK6	Activation
H2BK7	Activation
H2BK16	Activation
H2BK17	Activation

Table 1-2. Role of different histone acetylated sites on transcription.

Acetyl groups may be removed from acetylated histones through histone deacetylase enzyme (HDAC) (Kurdistani and Grunstein, 2003; Yang and Seto, 2003). There are numerous HDAC enzymes and they fall into three catalytic groups. Type I and type II have a related mechanism of deacetylation, which does not involve a cofactor, whereas type III (Sir-2 related enzymes) require the cofactor NAD. Many of

HDACs are found within large multisubunit complexes, components of which serve to target the enzymes to genes, leading to transcriptional repression (Kurdistani and Grunstein, 2003; Yang and Seto, 2003).

Phosphorylation

Phosphorylation is a histone posttranslational modification associated with active transcription. Indeed, when immediate-early genes are induced to become transcriptionally active a strong correlation is found with H3 phosphorylation (Allis et al., 2007; Mahadevan et al., 1991). The histone 3 serine 10 residue has turned out to be an important phosphorylation site for transcription (Nowak and Corces, 2004).

The precise mechanistic role of histone phosphorylation is still not known, but the collective negative charges resulting from the phosphorylation of clusters of nearby residues affects the affinity of binding of histone H1 to DNA, positively increasing the transcriptional potential (Dou and Gorovsky, 2002). Otherwise, phosphorylated residues of histones may dislodge proteins bound to chromatin (Fischle et al., 2005; Hirota et al., 2005) or, alternatively, they are bound by phospho-binding protein (Macdonald et al., 2005) that modify chromatin structure or or regulate transcription activity (Allis et al., 2007).

Methylation

Methylation is another histone posttranslational modification. It occurs on either lysines or arginines. Furthermore, there can be multiple methylated states on each residue, resulting in a higher level of complexity with respect to the other HPTMs. Indeed, lysines can be mono- (me1), di- (2me) or tri- (3me) methylated, whereas arginines can be mono- or di- methylated. The consequence of methylation can be either positive or negative toward transcriptional expression, depending on the position of the residue within the histone.

Given that there are at least 24 identified sites of lysine and arginines methylation on H3, H4, H2A and H2B, the number of distinct nucleosomal methylated sites is enormous. Such combinatorial potential of methylated nucleosomes may be necessary, at lest partly, to allow the regulation of complex and dynamic processes such as transcription and replication, which requires sequential and precisely timed events (Allis et al., 2007; Dimitrova and Gilbert, 1999; Wu et al., 2005).

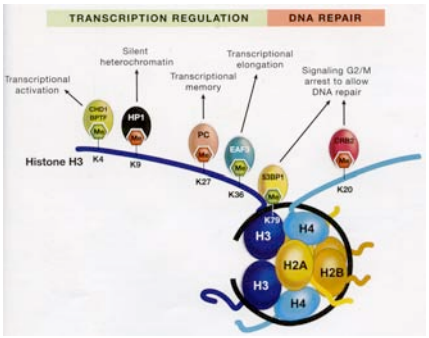

Figure 1-20. Sites of histone methylation, their protein binders, and functional role in genomic processes. Methylation of histones occurs at lysine residues in histones H3 and H4. Ceratin methylated lysine residues are associated with activating transcription (green Me flag), whereas others are involved in repressive processes (red Me flag). Proteins that bind particular methylated lysine residues are indicated. (Allis et al., 2007).

Histone lysine methyltransferases (HKMTs) have been identified and their sites of modification on histones are defined. All of these enzymes, except Dot 1, share the SET domain, which contain the catalytically active site and allows binding to the S-adenosyl-L-methionine cofactor. Of the many known methylated sites, six have been well characterized do date: five on H3 (K4, K9, K27, K36 and K79) and one on H4 (K20). The role of these modifications on transcription is reported in Table 1-3.

Specific protein binders recognize each of the six characterized methylation sites and, in turn, regulate chromatin condensation and gene expression. These proteins have one of three distinct types of methyl lysine recognition domains: the chromo, tudor and PHD repeat domains. For example, the methylation of lysine 9 of histone 3 by the methyltransferase SUV39H creates a binding site for HP1 (Nishigaki et al., 2000). Once HP1 binds through

Histone methylated site	Role in transcription
H3K4	Activation
H3K9	Repression
H3K27	Repression
H3K36	Activation
H3K79	Activation
H4K20	Repression

Table 1-3. Role of different histone methylated sites on transcription.

its chromodomain, it can spread onto adjacent nucleosomes, by its association with SUV39H, which further catalyzes neighboring histone methylation (Allis et al., 2007; Nakayama et al., 2001). In addition, HP1 self-associates via the chromoshadow domain, facilitating the spreading of heterochromatin.

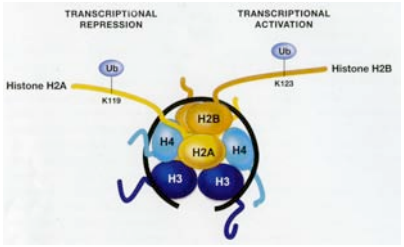

Figure 1-21. Sites of histone ubiquitylation and their consequence for transcriptional regulation. Ubiquitylation of H2A at Lys-119 is correlated with transcriptional repression. H2BK123 ubiquitylation is conversely associated with transcriptional activation. (Allis et al., 2007).

Ubiquitylation and Sumoylation

Ubiquitylation and sumoylation are different from the others HPTMs since ubiquitin and SUMO are large polypeptides, which increase the size of the histone by approximately two-third.

Ubiquitylation can be either repressive or activating, depending on the specific sites. Indeed, H2B monoubiquitylation is activating to transcription (Kim et al., 2005; Wood et al., 2003; Zhu et al., 2005), while Ub1H2A119, is repressive (Wang et al., 2004). The role of sumoylation may be generally negative-acting to prevent activating histone posttranslational modifications, such as acetylation (Shiio and Eisenman, 2003).

Histone posttranslational modifications are dynamic and rapidly changing. Acetylation, methylation and phosphorylation can appear and disappear on chromatin within minutes of stimulus arriving at the cell surface. Thus examining bulk histones under one specific set of conditions (with either antibodies or mass spectrometry) will identify only a proportion of the possible modifications. There are also problems of detection that are specific for antibodies. Firstly, there are the obvious issues of specificity. These are difficult to avoid, as there are no true controls for modifications in mammalian cells (unlike yeast) where it is impossible to mutate the residue to make sure reactivity is lost. In addition, an adjacent modification may disrupt the binding of the antibody or a protein may occlude its recognition, both of which may give a misinterpretation. Similarly, there are

problems of detection that are specific to mass spectrometry. Peptide coverage is not equivalent for all parts of the histone and this reduces the sensitivity of detection in these regions. These facts undoubtedly contribute to an underestimation of the extent of modifications present on histones (Kouzarides, 2007).

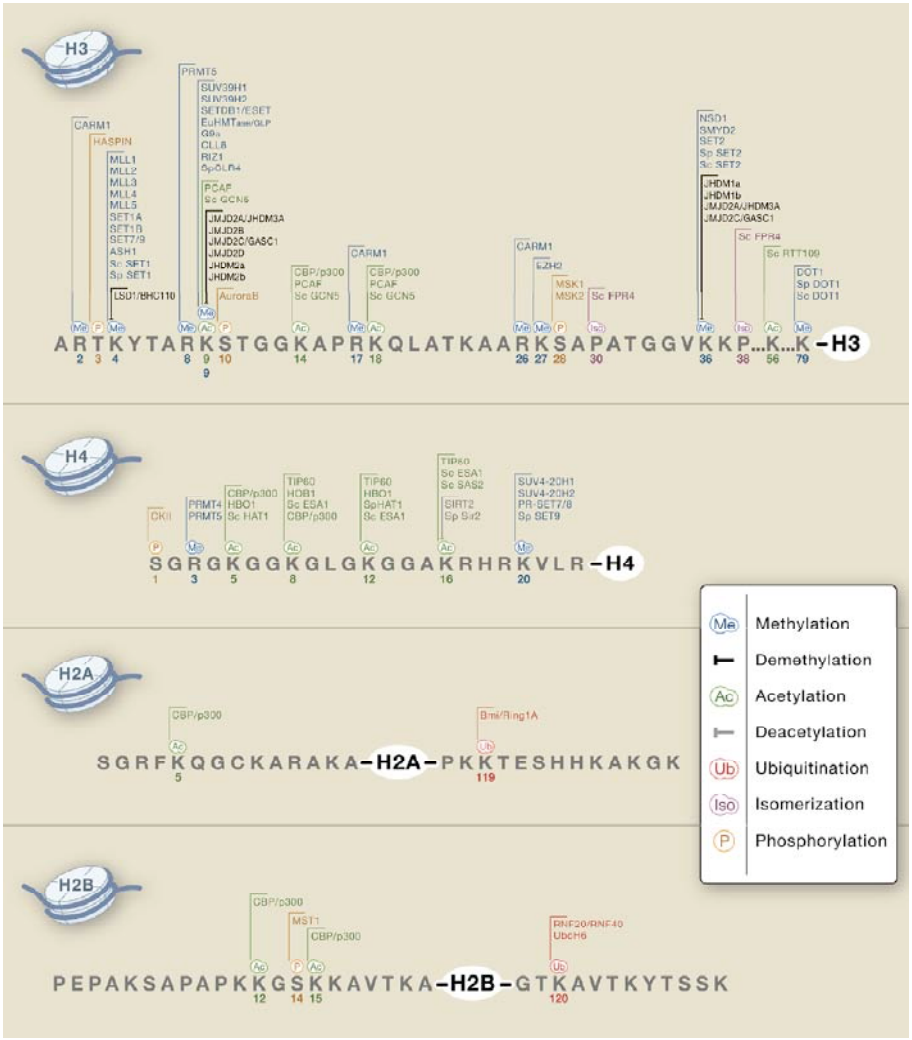

Figure 1-22. This picture depicts those histone-modifying enzymes whose specificity has been determined. (Kouzarides, 2007).

DNA Methylation

The DNA of vertebrate animals is covalently modified by methylation of the cytosine base in the dinucleotide sequence 5'CpG3'. CpG is an abbreviation for

cytosine and guanine separated by a phosphate, which links the two nucleotides together in the DNA. In mammals, nearly all DNA methylation occurs on cytosine residues of CpG dinucleotides.

Regions of the genome that have a high density of CpGs are referred to as CpG islands, and DNA methylation of these islands correlates with transcriptional repression (Goll and Bestor, 2005). Indeed, the methyl moiety of methyl cytosine resides in the major groove of the DNA helix, where many DNA-binding proteins make contact with DNA, and exerts its effect by attracting or repelling various DNA-binding proteins. A family of proteins that can bind to DNA containing methylated CpG dinucleotides, known as methyl-CpG-binding proteins, have been shown to recruit repressor complexes to methylated promoter regions and thereby contribute to transcriptional silencing. Certain transcription factors bind to CpG-containing DNA sequences only when they are nonmethylated. In these cases CpG methylation can prevent protein binding and affect transcription (Allis et al., 2007).

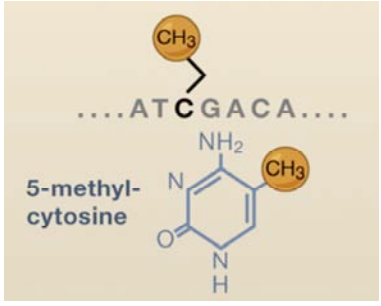

Figure 1-23. Schematic representation of cytosine methylation. (Bernstein et al., 2007).

Spatial Organization of Genomes

The most global level of cellular genome organization is the arrangement of genome regions within the whole 3D space of the cell nucleus (Meaburn and Misteli, 2007). The nonrandom nature of spatial genome organization is indicated by the above mentioned historical observation of segregation of transcriptionally active and inactive regions into physically separate domains of euchromatin and heterochromatin, respectively. New technologies and new methods, such as DamID (van Steensel et al., 2001), ChIP (Casolari et al., 2004), LacO/LacI tagging system (Taddei et al., 2006), have significantly extended this concept and have made it clear that chromosomes, genome regions, and single genes are nonrandomly arranged within the nucleus. Changes in positioning patterns occur during differentiation and development, which strongly suggests a link between positioning and genome function.

A simple way to assess the position of a genome region within the nucleus is by determining its distance from the nuclear periphery (Misteli, 2007). A general correlation between transcriptional silencing and localization toward the nuclear edge has long been suggested based on the observation that early-replicating and

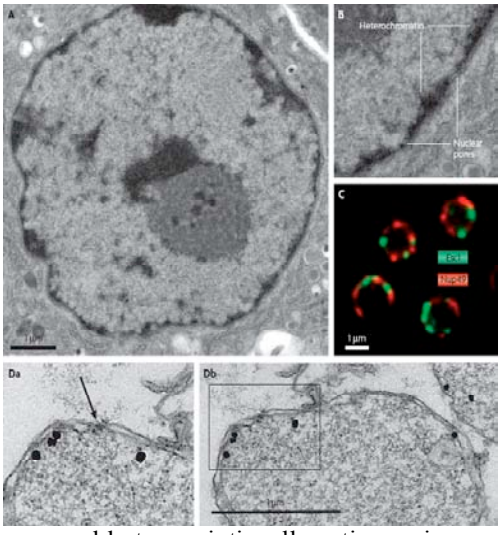

Figure 1-23. Heterochromatin in mammalian and yeast cells is distinct from nuclear pores. (A) An electron micrograph of the mammalian liver nucleus (with an enlarged section shown in part B), showing dense-staining heterochromatin located around the nucleolus and against the nuclear envelope. Nuclear pores open onto lighterstaining open chromatin. (C) In budding yeast, heterochromatin binds the nuclear envelope through Esc1 (enhancer of silent chromatin 1; labelled green), which forms distinct foci alternating with nuclear pores (visualized in red through labelling of Nup49 (nucleoporin 49)). (D) An electron micrograph showing Esc1 at non-pore sites along the yeast inner nuclear envelope. An arrow indicates the nuclear pore, and black dots represent the labelling of Myc-epitope-tagged Esc1 using fluoronanogold Alexa-488 anti-mouse antibody. (Akhtar and Gasser, 2007).

presumably transcriptionally active regions are generally found toward the center of the nucleus, whereas late-replicating, inactive regions are often located toward the periphery. Indeed, the position of single genes relative to the nuclear periphery is nonrandom and has been linked to their functional status. For example, the CD4 locus repositions from the periphery to the nuclear interior during T cell differentiation (Kim et al., 2004). Conversely, the radial position of a gene is generally not directly related to its activity, as indicated by the fact that in most cells the two alleles are positioned differently, even if their functional properties appear to be similar (Misteli, 2007).

The potential role of the nuclear periphery in genome regulation has become of particular importance due to the emergence of several human diseases that are caused by mutations in the LMNA gene, which encodes lamin A and lamin C, the two major architectural proteins of the peripheral lamina (Gruenbaum et al., 2005). Although the nuclear lamina has traditionally been considered to have purely structural properties, recent observations allow for the possibility that it more directly contributes to gene regulation by tethering specific genome regions.

Peripheral localization of genome regions might occur directly via interactions between lamin A and core histones (Gruenbaum et al., 2005).

The nuclear periphery, however, does not function exclusively as a repressive environment given that a large number of S. *cerevisiae* genes are repositioned to the periphery where they interact with nuclear pore components when they become activated (Gruenbaum et al., 2005; Taddei et al., 2006). In fact, by electron microscopy it has been possible to observe that in a differentiated nucleus of mammalian cell dense-staining, transcriptionally inactive heterochromatin is usually plastered against the inner face of the nuclear membrane. The heterochromatic patches are interrupted by nuclear pores, which contain the light-staining nucleoplasm of euchromatin (Akhtar and Gasser, 2007). This association with the periphery is not probably an absolute requirement for gene expression, but it might play a role in optimizing gene activity (Taddei et al., 2006).

Recent studies (Abruzzi et al., 2006) show that gene association with the nuclear periphery does not require ongoing transcription and suggest that the 3'UTR may contribute to the tethering of the gene gene-nuclear periphery tether.

Taken together these results demonstrate that some promoters alone are sufficient to establish strong promoter-pore interactions, others need 3'UTR-linked factors interaction for anchoring to nuclear pores (Akhtar and Gasser, 2007). In conclusion, the studies so far performed suggest that the positioning of chromatin at the nuclear envelope can contribute to gene regulation in both a positive and negative manner, probably depending on the subnulcear positioning.

RELATIONSHIPS BETWEEN VIRAL INTEGRATION AND CHROMATIN ORGANIZATION

Integration is an essential step for retroviral replication. This process leads to the irreversible and permanent viral DNA insertion into the host cell genome, allowing the transcription of viral genes by the cellular machinery. This peculiarity of retroviruses raised the possibility to exploit HIV-1 in gene therapy, as a vector to stably integrate genes into the genome of the target cells, in order to restore the functionality of defective endogenous genes.

However, integration is a mutagenic event, which may alter a cellular function depending on the targeted genetic site. For example, retroviral vectors have been used to treat patients with severe immunodeficiency (X-linked severe combined immunodeficiency; X-SCID). During this trial three out of ten children developed leukaemia; in two of these cases, in the leukaemic cells, the therapeutic retroviral vector was found to have integrated in the 5' region of the LMO2 oncogene, which probably contributed to the neoplastic transformation (Hacein-Bey-Abina et al., 2003a; Hacein-Bey-Abina et al., 2003b). Therefore, understanding weather there is a preferential target sequence in the host cellular genome and the mechanism that underlies the integration site selection of HIV-1 is important for both basic retrovirology and its clinical applications in gene therapy.

Initial experiments with murine retroviruses revealed that DNA assembled with nucleosomes constitutes a better substrate for integration as compared to naked DNA. *In vivo* genomic DNA is complexed with nucleosomes (chromatin). Incorporating DNA into nucleosomes *in vitro* does not reduce integration, as might have been expected from a steric hindrance model, but instead creates new hotspots for integration. Analysis of these integration hotspots indicates that these are sites at which DNA is probably distorted owing to the wrapping of DNA around nucleosomes (Bushman et al., 2005). Indeed, in chromatin the preferred integration sites are periodically spaced by 10 bp, indicating that HIV-1 integration occurs preferentially at positions where the major groove is on the exposed face of the nucleosomal DNA helix (Bushman, 1994; Muller and Varmus, 1994; Pruss et al., 1994; Pryciak et al., 1992).

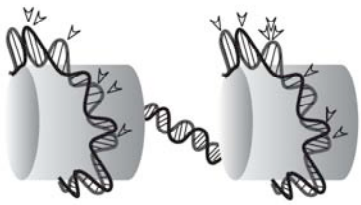

Figure 1-24. Preferred DNA integration sites into nucleosomal DNA. Favorable sites for retroviral integration are located into the major groove on the exposed face of the DNA that bends around nucleosomes (schematically represented by cylinders). The arrows indicate the favorable integration sites. (Cereseto and Giacca, 2004).

Since the nucleosomal complex usually restricts the accessibility of other proteins to DNA, the enhancement of retroviral integration into chromatinized DNA was an unexpected outcome. Indeed, the presence of DNA-binding proteins on the target DNA creates regions refractory to integration due to steric interference (Bor et al., 1995; Bushman, 1994; Pryciak et al., 1992). Therefore, other factors, such as DNA structure rather than the proteins themselves, probably influence the efficiency of virus integration. To distinguish the different roles played by DNA structure (bending around nucleosomes) and proteins (histones) during integration, the N-terminal tails of the histones protruding from the nucleosomes were removed from the target DNA. In these experiments, a similar distribution and frequency of integration were observed in intact or tailless histone-bound DNA, indicating that the wrapping of DNA around nucleosomes, rather than the presence of proteins, is the major determinant for integration site selection by the HIV-1 integrase (Pruss et al., 1994). The importance of DNA distortion is consistent with the idea that it is involved in the integrase mechanism, so that pre-distorting the target DNA favours the integration reaction. Indeed, *in vitro* experiments, using the *E. coli* IHF protein (integration host factor) that binds inside the DNA bend, showed an increased efficiency of integration at hotspots within the IHF site itself (Bor et al., 1995). This could be explained by the fact that the outside surface of the bend is easily accessible for integration. In addition, by modifying DNA structure with a variety of methods, it has been clearly demonstrated that the extent of integration enhancement upon bending correlates with the extent of the bending (Muller and Varmus, 1994). On the other hand, the presence of a DNA-binding protein on target DNA can block access of integration complexes, creating regions that are refractory to integration. For example, LEF protein (lymphoid enhancer factor) bends DNA but lies outside the bend covering the region of the greatest distortion favorable for integration, and therefore did not create integration hotspots (Bor et al., 1995).

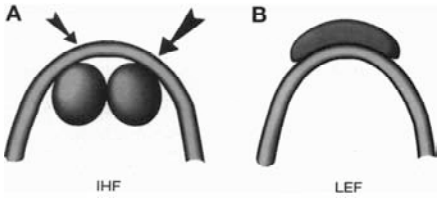

Figure 1-25. Schematic diagrams of the IHF-H' complex (A) and the LEF-DNA complex (B). Each protein is shown stippled. DNA is shown as the bent cylinder. Arrows mark approximate location of integration hotspots in the IHF site. (Bor et al., 1995).

Extensive analyses of the sequences flanking the integration sites have revealed some weak biases due to different primary sequence (Carteau et al., 1998; Pryciak and Varmus, 1992; Stevens and Griffith, 1996). However, a unique consensus DNA sequence necessary for retrovirus integration has not been identified (Bor et al., 1996; Fitzgerald and Grandgenett, 1994; Goodarzi et al., 1997), indicating that the primary sequence of the integration target site has a relatively minor influence on site selection during infection. In light of the evidence indicating the importance of the DNA structure on target site selection, the role of certain sequences influencing integration efficiency can be explained by the modifications of the local DNA structures induced by these sequences (Muller and Varmus, 1994; Pruss et al., 1994). This notion has been ultimately demonstrated using a supercoiled DNA containing an extensive inverted repeat as the integration target. In this study, integration by the HIV-1 and ASV integrase preferentially occurred in only one half of the inverted repeat, thus suggesting that this bias was due to the creation of a secondary structure favorable for integration rather than to the primary sequence (Katz et al., 1998). Indeed, several reports have correlated integration *in vivo* with the presence of nearby repeated sequences, including LINE-1 elements (Stevens and Griffith, 1994), clusters of Alu repeats (Alu islands) (Stevens and Griffith, 1996), or topoisomerase II cleavage sites (Howard and Griffith, 1993). However, in all these studies the number of integration sites analyzed was relatively low. In addition, their conclusions are challenged by another report in which no strong bias could be detected in favor of, or against, integration near Alu or LINE-1 elements (Carteau et al., 1998). Considered together, the overall conclusion of these studies is that DNA secondary structure, and not DNA primary sequence, is a major determinant for integration site selection.

It has been observed that centromeres are disfavored integration targets *in vivo*, despite the fact that centromeric alphoid repeats are used similarly to other sequences when tested as naked DNA *in vitro* (Carteau et al., 1998). Inside the cells, centromeres assume a heterochromatic conformation, which is known to be wrapped tightly by distinctive DNA-binding proteins, and this chromatin environment is unfavourable for the expression of most genes. Moreover, alphoid sequences become more resistant to digestion with DNase I than most DNA in isolated nuclei.

This indicates that the packing of DNA into centromeric heterochromatin renders it less accessible, and so it disfavours integration. In keeping with this observation, a number of other *in vivo* surveys of retroviral integration sites have revealed that viral gene insertion is statistically biased to regions close to DNase I hypersensitive sites, which are characterized by an open chromatin conformation (Goodenow and Hayward, 1987; Panet and Cedar, 1977; Robinson and Gagnon, 1986; Rohdewohld et al., 1987; Vijaya et al., 1986). Since open chromatin is a hallmark of actively transcribed areas, it is not surprising that most of these studies have also found an association between retrovirus integration and genomic regions containing transcriptionally active genes (Mooslehner et al., 1990; Scherdin et al., 1990). However, these early *in vivo* studies could be the results of a potential bias imposed by the relatively small sample size analyzed and the selection of cloned proviruses for analysis. In fact, if integration occurred near the genes affecting the growth of the infected cells, these cells could be either over or less represented in the analyzed population, thus providing a false impression of integration near active genes.

Recent progress made in the field of genome and transcriptome analysis has allowed for genome-wide surveys of HIV-1 integration preferences. Following large-scale sequence analysis, the distribution of HIV integration sites in the chromosomes of a human lymphoid cell line, SupT1, was investigated (Schroder et al., 2002). This study showed that genes were favoured targets for HIV integration, and later studies of HIV integration in other cell types reached the same conclusion (Mitchell et al., 2004; Wu et al., 2003). Further studies investigated whether there were any preferences in the location of HIV integration sites along the length of transcription units (Mitchell et al., 2004; Schroder et al., 2002; Wu et al., 2003). No biases were found. Evidently, the positive influence of transcription units on HIV integration extends across their entire length (Bushman et al., 2005).

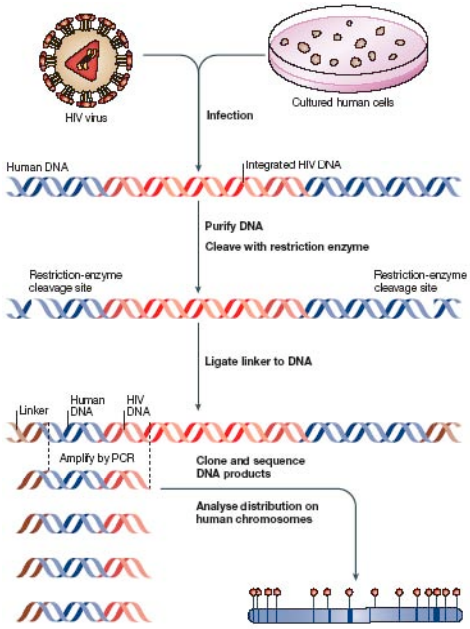

Figure 1-26. Analysing retroviral integration sites in the human genome. To analyse retroviral integration sites in the human genome, cultured cells are infected with HIV or another retrovirus. DNA from infected cells is isolated, cleaved with restriction enzymes and ligated to DNA linkers. Integration sites are then amplified using one primer that binds to the viral DNA end and another primer that binds to the DNA linker (see the figure). Amplification is carried out a second time with nested primers, and the PCR products, which contain host– virus DNA junctions, are cloned and sequenced (Schroder et al., 2002). Integration sites are mapped on the draft human genome sequence (see Figure 1-27), and local features at integration sites are quantified. Various control sites can be used for comparison in these experiments. Probably the best type of control takes advantage of integration in vitro. Schroder and colleagues purified DNA from uninfected SupT1 cells and used this DNA as a target for preintegration-complex integration in vitro (Schroder et al., 2002). Reaction products were purified and integration sites were cloned, as for the in vivo sites. The analysis then compared the in vivo and in vitro populations. Statistical analysis revealed that the distribution of integration sites in the in vitro population was indistinguishable from random sampling of the human genome (Schroder et al., 2002), supporting the idea that the clonino and analytical methods used did not bias the analysis. Another type of control takes advantage of random locations in the human genome that are generated computationally. These are used in statistical comparisons with the experimental population. A more sophisticated variation of this approach uses random sites that are selected in a way that takes into account the possible influence of the distribution of restriction-enzyme recognition sites used in the cloning of experimental integration sites. (Bushman et al., 2005).

Transcriptional profiling analysis has been carried out in some of the cell types studied as integration targets, allowing the influence of transcriptional activity on integration-site selection to be assessed. Some of these transcriptional profiling studies were carried out on retrovirus-infected cells (Lewinski et al., 2005; Mitchell et al., 2004; Schroder et al., 2002), so that the data reflected the influence of infection on cellular gene activity (Bushman et al., 2005; Corbeil et al., 2001;

Mitchell et al., 2003; Schroder et al., 2002; van 't Wout et al., 2003). Analysis of the microarray data revealed that the median expression level of genes hosting HIV integration events was consistently higher than the median expression level of all the genes assayed on the microarray. Transcriptional profiling studies were carried out for HIV vector integration in SupT1 cells (Schroder et al., 2002). This study showed that the trend towards integration in highly expressed genes increased when data from infected cells were used, which indicates that genes that are activated by infection are favoured integration targets.

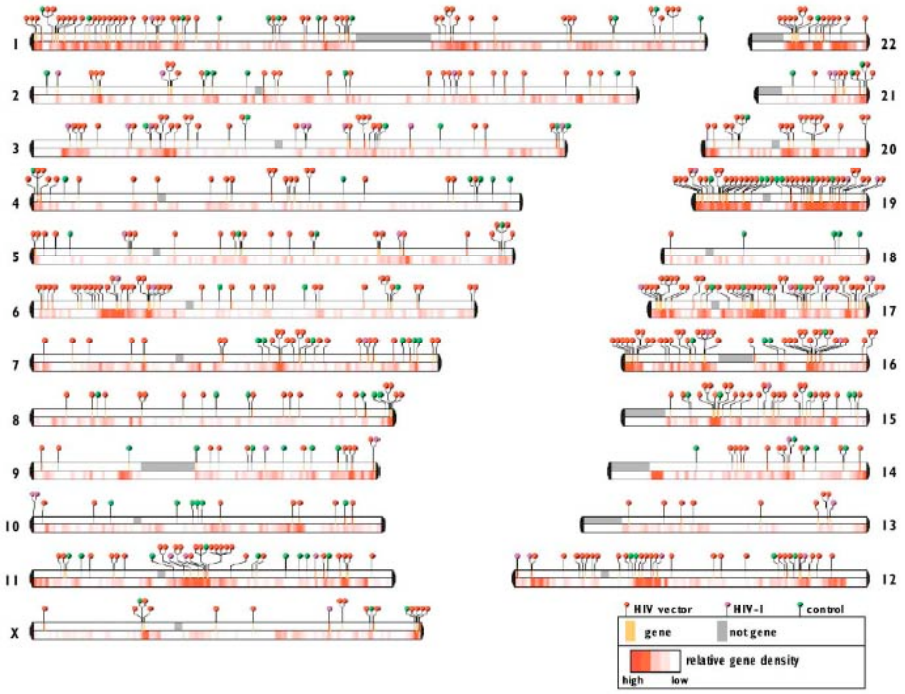

Figure 1-27. Sites of HIV-1 cDNA Integration in the Human Genome. Locations of chromosomal sequences matching HIV-1 integration site clones are shown as "lollipops" above the linear chromosomes. Purple indicates HIV-1; red, HIV-based vector; and green, PIC (in vitro control). The human chromosomes are shown numbered. For each chromosome, the color of the dashes on the upper bar indicates integration within genes (gold) or outside genes (gray). The lower bar indicates relative gene density, with more-gene-dense regions shown as a more intense red. Centromeres are shown by the gray rectangles. Karyotype analysis showed that the Y chromosome is not present in the SupT1 cells studied and the representation of chromosomes was roughly equal in the cells analyzed. (Schroder et al., 2002).

Since the majority of the HIV-1 infected cells die very shortly after infection due to cytopathic effects or by immunoclearance, it has been hypothesized that the bias for integration into transcriptionally active regions is a strategy to maximize its

expression to produce viral progeny. Conversely, a latent infection can be established by silencing the basal viral expression by integration into heterochromatic regions (Jordan et al., 2001).

Taken together, these data indicate that the integration is favoured in the transcriptionally active genes. These regions are characterized by an open chromatin structure, which is more accessible to the integration apparatus. Since histone posttranslational modifications are involved in chromatin condensation and gene regulation (Allis et al., 2007), a role for acetylation and methylation of histones in directing retroviral integration has been investigated (Wang et al., 2007). In this study 40,569 unique sites of HIV-1 integration have been sequenced. Analysis of integration site positions in the densely annotated ENCODE (Encyclopedia of DNA elements) regions revealed that integration was favoured near transcription-associated histone modifications, including H3 acetylation, H4 acetylation, and H3 K4 methylation, but was disfavored in regions rich in transcription-inhibiting modifications, which include H3 K27 trimethylation and DNA CpG methylation. Different hypothesis have been proposed to explain such correlations. One model takes in consideration a family of related integrase enzymes encoded by yeast retrotransposons that contain chromodomains (Hizi and Levin, 2005), which bind methylated histone tails, thus direct binding is a candidate explanation for integration targeting. However, retroviral integrases do not contain domains known to bind modified histones. Another possibility is that the cellular proteins recruited by specific histone posttranslational modifications tether integration complexes near sites of modification. Alternatively, epigenetic modifications may be only markers of favored integration sites and not directly involved in the targeting mechanism (Bushman et al., 2005). Recently, the cellular protein LEDGF/p75 has been identified as a HIV-1 IN co-factor (Cherepanov et al., 2003; Maertens et al., 2003; Turlure et al., 2004), which is functionally important for targeting the proviral DNA (Cherepanov et al., 2003; Ciuffi et al., 2005; Emiliani et al., 2005; Kang et al., 2006; Maertens et al., 2003) through a mechanism that is not linked with histone modifications (see subsequent sections).

INTERACTION OF HIV-1 INTEGRASE WITH HOST CELLULAR PROTEINS

HIV-1 has only a limited genome (Frankel and Young, 1998), nevertheless its replication in the human cell Interaction with host cellular proteins requires multiple and distinct activities. Consequently, the virus exploits cellular proteins and cellular pathways to complete the different steps in its life cycle (Goff, 2007; Van Maele et al., 2006).

As mentioned above, PICs contain linear viral DNA and several viral proteins including matrix, reverse transcriptase, integrase and nucleocapsid. Cellular proteins have also been identified in functional PICs, suggesting a functional involvement for the viral infectious process. Indeed, even though purified recombinant integrase is necessary and sufficient to carry out processing and strand transfer *in vitro*, a variety of viral and cellular proteins have been put forward as important partners in establishing the integrated provirus in the infected cell.

Cellular co-factors of integration have been identified in different ways: (I) by *in vitro* reconstitution of enzymatic activity of salt-stripped PICs; (II) by using the yeast two- hybrid assay; and (III) by co-immunoprecipitation.

PICs isolated from cells infected with HIV-1, show a strong preference for integration into the target DNA added to the reaction rather than into the viral DNA carried within the PIC. Indeed, HIV-1 PICs contain a cellular barrier-to-autointegration factor (BAF) that prevents suicidal autointegration (Lin and Engelman, 2003). BAF binds double-stranded DNA and is, therefore, probably recruited by infectious retroviruses during the late stage of reverse transcription (Harris and Engelman, 2000; Zheng et al., 2000). It has been suggested that BAF acts by bridging DNA molecules in order to condensate DNA, thus rendering the viral DNA inaccessible as a target for integration (Lee and Craigie, 1998; Zheng et al., 2000). BAF can also promote efficient intermolecular DNA recombination by anchoring PICs to target DNA prior to the integration reaction. Hence, the prevention to autointegration and the promotion of intermolecular integration by BAF may involve a unique mechanism of DNA bridging (Suzuki and Craigie, 2002). At the cellular level, the role of BAF still remains to be elucidated. However,

the ability of BAF to compact DNA suggests a possible role in chromatin organization. Findings that lamina-associated polypeptide 2 (LAP2), a protein associated with nuclear lamina, interacts with BAF reinforce this hypothesis (Furukawa, 1999; Shumaker et al., 2001).

Fractionation of an uninfected cell extract that restored *in vitro* PIC activity after salt-stripping yielded high mobility group chromosomal protein A1 (HMGA1; formerly HMGI(Y)), a non-histone DNA-binding protein that can modulate transcriptional regulation and chromatin structure (Farnet and Bushman, 1997). Two members of this protein family, HMGA1 and HMGA2, recognize specific sequences in the cellular genome and probably function by facilitating the binding of transcription factors to the chromatin (Thomas and Travers, 2001). HMGA1 and HMGA2 have been identified within the PICs of MLV and HIV-1, where they act by stimulating retroviral integration (Farnet and Bushman, 1997; Li et al., 2000). A recent attempt to investigate the role of these cellular proteins during the viral replication cycle has indicated that they are dispensable for retroviral integration, probably due to redundancy with other factors (Beitzel and Bushman, 2003). The mechanism by which HMGs stimulate intermolecular integration is still being debated, and several models have been proposed: (I) by binding specific DNA sequences in the LTR, HMGs may act by bridging distant DNA segments into proximity (Farnet and Bushman, 1997; Li et al., 2000); consistently, the cDNA ends in PICs are known to be protected from nuclease attack by bound proteins that also function as a protein bridge between the viral ends (Miller et al., 1997; Wei et al., 1997); (II) by binding both viral and target DNA, thus bridging the PIC to the cellular genome; this hypothesis, however, appears unlikely since no HMG binding sites have been identified close to the integration sites and HMGs act on viral DNA, while they have no effect on target DNA during the integration reaction (Aiyar et al., 1996); (III) by condensing the viral cDNA that, in turn, would stabilize the integrase in an active conformation (Farnet and Bushman, 1997; Li et al., 2000).

EED is a chromatin-remodeling protein that belongs to the widely conserved Polycomb group of proteins, and has very recently been found to interact with integrase (Violot et al., 2003). Interestingly, BAF, HMGs and EED share the

common feature of all being associated to condensed DNA structures. Although the data so far acquired indicate a primary effect of these proteins on donor viral DNA rather than on the acceptor cellular genome, it still remains an open question weather these factors might play a major role at the level of the integration site *in vivo*. In addition, these proteins may also function by bridging the interaction with other factors (e.g. transcriptional factors) that ultimately could favor integration as well as transcription.

By using yeast two hybrid approach Kalpana and coworkers (Kalpana et al., 1994) found another IN cellular co-factor, the integrase interactor 1 (INI1), also known as hSNF5. INI1 is the human homolog of yeast SNF5, a transcriptional activator and component of the chromatin remodeling SWI/SNF complex (Carlson and Laurent, 1994). Likewise, INI1 was shown to be part of the mammalian SWI/SNF complex (Wang et al., 1996). INI1 and integrase interact through direct binding and this association promotes integrase activity (Kalpana et al., 1994). Although INI1, as a component of the SWI/SNF complex, has been hypothesized to play a role in integration-site selection, no experimental evidence has been produced to support this idea (Van Maele et al., 2006). Interestingly, a possible role for INI1 in the post-integration steps of HIV-1 replication is stronger (Yung et al., 2001). Indeed, INI1 probably interacts with integrase within the context of Gag-Pol precursor and inhibits viral particle production (Yung et al., 2001). These results indicate that INI1 is required for late events in the viral life cycle, and that ectopic expression of the minimal integrase-interactor domain of INI1 (S6) inhibits HIV-1 replication in a transdominant manner via its specific interaction with integrase within the context of Gag-Pol (Yung et al., 2001). On the contrary, it has been reported that siRNA mediated silencing of SWI/SNF complex expression inhibited the formation of 2-LTR circles and integrated forms of viral DNA, suggesting a role for SWI/SNF complex in the early steps of HIV-1 replication (Maroun et al., 2006). In fact a single amino acid change, K71R, in integrase reduced its ability to interact with SNF5/ Ini1, leading to an increased viral infectivity (Maroun et al., 2006).

Ku, a chromatin-associated protein that functions by participating in double-stranded DNA break recognition and repair, has also been identified in PICs (Li et al., 2001;

Lin and Engelman, 2003). This protein seems to enhance the circularization of a portion of the total viral DNA produced by reverse transcription in infected cells. It has been hypothesized that free viral DNA ends could induce apoptosis in infected cells. By promoting viral DNA circularization, Ku might therefore protect cells from cell death, allowing the viral replication cycle to be efficiently completed (Li et al., 2001).

Recently, a new binding partner of HIV-1 integrase was identified following a study of the HIV-1 integrase complexes present in nuclei of human cells that stably overexpress the viral integrase from a synthetic gene (Cherepanov et al., 2003). Using co-immunoprecipitation, a novel cellular co-factor interacting with integrase was found. The same co-factor, known as *lens epithelium derived growth factor* (LEDGF/p75), has been independently confirmed by at least two other groups, by using co-immunoprecipitation (Turlure et al., 2004) or yeast-two-hybrid (Emiliani et al., 2005). LEDGF/p75 contains 530 amino acids and several functional domains (Van Maele et al., 2006). In the N-terminal region of LEDGF/p75, a PWWP (for Pro-Trp-Trp-Pro) domain of 92 residues is present that functions as a protein–protein interaction domain and/or DNA-binding domain. A functional nuclear

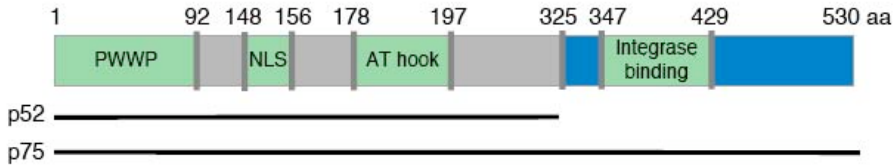

Figure 1-27. Domain structure of LEDGF/p75. The p75 and p52 splice variants and the different domains are highlighted. In the N-terminal region of LEDGF/p75, a PWWP domain of 92 residues is present that functions as a protein–protein interaction domain and/or a DNA-binding domain. A functional nuclear localization signal (NLS) has been identified. An evolutionarily conserved integrase-binding domain (IBD) was mapped to the C terminus. A possible AT-hook-like domain is also illustrated. (Van Maele et al., 2006).

localization signal (NLS, residues 148–156) is present. In accordance with its ability to interact with HIV-1 integrase, an evolutionarily conserved integrase-binding domain (IBD) of about 80 amino acids (residues 347–429) was recently mapped to the C terminus (Cherepanov et al., 2004). LEDGF/p75 is predominantly localized in the nucleus, where it is intimately associated with the chromosomes (Nishizawa et al., 2001). The precise stoichiometry of the integrase–LEDGF/p75 complex in the infected cell has not been elucidated, but the simplest model suggests a symmetrical

complex containing a pair of integrase tetramers and two subunits of LEDGF/p75 (Cherepanov et al., 2003).

The nuclear distribution of HIV-1 integrase perfectly matches that of LEDGF/p75 (Cherepanov et al., 2003; Maertens et al., 2003). Knock-down of endogenous LEDGF/p75 using small interfering RNA (siRNA) completely abolishes the nuclear localization of HIV-1 integrase and its association with chromosomes in cells transiently transfected with the integrase fused to enhanced GFP (EGFP) (Maertens et al., 2003). In pull-down assays using different recombinant integrases, it was subsequently demonstrated that LEDGF/p75 interacts with lentiviral but not retroviral integrases (Busschots et al., 2005). Direct interaction in cells was confirmed using fluorescence-correlation spectroscopy (FCS) (Maertens et al., 2005). Two approaches were used to validate the role of LEDGF/p75 during HIV replication. Transient and stable siRNA-mediated knock-down of LEDGF/p75 reduced HIV replication significantly, without effect on viability or growth kinetics of the target cells (Vandekerckhove et al., 2006). In the second approach, the Q168A (Gln/Ala) mutation in integrase, which abolishes interaction with LEDGF/p75 but not integrase catalytic activity, was exploited to show a stop in the replication process due to a specific block at the integration step, whereas the nuclear import was not hampered (Emiliani et al., 2005). Thus, both RNAi- and mutant-based experiments point to an important role of LEDGF/p75 in HIV replication. These data, however, are at odds with some findings from another group (Llano et al., 2004); this discrepancy might be owing to the inefficient siRNA-based knockdown of LEDGF/p75, leaving a very small amount of LEDGF/p75. In order to overcome this problem, Llano *et al.* (Llano et al., 2006) used intensified RNA interference and dominant-negative protein approaches to show that LEDGF/p75 is indeed an essential HIV-1 integration co-factor. Recently, the generation of LEDGF/p75 knockout mouse embryo fibroblasts (MEFs) (Shun et al., 2007b) allowed for the first time to analyze HIV-1 integration in the complete absence of LEDGF/p75 protein. The lack of LEDGF/p75 protein expression showed that HIV-1 replicates less efficiently and changes its integration bias from transcriptionally active regions to promoter regions and CpG islands (Shun et al., 2007b). Therefore, since LEDGF/p75 associates with transcriptionally active genes (Ge et al., 1998; Mitchell

et al., 2004; Shinohara et al., 2002), it acts as a tethering factor for IN, by specifically targeting viral integration toward LEDGF/p75-associated regions.

Based on the preferential integration of HIV-1 into transcriptionally active regions of chromatin, Cereseto *et al*. explored the association of IN with cellular proteins possessing HAT activity (Cereseto et al., 2005). Among these proteins, p300 resulted to interact with HIV-1 integrase both *in vitro* and *in vivo* (Cereseto et al., 2005; Topper et al., 2007). This factor regulates gene expression by bridging the transcriptional machinery to several known transcription factors, and by promoting histones acetylation. In addition to its HAT activity, p300 also acetylates a number of different cellular and viral proteins (Cereseto and Giacca, 2004). The carboxy-terminus domain (CTD) of IN (amino acids 212-288) binds specifically to p300 and gets acetylated on lysines 264, 266, and 273 (Cereseto et al., 2005; Topper et al., 2007). Acetylation of IN increases its binding to DNA *in vitro*, according with the fact that acetylation of DNA-binding proteins often increases their binding affinity to DNA (Cereseto et al., 2005). In addition, acetylation of IN increases its DNA strand transfer activity of approximately two-fold *in vitro*, indicating a potential role for p300-dependent acetylation of IN during virus infection (Cereseto et al., 2005). Mutational analysis revealed a reduced integration efficiency *in vivo* (Apolonia et al., 2007; Terreni, 2009; Topper et al., 2007).

PICS NUCLEAR IMPORT

The pre-integration complexes are formed by the retrotranscribed viral DNA and both cellular and viral proteins. Several factors intervene in PICs nuclear translocation. The active nuclear transportation is determinant for lentiviruses, including HIV, to infect non-dividing cells, such as terminally differentiated macrophages (Lewis et al., 1992). However, the mechanism governing the nuclear import is still poorly understood. Indeed, unlike other viral proteins such as reverse transcriptase or integrase, nuclear import is not accompanied by a measurable enzymatic activity (De Rijck et al., 2007). Moreover, HIV-1 proteins have a pleiotropic nature; since the genomic capacity of a lentivirus is restricted to about 9 kb, viral proteins evolved to play various roles in the replication cycle in close interaction with each other and with the proteins of the host. Therefore, deletions or

mutations in any viral protein are likely to alter many steps in viral replication, hindering the interpretation of the results obtained.

Matrix is one of the viral proteins involved in the nuclear import. It has a basic-type nuclear localization signal (NLS) at the N-terminus (Bukrinsky et al., 1993a), resembling the NLS of SV40 large T antigen. Later on, it was shown that matrix NLS was capable of binding to Rch1, a member of the importin-α family (Gallay et al., 1996). However, the matrix NLS hypothesis is controversial (Fouchier et al., 1997; Heinzinger et al., 1994). The ultimate proof that matrix is not the only factor involved in nuclear import was the finding that a virus lacking the complete globular head of matrix was still capable of replicating in macrophages (Reil et al., 1998). Recently, the replacement of HIV-1 MA protein with that of MLV, which is not able to infect non-dividing cells, did not have any adverse effects on viral infection in interphase cells (Yamashita and Emerman, 2004). These data suggest that the importance of MA for nuclear import of the PIC is still highly controversial and redundancy exists with other factors.

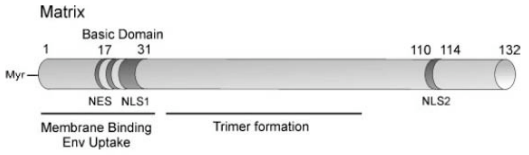

Figure 1-28. Schematic overview of the matrix protein. NLS, nuclear import signal; NES, nuclear export signal; Env, envelope. Numbers refer to the amino acid number. (De Rijck et al., 2007).

Another viral protein that has been investigated for its role in PIC nuclear translocation is Vpr. Speculations about its involvement in nuclear import started when Vpr was shown to play an important role in facilitating viral replication in macrophages (Bukrinsky et al., 1992; Eckstein et al., 2001; Heinzinger et al., 1994; Popov et al., 1998; Vodicka et al., 1998). The first indication for a direct role of Vpr in nuclear translocation came from the observation that PICs containing a mutated matrix NLS were still able to replicate in macrophages in presence of

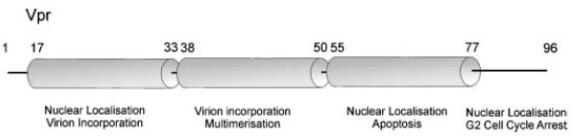

Figure 1-28. Schematic overview of viral protein R. The three a-helices are shown in gray. Potential functions of the three a-helices and the C-terminal domain are indicated. Numbers refer to the amino acid number. (De Rijck et al., 2007).

functional Vpr, but a severe replication defect was observed when both these proteins where mutated (Heinzinger et al., 1994). However, these data were not confirmed by Kootstra *et al*. (Kootstra and Schuitemaker, 1999). It was also shown that Vpr associates with the nuclear envelope and even more specifically with nucleoporins (Vodicka et al., 1998). Next to this, HIV-1 replication is inhibited by addition of a Nup98 inhibitor or RNAi-mediated knockdown of Nup98 (Ebina et al., 2004).

These interactions seem to indicate that Vpr is involved in docking of the PIC to the NPC. Next to interactions with the NPC, Vpr was shown to interact with importin α (Vodicka et al., 1998). Given that importin α also binds other components of the PIC such as integrase or matrix, it was suggested that Vpr acts like an importin β-like protein (Vodicka et al., 1998). In this hypothesis, importin α binds to the preintegration complex through interaction with integrase or matrix, while Vpr binds to importin α and docks the preintegration complex to the nuclear envelope (Vodicka et al., 1998). A second theory suggests that Vpr facilitates nuclear import by stabilizing the interactions of matrix or integrase with the nuclear import machinery (Popov et al., 1998).

In the complex mechanism of nuclear import it seems that another viral component is involved: the central DNA flap. Mutations in this sequence showed controversial results: some groups found replication defect of HIV-1 virus in different cell lines (Arhel et al., 2006b; Charneau et al., 1992; Charneau et al., 1994; Zennou et al., 2000), others reported only a delay in the viral replication and some others showed even no effect (Dvorin et al., 2002; Hungnes et al., 1992; Limon et al., 2002b). Recently, it was demonstrated unambiguously that the DNA flap stimulates HIV replication in a dose-dependent manner (De Rijck and Debyser, 2006). At the lowest virus dose used, the absence of the DNA flap resulted in a 100-fold defect in viral replication in various cell lines and in PBMC. This dose-dependent effect might explain part of the existing controversy. At high doses of virus, the impact of the DNA flap is subtler. The replication defect was pinpointed to a step between reverse transcription and integration. Apparently, the DNA flap can overcome a rate limiting

step that can be bypassed using a high MOI (De Rijck and Debyser, 2006; De Rijck et al., 2007).

Several groups showed, as mentioned before, no replication defect in presence of both matrix and Vpr mutants (Gallay et al., 1997). These data were explained by postulating a bipartite NLS (NLSP 186–189 and NLSD 211–219) in integrase. This bipartite NLS was shown to interact with importin α and NLS mutations inhibited this interaction. Moreover, an HIV-1 strain mutated in both NLSs was replication-defective even in the presence of functional Vpr and matrix. However, the effect of NLSP and NLSD on nuclear localization of integrase was confirmed by some groups (Ao et al., 2005; Petit et al., 2000), but not by others (Depienne et al., 2001; Lu et al., 2004; Tsurutani et al., 2000). A more recent *in vitro* study showed that integrase mediates the import of viral DNA into the nucleus using the Impα/β pathway, suggesting the potential for IN to fulfill such a role *in vivo* (Hearps and Jans, 2006).

HIV-1 viral components, however, are not the only ones that putatively take part in the PICs nuclear import. Indeed, there is growing body of evidence for the involvement of cellular proteins. The hypothesis that LEDGF/p75 is involved in the nuclear import arises from the requirement of this cellular co-factor to relocalize transfected viral IN from the cytoplasm to the nucleus (Llano et al., 2004; Maertens et al., 2003; Vanegas et al., 2005). However, a direct effect of the nuclear translocation on PICs has not been observed (De Rijck et al., 2006; Emiliani et al., 2005; Vandekerckhove et al., 2006). It has been showed that the interaction between IN and LEDGF/p75 already occurs in the cytoplasm within the PICs (Llano et al., 2004) and might increase the affinity of IN for DNA (Busschots et al., 2005) or stabilize the whole pre-integration complex. In this case, LEDGF/p75 could indirectly influence the nuclear import of PICs.

Recently another cellular co-factor has been shown to be one of the key actors of HIV-1 PICs nuclear import: transportin-SR (TRN-SR, TNPO3) (Brass et al., 2008; Christ et al., 2008). This factor was initially reported to play a role in HIV-1 replication (Brass et al., 2008) and subsequently to promote PICs nuclear import through its interaction with IN (Christ et al., 2008). TNPO3 has been identified

independently by two different approaches: (I) a large-scale siRNA screen (Brass et al., 2008) and (II) yeast-two-hybrid screen. TNPO3 (Lai et al., 2000) was initially described as the human homolog of the yeast nuclear import factor Mtr10. TNOP3 is a karyopherin, which import multiple proteins into the nucleus, including histone mRNA stem-loop binding protein, serine/arginines-rich proteins that regulate splicing of mRNA. The recognition of the SR-proteins by TRN-SR relies on the conserved SR-domain and requires phosphorylation (Kataoka et al., 1999; Lai et al., 2000; Lai et al., 2001). The gene *tnpo3* encodes two isoforms via alternative splicing: TRN-SR1 and TRN-SR2 (Yun et al., 2003). In most tissues and in all cell lines only TRN-SR2 is expressed, whereas the TRN-SR1 isoform is undetectable (Yun et al., 2003). Christ *et al*. showed that TRN-SR2 interacts with IN and the relevance in HIV-1 replication has been demonstrated by using iRNA (Christ et al., 2008). In fact, the depletion of TRN-SR2 severely affects HIV-1 replication in HeLaP4 cells and in primary macrophages (Christ et al., 2008). In addition, they showed that TNPO3 mediates the translocation of PICs in the nuclear compartment (Christ et al., 2008). One of the most used nuclear import assay is an *in vitro* transport system, in which recombinant transport factors and their potential cargos are added to digitonin-permeabilized cells (Liu et al., 1999b). However, this import assay lacks the use of intact cells and intact nuclei. To overcome this problem, nuclear import was studied upon infection of intact living cells with fluorescently labeled HIV-1 virions (Albanese et al., 2008). Data obtained with such novel approach showed a decreased PIC nuclear import by more than 5-fold in TRN-SR2 knockdown cells, showing that TNPO3 is indeed the cellular import factor of HIV-1 (Christ et al., 2008).

FLUOROPHORES AND THEIR APPLICATION

In the past years many different aspects of life science have been extensively studied using a wide array of molecular biology, genetic, biochemistry, bioinformatic and structural biology approaches. However, in order to identify the subcellular compartments and the timing in which different molecules are localized and/or interact with each other is critical to directly visualize all these components. Two things are requested to reach such purpose: (I) to label proteins and cellular

structures by fluorescence and (II) to observe the fluorescent signal coming from these microscopic structures with the microscope. This approach was made possible by the use of fluorescent proteins, such as green fluorescent protein (GFP) (Chalfie et al., 1994; Crameri et al., 1996; Pines, 1995; Prasher, 1995), and the introduction of confocal microscopy (Minsky, 1988; Wilson and Carlini, 1988).

Fluorescence microscopy allows the examination of all biological specimens, fixed or alive, because it allows the selective and specific detection of molecules at small concentrations with good signal-to-background ratio. At the same time, although traditional fluorescence microscopy affords excellent detection of fluorophores in thin samples, when applied to thick or living samples, it has always been hampered by the fact that the entire sample is excited indiscriminately and therefore most of the fluorescent photons arise from out-of-focus fluorophores. Confocal scanning microscopy, developed in the last several decades, solved this problem by restricting photodetection to light originating from the focal point. Thus, optical sectioning became possible and afforded three-dimensional microscopic reconstruction of biological specimens, as it will be described later (Yuste, 2005). Thanks to fluorescent microscopy, and in particular to confocal microscopy, it is possible to visualize viral proteins tagged to fluorescent proteins, and observe their behavior in the cell, with respect to some specific structures.

Fluorescent Proteins

The first fluorescent protein that has been discovered is GFP. It has been discovered by Shimomura *et al*. (Shimomura et al., 1962) as a companion protein to aequorin, the famous chemiluminescent protein from *Aequorea victoria* jellyfish. The peculiarity and the potential of GFP is, indeed, its fluorescence. The GFP from *A. victoria* has a major excitation peak at a wavelength of 395 nm and a minor one at 475 nm, while the emission peak is, as suggested by its name, in the green portion of the visible spectrum, at 509 nm.

Figure 1-29. Ribbon representation of the structure of GFP, showing 11 β-strands forming a hollow cylinder through which is threaded a helix bearing the chromophore, shown in ball-and-stick representation.

Although GFP was first crystallized in 1974 and diffraction patterns reported in 1988, the structure was

first solved in 1996 by two groups: Ormö *et al.* (Ormo et al., 1996) (Protein Data Bank accession number 1EMA), and by Yang *et al.* (Yang et al., 1996) (accession number 1GFL). GFP consists of 238 amino acids organized in an 11-stranded β-barrel threaded by an α-helix running up the axis of the cylinder.

Fluorescence property of GFP is given by a functional group known as *chromophore*. It absorbs energy of a specific wavelength (excitation) and emits energy at a longer wavelength (emission). The chromophore of GFP is attached to the α-helix and is buried almost perfectly in the center of the cylinder, which has been called a β-can. The chromophore is a p-hydroxybenzylideneimidazolinone (Cody et al., 1993; Prasher et al., 1992) formed from residues 65–67, which are Ser-Tyr-Gly in the native protein. According to the currently accepted mechanism (Cubitt et al., 1995; Heim et al., 1994; Inouye and Tsuji, 1994) for chromophore formation, first GFP folds into a nearly native conformation, then the imidazolinone is formed by nucleophilic attack of the amide of Gly 67 on the carbonyl of residue 65, followed by dehydration. Finally, molecular oxygen dehydrogenates the α-β bond of residue 66 to put its aromatic group into conjugation with the imidazolinone. Only at this stage does the chromophore acquire visible absorbance and fluorescence (Tsien, 1998).

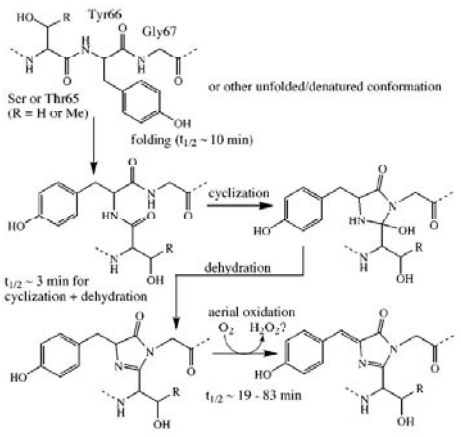

Figure 1-30. Mechanism proposed by Cubitt *et al.* (Cubitt et al., 1995) for the intramolecular biosynthesis of the GFP chromophore, with rate constants estimated for the Ser65→Thr mutant by Reid & Flynn (Reid and Flynn, 1997) and Heim *et al.* (Heim et al., 1994). (Tsien, 1998).

The fluorescent property of GFP has been widely and deeply exploited in biology. Indeed, this protein is a fluorescent dye that is gene encoded. Therefore, by using standard molecular biology techniques, it is possible to express it in any cell type as reporter. In addition, GFP can be fused to another protein of interest and see at the fluorescent microscope its localization in the cell, its mobility, and its interaction with other proteins (Chalfie et al., 1994; Pines, 1995; Prasher, 1995). However,

while GFP from *A. victoria* folds fairly efficiently when expressed at or below room temperature, its folding efficiency declines steeply at higher temperatures. This is not desirable for biology applications, where all enzymatic reactions work well at 37°C. Therefore a GFP mutant able to fold efficiently at 37°C was widely desired. The most extensive attempt to develop such a mutant while preserving the complex wild-type spectrum utilized DNA shuffling (Crameri et al., 1996), a technique for recombining various mutations while creating new ones. This approach produced a triple mutant, F99S, M153T, V163A, which improved 37°C-folding, reduced aggregation at high concentrations, and increased the diffusibility of the protein inside cells (Tsien, 1998).

Many other mutations have been made, including improvement in the spectral characteristics of GFP and color mutants. Indeed, to date it is possible to choose among variants that differ in their excitation/emission spectra: BFP, ECFP, Cerulean, EGFP, EYFP, Venus, mCitrine, mOrange, DsRed, mRFP, mCherry, tdTomato, mStrawberry, mPlum (Shaner et al., 2007; Shaner et al., 2005). So, the vast range of fluorescent protein variants developed over the past years feature fluorescence emission profiles spanning almost the entire visible light spectrum, giving the opportunity to express in the cell more than one fused protein and see how these proteins interact among them or with cell structures.

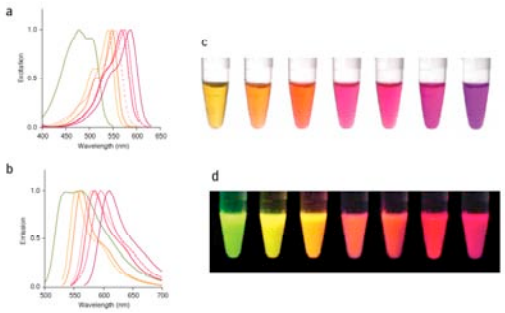

Figure 1-31. Excitation and emission spectra for new RFP variants. Spectra are normalized to the excitation and emission peak for each protein. (a,b) Excitation (a) and emission (b) curves are shown as solid or dashed lines for monomeric variants and as a dotted line for dTomato and tdTomato, with colors corresponding to the color of each variant. (c,d) Purified proteins (from left to right, mHoneydew, mBanana, mOrange, tdTomato, mTangerine, mStrawberry, and mCherry) are shown in visible light (c) and fluorescence (d). The fluorescence image is a composite of several images with excitation ranging from 480 nm to 560 nm. (Shaner et al., 2004).

Confocal microscope

A confocal microscope creates sharp images of a specimen that would otherwise appear blurred when viewed with a fluorescent microscope. This is achieved by

excluding most of the light from the specimen that is not from the microscope's focal plane. Therefore, the image has less haze and better contrast than that of a wide-field fluorescent microscope and represents a thin cross-section of the specimen. Thus, apart from allowing better observation of fine details it is possible to reconstruct 3D images of the specimen.

The first example of confocal microscopy as been set up by Marvin Minsky in 1955 (Minsky, 1988; Semwogerere and Week, 2005). His invention would perform a point-by-point image construction by focusing a point of light sequentially across a specimen and then collecting some of the returning rays. By illuminating a single point at a time Minsky avoided most of the unwanted scatter light that obscures an image when the entire specimen is illuminated at the same time. Additionally the light returning from the specimen would pass through a second pinhole aperture that would reject rays that were not directly from the focal point. The remaining "desirable" light rays would then be collected by a photomultiplier and the image gradually reconstructed using a long-persistence screen. Modern confocal microscopes have kept the key elements of Minsky's design: the pinhole apertures and point-by-point illumination of the specimen. Advances in optics and electronics have been incorporated into the current designs and provide improvements in speed, image quality, and storage of the generated images.

In the modern laser scanning confocal microscope, the light exciting the fluorophore comes from a laser light source. The advantages to use this light source are: high intensity, point-by-point illumination, and a wide range of wavelength available. The laser beam passes through a light source aperture and is reflected by a dichroic mirror that directs the laser to the objective lens, which, in turn, focuses the light source into a small focal volume. However, since the laser beam generates a point-by-point illumination a scanning of the light source is necessary to excite point-by-point an area of the specimen to generate an image. Therefore, between the dichroic mirror and the objective lens there is an assembly of vertically and horizontally scanning mirrors. These motor-driven mirrors scan the laser across the specimen. When light is incident on a fluorescent molecule or on the chromophore of a fluorescent protein, it absorbs a photon of light that increases its energy causing an

electron to jump to a discrete singlet excited state. Typically, the molecule quickly (within 10^{-8} sec) dissipates some of the absorbed energy through collisions with surrounding molecules causing the electron to drop to a lower energy level. If the surrounding molecules are not able to accept the larger energy difference needed to further lower the molecule to its ground state, it may undergo spontaneous emission, thereby losing the remaining energy, by emitting light of a longer wavelength (for example, green light in the case of GFP). The light emitted by the fluorescent molecules of the sample is descanned by the same mirrors that are used to scan the exciting light from the laser and then passes through the dichroic mirror without being reflected. Thereafter, it is focused onto the pinhole. The light that makes it through the pinhole is measured by a detector such a photomultiplier tube. In confocal microscopy, there is never a complete image of the specimen because at any instant only one point is observed. Thus, for visualization the detector is attached to a computer, which builds up the image one pixel at a time. The image created by the confocal microscope is of a thin planar region of the specimen, an effect referred to as optical sectioning. Out-of-plane unfocused light has been rejected, resulting in a sharper, better-resolved image. The ability of a confocal microscope to create sharp optical sections allows the 3D image reconstruction of the specimen. Data gathered from a series of optical sections imaged at short and regular intervals along the optical axis are used to create the 3D reconstruction (Semwogerere and Week, 2005).

Fluorescent viruses

In a typical viral replication cycle, virus binds to the cell surface, enters the cell and the viral genome is transported to specific sites in the cytoplasm or in the nucleus, depending on the viral species. Newly synthesized viral proteins and genetic material are subsequently transported to specific sites for assembly into progeny viruses. All these viral steps have been extensively investigated with molecular biology, bioinformatic, structural biology and biochemical studies, leading to the actual knowledge on the viral replication cycles. The recent use of fluorescent probes together with the confocal microscope opened new perspectives in studying virus-host interaction, complementing previous studies. In fact, such approach

allows to directly visualize single viral particles, enabling researcher to follow virions within intact living cells and to probe the dynamic interactions between these virions and the cellular machinery. In the last decade there was an increasing and exponential interest in this field, therefore many authors exploited this approach with different viruses to answer many unsolved issues (Arhel et al., 2006a; Brandenburg and Zhuang, 2007; Campbell et al., 2007b; Damm et al., 2005; del Rio et al., 2005b; Jouvenet et al., 2008; Lakadamyali et al., 2003; Lampe et al., 2007; Lehmann et al., 2005; McDonald et al., 2002; McDonald et al., 2003; Muller et al., 2004; Nicola and Straus, 2004; Rudner et al., 2005; Rust et al., 2004).

The first step towards single-virus tracking is labeling the viral components and relevant cellular structures. A crucial requirement is that both viruses and cellular structures need to be labeled with a sufficient number of fluorophores for detection at the single particle level without inhibiting viral infectivity and cell functions. The external components of a virus, such as the capsid of a non-enveloped virus or the membrane of an enveloped virus, can be readily labeled with chemical fluorescent dyes, such as cynine or Alexa dyes (Lakadamyali et al., 2003; Pelkmans et al., 2001; Seisenberger et al., 2001; Suomalainen et al., 1999). Tracking virions labeled in this manner can provide important insights into the uncoating or cellular trafficking mechanisms of viruses. On the contrary, internal components of assembled viral particles are typically inaccessible to chemical dyes. Therefore, viral proteins within the virions are labeled with fluorescent proteins, so as that the resulting fusion protein is incorporated in the viral particle during the assembly in the producer cells (Campbell et al., 2007b; Lampe et al., 2007; McDonald et al., 2002; Muller et al., 2004). These can be even used to label endogenous cellular proteins, facilitating the study of virus-cell interactions.

Labeled viruses are then visualized in the cells using one of the following fluorescence microscopy set-up: (I) epifluorescence microscopy, that is often the method of choice for studies on long-range viral trafficking or transport, (II) confocal microscopy, and (III) total internal reflection fluorescence (TIRF) microscopy, whose excitation depth is of 100-200 nm. Therefore, this technique is

used to monitor events occurring near the cell surface, such as entry or budding of viral particles.

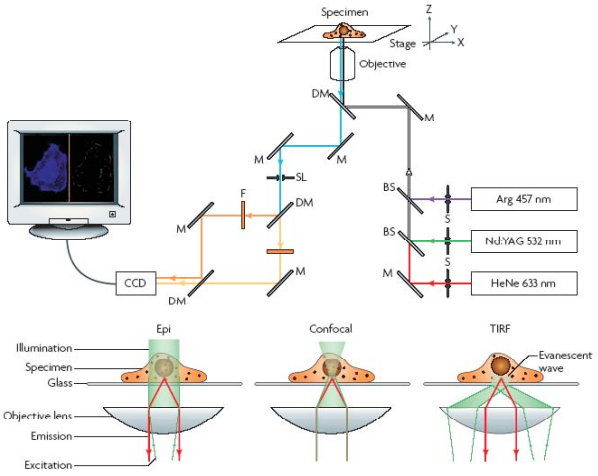

Figure 1-32. A typical single-virus tracking setup includes an inverted microscope with a temperature controlled stage, several lasers, optics and a sensitive detector. The figure shows the microscope setup. Various laser lines, such as Argon ion (Arg; 457 nm, 488 nm and 514 nm), Krypton ion (647 nm; not shown), helium-neon (HeNe; 543 nm, 594 nm and 633 nm) and Nd:YAG (532 nm) lasers, can function as light sources to excite different fluorophores. Multicolour imaging is enabled by a combination of several different laser lines with specific excitation and detection optics that allow different coloured excitation to be combined at the sample, and different coloured fluorescence emissions to be separately detected. The lower part of the figure shows imaging geometries. In the epi-fluorescence geometry (left panel), a collimated light beam illuminates a large sample area (~ 100 μm in linear dimension) (Stephens and Allan, 2003). Fluorescence emission from the sample is collected by a high numerical aperture objective and detected by a CCD camera. The advantages of this scheme are the low signal loss, rapid wide-field detection and large excitation depth, which allow single particles to be tracked in a large sample volume. The disadvantage is its poor rejection of the fluorescence background signal from the cell. Confocal microscopy (middle panel) uses a focused light beam and spatial filtering techniques (pinholes in excitation and detection paths) to eliminate out-of-focus background fluorescence, but at the cost of signal reduction (Amos and White, 2003). For the observation of fast dynamics in live cells, a spinning disk confocal setup is often preferred over the relatively slow scanning confocal microscope, which relies on rotating mirrors to scan a focused laser beam in the imaging plane and a point detector, such as avalanche photodiode or photomultiplier tubes, for signal acquisition (Stephens and Allan, 2003). The spinning disk confocal microscope relies on a pair of rapidly rotating discs, one with an array of pinholes and the other with correspondingly aligned micro-lenses. Thereby the excitation light is subdivided into thousands of beams, which simultaneously scan the entire field at a rate of >1000 frames per second. This scheme effectively creates a wide-field image detected by a CCD camera. When combined with Z-direction scanning of the sample stage, both confocal schemes allow the construction of 3-dimensional images. In a TIRF microscope (right panel), the incident light strikes the interface between two optical media of different refractive indices (for example, a glass substrate and a cell) at a sufficiently large angle to induce total reflection (Axelrod, 2001). As a result, an evanescent excitation field is generated, extending only a few hundred nanometers into the second medium. This wide-field imaging geometry offers the best rejection of background signal, but can only be used to detect events occurring close to the adhering surface of the cell. In order to simultaneously track a large number viruses, a camera chip with a high number of pixels is needed, which allows a large field of view. BS, beam splitter; CCD, charge-coupled device; DM, dichroic mirrors; F, filter; M, mirrors; SL, optical slits to control image size; S, shutters; TIRF, total internal reflection fluorescence. (Brandenburg and Zhuang, 2007).

Due to the limiting size of the virus (the smallest virus has a diameter of only 20-30 nm), restricted number of fluorescent probes that can be attached to each single viral particle, in order to avoid impairment of viral infectivity. For example, whereas hundreds to thousands of dye molecules can be attached to a relatively large influenza virion without affecting its infectivity (Lakadamyali et al., 2003), only 30-50 dye molecules can be attached to a polio capsid owing to its small size (Brandenburg and Zhuang, 2007) and attaching more than a few dye molecules to the capsid of adeno-associated virus, renders the virus non-infectious (Seisenberger et al., 2001).

Imaging viral entry

Viruses exploit specific receptors on the cell surface to identify and infect target cells. However, these receptors are often rare or distributed in regions that are not readily accessible to incoming virions. Therefore, many viruses first bind to relatively non-specific attachment factors, such as carbohydrates, and migrate along the cell surface to locate specific receptors (Marsh and Helenius, 2006). Specific virus–receptor interactions activate signaling cascades, guide the virus into endocytic pathways and/or trigger conformational changes in the virus envelope or capsid proteins for genome release (Marsh and Helenius, 2006). Single-virus tracking offers an ideal method for the visualization of virus movement. Multicolor live-cell imaging that allows tracking of single-virus particles together with fluorescent-protein labeled cellular structures provides a powerful tool for studying viral entry mechanisms. Using this approach, even transient interactions between viruses and cellular proteins can be detected. Multicolour labelling of distinct virus components also allows viral disassembly during entry to be monitored. Such dynamic information is crucial for a more complete understanding of viral entry mechanisms.

Several viruses, such as murine leukaemia virus, Avian leukosis virus and vesicular stomatitis virus (VSV) use the cortical actin cytoskeleton, together with myosin II, for directed movement along microvilli or filopodia, surfing towards the cell body before entry (Lehmann et al., 2005). Differently, murine polyoma virus-like particles have distinct modes of movement on the cell surface: an initial phase of free

diffusion is followed by actin-dependent confined movement in small domains (Ewers et al., 2005). Together, these imaging experiments show that viral attachment is followed by organized transport on the cell surface, probably to locate specific receptors or special active zones that are efficient in virus uptake. These data reveal a crucial role for fluorescent viruses in the study of viral entry.

Multicolor live-cell imaging provides additional information on the interactions between virus and cellular structures, further elucidating viral-entry mechanisms. Using this approach, single Simian virus 40 (SV40) particles were simultaneously tracked with GFP-tagged caveolae. These experiments revealed the dynamic SV40 entry process and a new endocytic organelle, the caveosome (Pelkmans et al., 2004; Pelkmans et al., 2001; Tagawa et al., 2005). The majority of SV40 viral particles colocalize with caveolae, activating tyrosin kinases and inducing rearrangement of actin stress fibers to form actin tails on virus-loaded caveolae (Pelkmans et al., 2002). After a dynamin-dependent pinching process, the SV40-loaded caveolae leaves the plasma membrane and enters the caveosome before finally reaching the ER through microtubule-dependent transport. Polyoma virus and echovirus 1 also enter cells through a similar pathway to SV40 (Elphick et al., 2004; Pietiainen et al., 2004; Upla et al., 2004).

Fluorescently labeled influenza virus showed to use a distinct entry mechanism (Matlin et al., 1981; Rust et al., 2004; Sieczkarski and Whittaker, 2002). As directly visualized in a viral tracking experiment, influenza viruses can simultaneously use two pathways to enter cells (Rust et al., 2004): most viral particles are internalized through clathrin-mediated endocytosis by promoting the de novo formation of clathrin-coated pits (CCPs) at the viral binding site; the remaining virions enter cells through a clathrin- and caveolin-independent pathway. After entry by these pathways the virus particles have similar post-endocytic trafficking behaviour, which leads to viral fusion with similar efficiencies. Live imaging of cells infected with fluorescently labeled influenza virus revealed that viral particles are preferentially delivered, by microtubule-dependent transport, to the dynamic early endosomes (Lakadamyali et al., 2006).

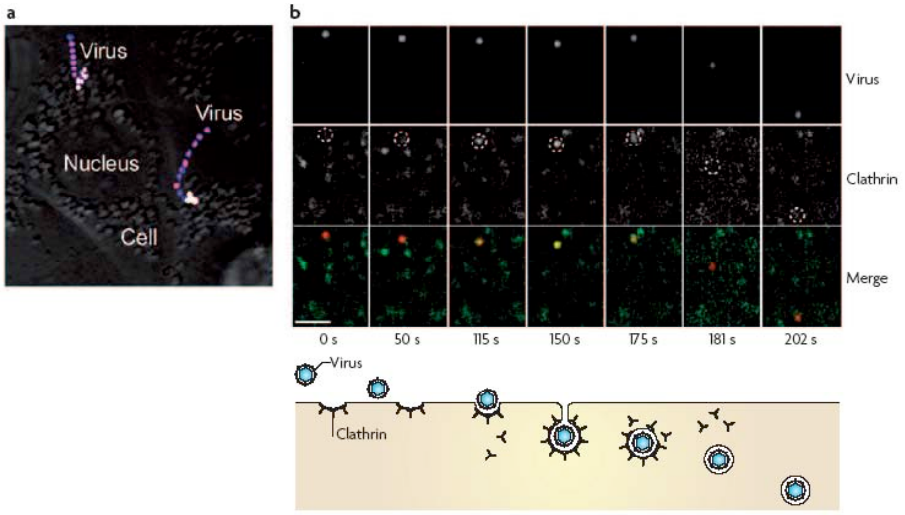

Figure 1-33. Time-lapse images of influenza viruses in live cells. (a) Stacked, time-lapse images of influenza viruses in living cells, revealing actin and microtubule-dependent transport. The virus is labelled with the lipophilic dye, DiD. The sudden colour change from blue/pink to yellow/white indicates a dramatic increase in the fluorescence signal of DiD, indicating the fusion of the virus with an endosome. (b) Simultaneous images of a DiD-labelled virus (upper panels and red in lower panels) and fluorescent protein-labelled clathrin (middle panels and green in lower panels) in a cell show the internalization of the virus by a clathrin-coated vesicle. The centres of dotted circles in the middle panels indicate the virus positions. Overlay of green and red signals appears yellow. The time (in seconds) after viral attachment and different stages of viral entry are shown below the images.

Other fluorescent viruses have also been observed to colocalize with CCPs in live cells, including reovirus and adenovirus (Ehrlich et al., 2004; Meier et al., 2002). In common with influenza, reovirus enters by the *de novo* formation of CCPs (Ehrlich et al., 2004). Experiments tracking reoviruses, transferrin, LDL and labelled CCPs revealed a random initiation behaviour of coated pits, which are only stabilized after cargo binding (Ehrlich et al., 2004).

Besides clathrin- or caveolin-mediated endocytosis, various viruses, including polyoma virus and herpes simplex virus (HSV) (Damm et al., 2005; Liebl et al., 2006; Nicola and Straus, 2004), exploit other clathrin- and caveolin-independent entry pathways.

As shown by these examples, the ability to monitor time-dependent behaviour of individual viral particles and to probe dynamic interactions between viral and cellular structures has revealed its relevance in understanding the mechanisms of

viral entry. These studies have showed to be helpul in unravelling previously unknown virus–cell interactions that are crucial for infection.

Following viral cytoplasmic trafficking

After uncoating, the viral contents need to be transported to proper sites for replication. Objects larger than 20 nm (or significantly heavier than 500 kDa), such as viruses, cannot freely diffuse through the crowded cytoplasm (Luby-Phelps, 2000). Therefore, to reach the site of replication viruses have successfully hijacked cellular transport systems, such as microtubule and actin filaments.

As shown with different single-virus trajectories, many viruses are transported by minus and plus end-directed motor proteins along microtubules towards the microtubule organizing centre (MTOC), either by directly interacting with molecular motors or through inclusion in a motor-interacting vesicle. This was observed for reovirus, adenovirus, HSV and influenza virus (Dohner et al., 2002; Georgi et al., 1990; Lakadamyali et al., 2003; Suomalainen et al., 1999). Cytoplasmic trafficking of viral particles is often highly regulated as with, for example, HSV in neurons. After fusion of incoming virions with the plasma membrane, HSV capsids are transported towards the minus end of microtubules by dynein and its cofactor dynactin (Dohner et al., 2002). In the axons of sensory neurons, incoming HSV

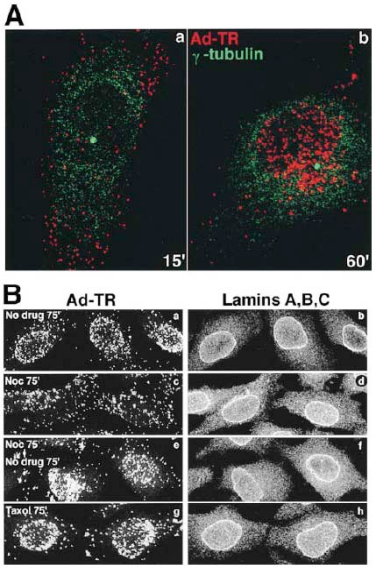

Figure 1-34. Microtubule-dependent transport of Ad2 to the MTOC/nuclear envelope. (A) TR-labeled Ad2 was bound to HeLa cells in the cold and internalized for 15 (panel a) or 60 min (panel b). Cells were labeled for γ-tubulin and analyzed by confocal laser scanning microscopy (shown are the sections that contained the perinuclear punctate g-tubulin signal only). Virus particles (red) and g-tubulin (green) are pseudocolored. (B) TR-labeled Ad2 was bound to HeLa cells in the cold in the absence (panels a and b) or presence of either 20 mM nocodazole (panels c-f) or 25 nM taxol (panels g and h). Drug treatment included a 30-min preincubation with drugs before virus binding. Cells were warmed to 378C in the presence or absence of drugs for 75 min (panels a-d, and h) or treated with nocodazole for the same time followed by an incubation without drug for 75 min (panels e and f). Cells were fixed in PFA and stained for lamins A, -B, and –C using anti-rabbit FITC and analyzed by confocal microscopy for TR and FITC fluorescence. Complete stacks of optical sections are shown. (Suomalainen et al., 1999)

capsids are moved by retrograde transport, whereas newly assembled capsids undergo bidirectional and saltatory motions, indicating a modulation of the plus-end directed motility (Smith et al., 2004).

The mechanisms by which capsids are transported to the nuclear pore complex for the import of viral genomes are less well known. Capsids might be transported by kinesin from the MTOC towards the nuclear pore complex and nuclear import factors might be involved in the unloading of capsids from microtubules that are proximal to the nucleus (Strunze et al., 2005). The direct tracking of an incoming viral genome in live cells has been challenging due to difficulties encountered in generating infectious virions harbouring labelled viral DNA or RNA. Tracking microinjected viral ribonucleoprotein (vRNP) particles from influenza showed diffusion as the predominant mechanism for the transport of vRNPs both towards the nuclear pore complexes and inside the nucleus (Babcock et al., 2004).

Visualizing viral assembly

A successful viral infection is ultimately marked by the assembly and release of progeny virus particles. After genome replication and protein synthesis, the subviral components are transported to the assembly site and progeny virions leave the cell by directly budding from the plasma membrane, controlled exocytosis or lysis of the cell. Labelling viral structural components with fluorescent proteins allows the assembly of individual virions to be monitored, and shows the location and kinetics of assembly as well as the exit mechanisms of matured viruses.

A series of imaging experiments by time-lapse microscopy revealed the exit mode of vaccinia virus (Greber and Way, 2006). Intracellular enveloped vaccinia virus particles move from their perinuclear assembly site to the plasma membrane along microtubules (Herrero-Martinez et al., 2005; Hollinshead et al., 2001; Rietdorf et al., 2001; Ward, 2005; Ward and Moss, 2001a; Ward and Moss, 2001b) These particles fuse with the plasma membrane, but remain attached as cell-associated enveloped virus (CEV) (Smith et al., 2003). It was recently discovered that African swine fever virus also shows a microtubule-dependent movement towards the plasma membrane, followed by actin polymerization that propels the virus away from the cell (Jouvenet et al., 2004; Jouvenet et al., 2006).

Compared with imaging the entry and transport of single virions, which typically involves labelling incoming viruses and therefore does not suffer from strong background cell fluorescence, it is more challenging to probe the assembly and egress of viruses at the single particle level. The background fluorescence from newly synthesized viral components makes it extremely difficult to monitor early assembly steps, while determining the distribution of viral proteins in living cells is currently more tractable. For example, the bluetongue virus core protein VP3 has highly distinct cellular distributions in the presence and absence of other viral proteins (VP7 and NS2) that are related to assembly (Kar et al., 2005). After initial stages of assembly, which accumulate sufficient proteins to form a virion, the signal might become sufficiently large to allow viral egress to be tracked at the single-virion level. Experiments with labelled pseudorabies virus tegument and capsid proteins demonstrate viral assembly in the cell body before entering the axon of cultured neurons (del Rio et al., 2005a), while the association of human cytomegalovirus tegument and capsid proteins occurs inside nuclear inclusions (Sampaio et al., 2005).

Fluorescent HIV-1 viruses

In the last 25 years since the discovery of HIV-1, the development of new techniques and technologies based on fluorescent probes and microscopy also allowed to visualize the trafficking of HIV-1 viral particles and proteins in their natural context of living cells, greatly increasing our knowledge throughout the different stages of viral life cycle.

Imaging HIV-1 entry

The ability to fluorescently label membranes of individual virions has offered the opportunity to monitor the process of fusion occurring between individual virions and target cells in real time. This method relies on the possibility to observe the mixing of target cell and fluorescently labeled viral membranes. This technique has been used by Markosyan and colleagues to analyze the events occurring during fusion mediated by HIV-1 envelope (Markosyan et al., 2005). They used both a fluorescent lipid dye (DiD) to label the viral membrane and a fluorescent nucleocapsid-GFP protein that freely diffuses away from virions after the

permeabilization of virions or effective mixing of viral and cytoplasmic compartments (Markosyan et al., 2005). This experimental set up allowed to quantitatively analyze lipid mixing of membrane components from the formation of a fusion pore large enough to allow mixing of cytoplasm and viral contents. They showed that hemifusion (the mixing of membrane contents) occurred more rapidly and before the nucleocapsid-GFP protein entered the target cell, demonstrating that fusion pore formation is a multistep process occurring during HIV-1 envelope fusion (Markosyan et al., 2005).

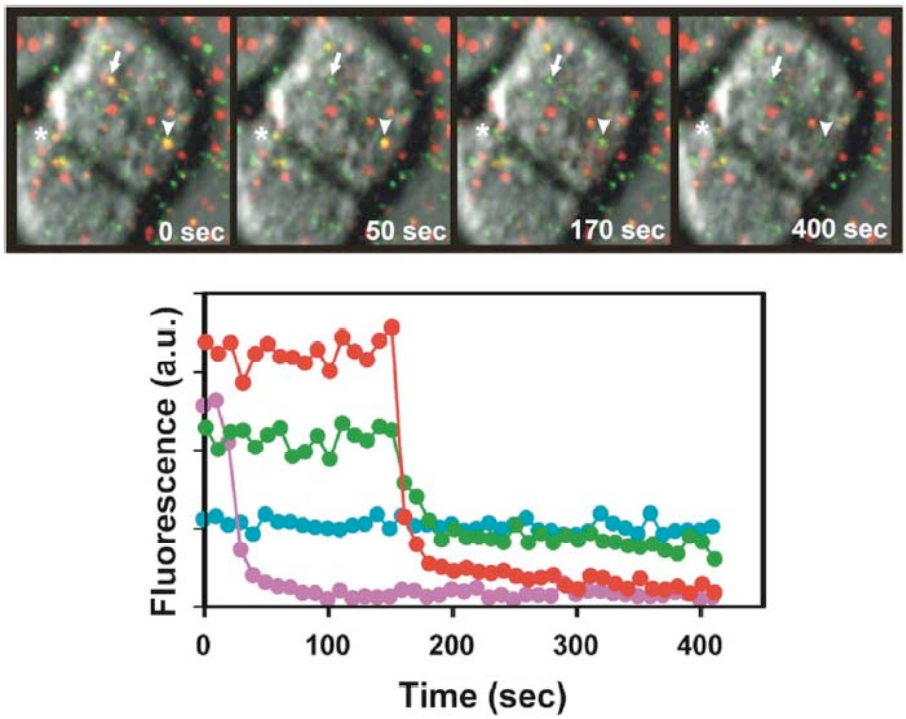

Figure 1-35. Imaging and analysis of individual virus-cell fusion events. Top panel, virions colabeled with NC-GFP and DiD are colored yellow, and those that do not contain DiD are green; DiD-only labeled vesicles are red. The first image (time 0) shows a U87 cell adhered to virions immobilized on a coverslip. Fusion was triggered immediately after the first frame by a temperature-jump to 37°C. The virus marked by arrowhead transferred its lipid and content into the target cell (third and fourth frames, respectively). Two viral particles that exhibited only DiD mixing activity are marked by arrow and an asterisk. Bottom panel, the DiD (red circles) and NC-GFP (green circles) fluorescence signals of the fusing virus (top panel, arrowhead) as a function of time at 37°C. The fluorescence traces for the virus marked by arrow are shown in magenta (DiD) and dark cyan (NC-GFP). (Markosyan et al., 2005).

The development of a dually labeled HIV-1 allowed discriminating virions that have productively entered the target cell via fusion from those virions that have been nonspecifically endocytosed and remain within the endosomal compartment (Campbell et al., 2007b). Campbell *et al*. labeled the HIV-1 viral core by incorporating EGFP fused to Vpr within the virions (Campbell et al., 2007b). In addition, they labeled the envelope of the viral particles with mCherry fluorescent protein fused to the N-terminal 15 aminoacid sequence of c-Src (S15) (Campbell et al., 2007b). This short tag specifically targets the fluorescent protein to the plasma membrane, generating a cell with a labeled membrane. Therefore, exploiting these cells to produce EGFP-Vpr labeled virions, they generated HIV-1 particles dually labeled. Following infection, S-15 mCherry fluorescent signal is lost as a consequence of membrane fusion, and EGFP-Vpr viral particles are visualized in the cytoplasm (Campbell et al., 2007b). The ability to separate these two viral populations allows a more careful analysis and quantification of those virions that have actively undergone postentry steps during infection (Campbell et al., 2008; Campbell et al., 2007b; Yamashita et al., 2007).

Following HIV-1 cytoplasmic trafficking

The observation of individual virions in target cells has provided critical insight into the biology of HIV-1 infection. The EGFP-Vpr labeled virus (McDonald et al., 2002) was monitored in the cytoplasm of infected cells. The authors proved that the fluorescent signals indeed derive from HIV-1 complexes by (1) sedimentation of EGFP-Vpr with viral proteins, (2) co-immunostaining with $p24^{CA}$ and with $p17^{MA}$, (3) colocalization with virion membranes and (4) association with newly synthesized cDNA in infected cells (McDonald et al., 2002). Therefore, labeling individual virions with this protein allowed to visualize with fluorescence microscopy the cytoplasmic behavior of individual viral complexes in both live and fixed cells (McDonald et al., 2002). These studies have been performed by pseudotyping virions with the glycoprotein of vesicular stomatitis virus (VSV-g), in order to increase viral tropism. Live cell observation of viral trafficking demonstrated that virions can move in the cell at speeds consistent with microtubule-mediated movement in cells, resulting in the perinuclear accumulation of viral complexes (McDonald et al., 2002). This was confirmed by the microinjection of target cells

with fluorescently labeled tubulin, which allowed the trafficking of individual viral cores along microtubules to be visualized in living cells (McDonald et al., 2002). This trafficking required the minus-end microtubule motor dynein, as microinjection of target cells with antidynein antibodies prevented the perinuclear accumulation of viral complexes.

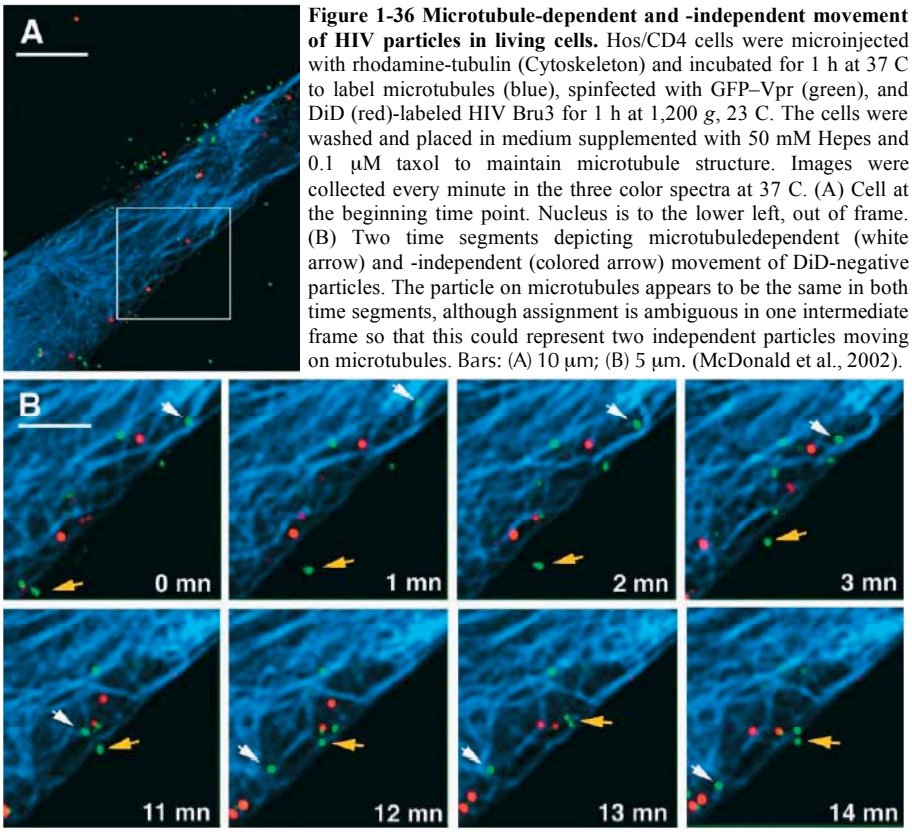

Figure 1-36 Microtubule-dependent and -independent movement of HIV particles in living cells. Hos/CD4 cells were microinjected with rhodamine-tubulin (Cytoskeleton) and incubated for 1 h at 37 C to label microtubules (blue), spinfected with GFP–Vpr (green), and DiD (red)-labeled HIV Bru3 for 1 h at 1,200 *g*, 23 C. The cells were washed and placed in medium supplemented with 50 mM Hepes and 0.1 μM taxol to maintain microtubule structure. Images were collected every minute in the three color spectra at 37 C. (A) Cell at the beginning time point. Nucleus is to the lower left, out of frame. (B) Two time segments depicting microtubuledependent (white arrow) and -independent (colored arrow) movement of DiD-negative particles. The particle on microtubules appears to be the same in both time segments, although assignment is ambiguous in one intermediate frame so that this could represent two independent particles moving on microtubules. Bars: (A) 10 μm; (B) 5 μm. (McDonald et al., 2002).

Recently, Arhel *et al*. developed an alternative method to visualize the trafficking of individual virions (Arhel et al., 2006a). They inserted a tetracystein motif into HIV-1 IN. This small tag, consisting in two pairs of cysteines held in a hairpin configuration (Cys-Cys-Pro-Gly-Cys-Cys), can specifically be bound and labeled by fluorescent biarsenical derivatives (Adams et al., 2002; Griffin et al., 1998). The advantage of this tag is to be relatively small with respect to EGFP, overcoming problems related to the steric hindrance of the fluorescent proteins which might lead to disruption of viral functions or marked loss of infectivity (Engelman et al., 1995;

Muller et al., 2004). Labeling is achieved with membrane-permeable biarsenical compounds that fluoresce in either green (FlAsH) or red (ReAsH) wavelenghts. The

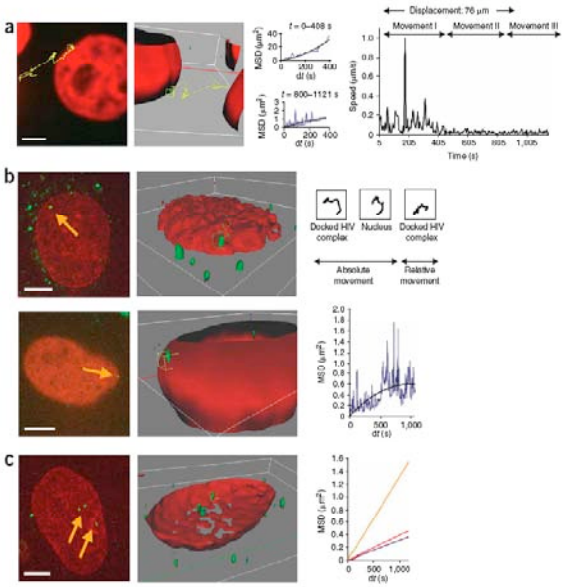

Figure 1-37. FlAsH labeling of HIV-1 integrase allows detection and characterization of HIV-1 complexes docked at the nuclear membrane and within the nuclear compartment. P4 cells were observed between 20 and 24 h after infection with FlAsHlabeled HIV$_{LAI}$(vsv)IN-C4 virus. Image stacks (z 1/4 0.8 mm) were acquired at 5-s intervals for a and b (bottom) and at 90-s intervals for b (top) and c for 21–32 min. All scale bars indicate 5 mm. (a) 4D tracking of an individual HIV-1 complex reveals passage from movement I (with peaks up to 1 mm/s) to II and finally to association with the nuclear membrane (movement III). MSD plots contrast initial directed movement (movement I; t 1/4 0–408 s) with restricted movement upon docking (movement III; t 1/4 800–1121 s). (b) Characterization of the movement of HIV-1 complexes at the nuclear membrane. Images show confocal slices and 3D surface reconstructions with individual docked HIV-1 complexes (arrows). As the nucleus moves over time, the relative movement of the docked complex was accurately calculated by subtracting the movement of the nucleus from that of the complex (top right panels). The MSD plot (bottom right) indicates confined movement within a volume of 0.7 mm average diameter. (c) Characterization of movement of HIV-1 complexes within the nucleoplasm of infected cells. Images show a confocal slice and 3D reconstruction with individual HIV-1 complexes within the nuclear compartment (arrows). Each line color refers to an individual intranuclear complex. MSD plots are linear in fit, indicating diffuse movement. (Arhel et al., 2006a).

primary disadvantage of this labeling technique is a relatively high degree of background signal detectable even in the absence of proteins carrying tetracystein motifs (Rudner et al., 2005). Arhel *et al*. overcome this obstacle by labeling the virus in the supernatant, prior infection, instead of at the intracellular level (Arhel et al., 2006a).

Using these integrase-labeled virions, they measured the trajectories obtained by these virions using live cell microscopy. They observed that virions exhibited rapid,

curvilinear, saltatory trafficking, indicative of microtubule-based movement, which resulted in the perinuclear accumulation of viral complexes (Arhel et al., 2006a). Arhel *et al*. could also visualize a decrease in the motility of viral complexes after their perinuclear deposition, which the authors suggest represent a docking interaction between the nuclear membrane and reverse transcription complex (Arhel et al., 2006a). In addition, they could detect the accumulation of these complexes within the nuclear compartment. They observed that, inside the nucleus, movement of the viral nucleoprotein complex becomes severely restricted, and they could occasionally observe the disappearance of their integrase-labeled signal, which could represent the occurrence of individual integration events during infection (Arhel et al., 2006a).

Another study labeled retrotranscribed viral DNA in order to visualize pre-integration complexes (Turelli et al., 2001). Turelli and co-workers took advantage of the fact that reverse transcription is initiated at the time of viral particle formation and can be promoted within purified virions by the addition of deoxynucleotides, divalent cations, and polyamines (Zhang et al., 1996). This reaction, commonly called natural endogenous reverse transcription (NERT), was performed with a mixture of nucleotides that included rhodamine-conjugated dUTPs (Turelli et al., 2001). To ascertain first that this technique allowed the visualization of the viral genome once delivered in the target cells, another marker of pre-integration complexes was created by producing virions from cells expressing an EGFP derivative called EGFP-WXXF (Turelli et al., 2001). In this protein, EGFP is linked to a short peptide that allows the incorporation of heterologous proteins into HIV-1 virions in a Vpr dependent manner (BouHamdan et al., 1998). Dually labeled virions were used to infect HeLa cells, revealing the presence of intracytoplasmatic dots positive for both EGFP and rhodamine (Turelli et al., 2001). At early time points, the signal was first observed at the plasma membrane and then more dispersed in the cytoplasm, while at 2.5 hours post-infection it concentrated around the nuclear envelope, confirming that the rhodamine label is effectively incorporated into nascent reverse transcripts, and therefore provide an adequate tool for detecting incoming viral genomes (Turelli et al., 2001). This fluorescently labeled virus has been exploited to study the role of cytoplasmic recruitment of INI1 and PML in the

early steps of viral replication (Turelli et al., 2001). They infected HeLa cells with this fluorescent virus, showing that incoming retroviral pre-integration complexes trigger the exportin-mediated cytoplasmic export of the SWI/SNF component of INI1 and of the nuclear body constituent PML through (Turelli et al., 2001). These two nuclear proteins are relocalized in the cytoplasm within 30 minutes from infection, presumably long before any viral protein reaches the nucleus. This event is therefore most likely signal mediated. In addition, when rhodamine-labeled virions were used to infect HeLa cells transfected with EGFP-INI1, they observed cytoplasmic colocalization between incoming viral genomes and INI1 (Turelli et al., 2001). They hypotesized that, once loaded on the PIC, INI1 and PML could recruit the other components of the SWI/SNF complex as well as PML binding histone acetyltransferases such as CBP/p300 (Turelli et al., 2001). This could result in both facilitating integration and promoting transcription of the provirus by inducing remodelling of chromatin at the integration site through a combination of ATP-dependent DNA translocation and histone acetylation. This would temporarily maintain the proviral DNA in an open state favourable for the loading of transcription factors on the viral promoter, thereby allowing for the priming of viral gene expression (Turelli et al., 2001).

Monitoring interactions with cellular restriction factors

Live and fixed cell microscopy techniques have also proven particularly valuable in understanding the cell biology of the retroviral restriction factor TRIM5α (Bieniasz, 2004; Stremlau et al., 2004). Members of the TRIM family localize to various regions of the cytoplasm and nucleus (Reymond et al., 2001), and TRIM5α is known to multimerize into discrete regions in the cytoplasm known as *cytoplasmic bodies* (Stremlau et al., 2004). It was originally suggested that these structures represented nonfunctional, static accumulations of protein, but live cell microscopy has revealed that these bodies are dynamic structures that appear relevant to the ability of TRIM5α to restrict HIV-1 virions during infection. Using TRIM5α proteins fused to EGFP and EYFP proteins, TRIM5α cytoplasmic bodies were shown to utilize the microtubule cytoskeleton to traffic throughout the cell (Campbell et al., 2007a). Although it is unclear if it is cytoplasmic bodies

themselves or instead properties inherent to the TRIM5α protein that allow it to dynamically multimerize into such structures that are critical to mediate restriction, the ability to visualize the interactions occurring between virions and restriction factors *in situ* has provided a better understanding of this process.

Live and fixed cell imaging techniques have also been used to directly observe the interactions that occur between TRIM5α and HIV-1 virions. A stable accumulation of individual viral complexes associating with TRIM5α cytoplasmic bodies after proteasome inhibition was observed using fixed cell microscopy (Campbell et al., 2008), providing a mechanistic explanation for previous biochemical studies which inferred that proteasome function was required for a step in the restriction process. Live cell microscopy was used to observe the interactions between viral complexes and restriction factors in real time. These experiments revealed that restriction-sensitive HIV-1 viral complexes could both interact with preexisting TRIM5α cytoplasmic bodies and induce the *de novo* formation of cytoplasmic bodies around individual virions (Campbell et al., 2008).

Visualizing HIV-1 assembly and budding

The complex interactions occurring between viral and host cell proteins that affect the formation and release of individual virions has also been successfully investigated through cell imaging. The labeling of HIV-1 Gag protein precursor with EGFP has been useful for studying its localization in the cell and the mechanism that governs it. In fact, Hermida-Matsumoto and Resh showed that Gag-EGFP associates with cellular membranes in transfected cells, displaying a punctate pattern (Hermida-Matsumoto and Resh, 2000). In addition, they observed that Gag-EGFP relocalizes in cytosolic complexes in the presence of the myristoylation inhibitor 2-OH-Myr, revealing myristoylation as a necessary event for plasma membrane targeting of HIV-1 Gag (Hermida-Matsumoto and Resh, 2000).

Visualization and quantification allowed detailed analyses of Gag multimerization and its subsequent involvement in viral assembly. These studies have been performed by studying the virus-like particles (VLPs) formation following Gag multimerization. However, expressing Gag-EGFP by itself resulted in a variety of

aberrant viral particle structures (Larson et al., 2005; Muller et al., 2004) and in a reduction of infectivity of about 2 orders of magnitude (Muller et al., 2004). In order to overcome this problem, equimolar amount of Gag and Gag-EGFP were expressed (Larson et al., 2005). Fixed cell studies using correlative light and electron microscopy, which allows individual fluorescent punctum to be examined by electron microscopy, clearly demonstrate that fluorescent puncta observable by light microscopy are indeed budding virions (Larson et al., 2005). However, one of the difficulties in the field has been determining if a given punctum is a developing VLP or one that has formed, been released from the cell and has become reassociated with the cell after release. This could partly explain number of conflicting reports in this area of study, and requires an accurate interpretation of these results.

Aspects of cell biology that govern VLP behavior in cells have been examined with microscopy. An examination of the intracellular mobility of Gag-EGFP signals in cells demonstrated that the Gag-EGFP protein is extremely mobile in cells, and that mobility is increased when the determinants that mediate the later stages of assembly are removed, suggesting that as the assembly process proceeds, Gag mobility is reduced (Gomez and Hope, 2006). In addition, fluorescence recovery after photobleaching (FRAP) and photoactivatable-GFP (PA-GFP) analysis revealed that the mobility of membrane-associated forms of Gag-GFP requires cholesterol (Gomez and Hope, 2006). FRAP involves the photobleaching of fluorescent fusion proteins, such as Gag-EGFP, in a discrete region of the cell and the measurement of the rate at which fluorescence returns (or does not) to that region. PA-GFP is a GFP variant that is only weakly fluorescent before its activation by 413 nm light (Patterson and Lippincott-Schwartz, 2002). Activation of this protein in a discrete region of the cell allows the trafficking of the protein originally present in this region to be followed over time. Depletion of cholesterol reduced Gag-GFP or Gag-PA-GFP motility in live cell experiments, which could be rapidly restored by cholesterol replenishment. This work, consistent with the observation that cholesterol depletion reduces viral production (Ono and Freed, 2001), cumulatively suggests that VLP formation can be mediated by interactions that occur as a result of the lateral mobility of membrane-associated Gag molecules in a cholesterol-dependent manner.

The Resh laboratory has used FlAsH labeling to observe Gag protein trafficking after its ribosomal translation (Perlman and Resh, 2006). One of the advantages of FlAsH labeling is that labeling can be achieved concurrently with translation, without the requirement for protein maturation that can be a factor in the observation of fluorescent fusion proteins. Moreover, a combinatorial use of FlAsH and ReAsH reagents allows tracking newly synthesized protein populations. This is accomplished by labeling existing proteins in a cell with one reagent, followed by exposure of cells to the second reagent. Under these circumstances, the second reagent used will occupy the binding sites present on newly synthesized protein. The Resh group has used this technique to follow newly synthesized Gag proteins from an initial, perinuclear localization to localization in a multivesicular body-like compartment before its accumulation at the plasma membrane in COS-1 cells (Perlman and Resh, 2006). However, Rudner *et al*. used a similar technique to visualize the same phenomenon in HeLa cells, but observed that the perinuclear loci in which newly synthesized protein appeared to be located did not contain appreciable levels of the p6Gag epitope by immunostaining, leading the authors to conclude that these intracellular FlAsH-positive loci represent background staining rather than authentic Gag protein (Rudner et al., 2005).

One of the most elegant and efficient approaches used to study the interaction of Gag proteins during VLP formation took advantage of fluorescence resonance energy transfer (FRET) to measure the interaction between Gag molecules fused to fluorescent FRET partners. FRET exploits the fact that excitation of some fluorophores can transfer energy to an acceptor fluorophore in very close proximity, such that the wavelength-specific excitation of one fluorescent protein can result in the excitation of a separate, neighboring fluorescent protein. FRET signals can therefore be used to monitor the close association (5 nm) between proteins in cells by exciting one protein (called the donor) and measuring emission occurring from a separate protein (called the acceptor) (Piston and Kremers, 2007). Derdowski *et al*. used FRET to measure the multimerization occurring between YFP-labeled and CFP-labeled HIV-1 Gag constructs in cells during VLP formation (Derdowski et al., 2004). Protein–protein interactions between the individual Gag proteins required for FRET occurred predominantly at the plasma membrane and required Gag

myristoylation. Gag mutants with the G2A mutation, which prevents myristoylation, did not exhibit similar FRET activity. Furthermore, plasma membrane localization was required for Gag-Gag multimerization and measurement of FRET signal, but by itself plasma membrane localization was not sufficient to induce FRET between individual Gag proteins. Regions within the I domain of Gag, which is known to mediate the ability of Gag to multimerize (Sandefur et al., 1998), were required to allow plasma membrane localized Gag proteins to generate FRET signal (Derdowski et al., 2004). A similar finding was made by Hubner and colleagues, who performed FRET analysis of Gag protein assembly (Hubner et al., 2007). These authors inserted a fluorescent protein between the matrix and capsid regions of the Gag precursor protein, flanked by protease cleavage sites (Gag internal GFP, Gag-iGFP) (Hubner et al., 2007). Unlike traditional Gag-GFP constructs, this approach allows the observation during the formation of infectious virions rather than VLP formation. They could also observe FRET between Gag donor and acceptor proteins. In this case they exploited Venus and cerulean fluorescent proteins, which are recently developed variants of YFP and CFP exhibiting improved brightness and FRET characteristics (Kremers et al., 2006). Consistently with Derdowski *et al.* (Derdowski et al., 2004), FRET measurements between Gag-iCerulean and Gag-iVenus were greatly impaired when the functional assembly domain within the nucleocapsid region of Gag was mutated.

FRET analysis has also been used to quantify interactions occurring in the final stages of viral assembly. During virus release, components of the host cell endocytic sorting machinery are required to facilitate the release of infectious virions from the target cell (Morita and Sundquist, 2004). Tsg101 is a component of this machinery and was identified as a Gag binding protein that is required for the release of virions from cells (Garrus et al., 2001). A CFP-Gag and YFP-Tsg101 construct interacts in living cells during virus assembly. Gag expression induced Tsg101 to localize to the plasma membrane from a cytoplasmic and vesicular localization that was assumed in the absence of Gag, and this interaction was sufficient to induce FRET between these two fluorescent proteins (Derdowski et al., 2004).

A recent study has also used live cell imaging to examine virus production. This study used total internal reflection fluorescent microscopy (TIR-FM) to monitor the formation of VLPs at the plasma membrane (Jouvenet et al., 2008). By using TIR-FM, these authors were able to concentrate their analysis on assembling virions or

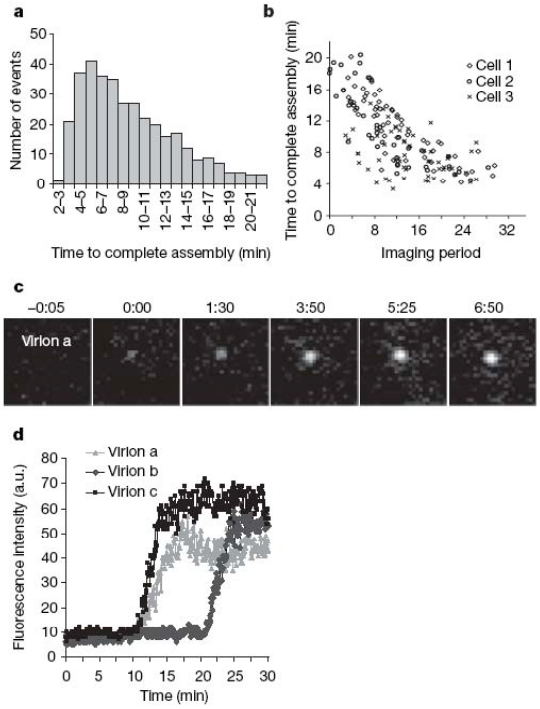

Figure 1-38. Variation in HIV-1 assembly kinetics. (a) Distribution of the time to complete assembly for 370 individual VLPs in 11 HeLa cells expressing Gag/Gag–GFP. Time to complete assembly was defined as the interval between the points of inflection on plots of fluorescence intensity against time, for each VLP. (b) Time to complete assembly is plotted against the time at which assembly commenced in three cells imaged for 40 min. Zero time is defined as the time at which observation began; that is, when more than 1 but fewer than 20 VLPs were visible in the TIR field for each cell. R=-0.71; R^2=0.5. (c, d) Assembly of HIV-1 particles from fulllength proviral plasmids. c, Images of an individual HIV-1 virion assembly event. Fields are 5.5 mm35.5 mm. Numbers above the fields are minutes:seconds. (d) Plots of the fluorescence intensity over time for three assembly events, including that shown in c. (Jouvenet et al., 2008).

puncta in specific regions of the plasma membrane. TIR-FM signals decay exponentially with increasing distance from the region of the plasma membrane being analyzed, allowing for high sensitivity in the analyzed region (Toomre and Manstein, 2001). The formation of individual Gag-GFP puncta could be measured, and events were divided into slow-forming and fast-forming populations. The slowly forming puncta were largely immobile compared with those that rapidly

appeared. Moreover, the colocalization of puncta with fluorescently labeled endocytic proteins, such as clathrin and CD63, predominated in the rapidly appearing population, whereas the slowly developing puncta did not associate with these markers. This allowed subsequent analysis to concentrate on these slowly appearing puncta, which were concluded to represent genuine VLP assembly events. Moreover, these slowly appearing puncta shared a similar fluorescent threshold at which no additional fluorescence appeared in these puncta, a point that indicates that a complete VLP has assembled. Careful analysis of these slow appearing puncta allowed the kinetics of VLP assembly to be quantified, with an average of 8.5 min passing between the time a punctum is first visible and when its maximal fluorescence is achieved. Lastly, Jouvenet *et al*. monitored the final event in viral particle formation (Jouvenet et al., 2008) using a pH-dependent GFP variant called pHlourin (Miesenbock et al., 1998), whose property is to lose fluorescence at low pH. When HIV-1 particles accomplished the fission of virion and cell membranes, they are not able to exchange any molecules –even protons– with the cell cytoplasm. Lowering the pH of the cytoplasm by raising the pCO_2 lowered cytosolic pH, resulted in a dramatic quenching in the fluorescence of Gag-pHlourin in the cytoplasm more than in cell-free VLPs (Jouvenet et al., 2008). This experiment allowed to clearly visualize budded VLPs, distinguishing them from those that are nascent VLPs, whose interiors are continuous with the cytosol.

Visualization of viral synapses

Contact between cells of the immune system results in the accumulation of numerous cell surface proteins, cytoplasmic proteins and other components at the point of cell-to-cell contact. The ability to visualize the dynamic redistribution of cellular proteins and compartments that is induced by contact between cells of the immune system has been critical in facilitating our understanding of these events. Jolly and coworkers have demonstrated that cell-to-cell transmission of HIV-1 virions is facilitated by exactly the same types of interactions between cells that mediate the immunological synapse (Jolly et al., 2004; Kupfer and Kupfer, 2003). Using immunofluorescence microscopy, they observed that the interactions between infected T cells and uninfected T cell targets induced the accumulation of HIV-1

Env and Gag at the point of cell-to-cell contact, which they defined as the virological synapse (VS). This interaction also induced the accumulation of target cell CD4 and CXCR4 coreceptor at the virological synapse. Using imaging-based assay systems, they demonstrated that the accumulation of these molecules at the virological synapse required the actin cytoskeleton and microtubule network, and the transfer of virus to target cells and their subsequent infection was reduced when this accumulation was prevented using pharmacological inhibitors (Jolly et al., 2004; Jolly et al., 2007). Chen and colleagues have subsequently demonstrated that this way of transmission could be the predominant mechanism by which viral infection occurs, estimating that VS-mediated infection is 18,000 times more efficient than infection by cell-free virus (Chen et al., 2007).

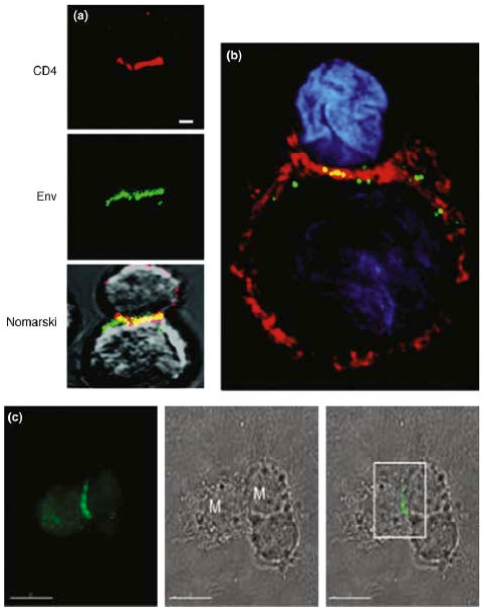

Figure 1-39. Visualizing the cell-to-cell contacts that mediate viral transfer. (a) The virological synapse visualized by Jolly and coworkers (Jolly et al., 2004). Cell-to-cell contact mediates the recruitment of CD4 receptor (red) on the target cell and viral envelope in the infected cell (green) to the VS. Scale bar, 1 μm. (b) The recruitment of individual HIV-1 virions (green) in the dendritic cell (bottom) to regions of the cell in contact with a T cell (top cell), as described by McDonald et al. (McDonald et al., 2003). Cells are visible by nuclear (blue) and actin (red) staining. (c) The recruitment of FlAsH labeled Gag protein (green) expressed in primary macrophages (M) to the point of cell-to-cell contact. Scale bar, 15 μm (Yu et al., 2008). The left panel shows the Gag fluorescence, the middle panel shows the macrophages, and the right panel combines these images and the point of cell-to-cell contact is highlighted the boxed region. (Kupfer, 2003; Jolly et al., 2007; Chen et al., 2007).

A similar phenomenon has also been observed between T cells and dendritic cells that had been exposed to HIV-1 virions (McDonald et al., 2003). Fixed and live cell imaging were used to demonstrate that HIV-1 virions enter the endosomal compartment of dendritic cells and accumulate in regions of the cell that come in contact with neighboring T cells (McDonald et al., 2003). Imaging-based assays were also used to detect the spatial redistribution of internalized virions in dendritic cells (McDonald et al., 2003). Yu *et al.* have recently demonstrated that these internalized virions reside in a compartmentalized invagination of the plasma membrane of the dendritic cell, where they remain susceptible to membrane impermeable gp120 inhibitors (Yu et al., 2008). They have also demonstrated the cell-to-cell transfer of these compartmentalized virions from dendritic cell to target T cells (Yu et al., 2008). This accumulation of virions at the point of cell-to-cell contact, termed the infectious synapse (Jolly et al., 2004), provided a mechanistic understanding of how dendritic cells can enhance HIV-1 infection of T cells without becoming infected themselves, a process known as *trans*-infection.

Cell-to-cell transfer of virus from antigen-presenting cells has also been observed in macrophages (Gousset et al., 2008). In this case, Goussett *et al.* introduced a tetracysteine motif inside *gag*, without interfering with Gag trafficking, virus assembly or release, particle infectivity, or the kinetic of virus replication (Gousset et al., 2008). They exploited this construct to follow viral Gag protein produced after infection of macrophages (Gousset et al., 2008). Gag accumulated in multivesicular bodies during virus production, and these particles contained structures recruited to the point of cell-to-cell contact in a fashion precisely resembling the synapse structures described above (Jolly et al., 2004; McDonald et al., 2003).

In addition to accumulating at points of cell-to-cell contact, recent reports have also demonstrated that extensions termed membrane nanotubes might also be exploited by viruses during cell-to-cell transmission of virus. These structures were first identified with live cell imaging as structures capable of facilitating the spread of murine leukemia virus (Sherer et al., 2007). More recently, these structures were shown to mediate the transport of HIV-1 Gag and Env proteins during cell-to-cell transmission (Sowinski et al., 2008).

These works cumulatively demonstrate the power of imaging techniques to observe and quantify critical aspects of cell biology that are simply not apparent when using more classical approaches.

CHAPTER 2

MATERIAL AND METHODS

CELLS AND ANTIBODIES

HeLa, 293T and HeLa-H2B-EYFP cells (generously supplied by Jörg Langowski) were maintained in DMEM supplemented with 10% FCS. HeLa-H2B-EYFP cells were cultured in medium containing 500 μg/ml of G418 (Gibco BRL, Milan, Italy). Primary antibodies used for immunofluorescence were: mouse mAb AG3.0 anti-HIV p24CA and rabbit anti-HIV p17MA (AIDS Research and Reference Reagent Program), goat anti-Lamin A/C (Santa Cruz Biotechnology, Inc., Santa Cruz, CA), rabbit anti-trimethyl-Histone H3 Lysine 9 (Upstate Biotechnology, NY, USA). Primary antibodies used for western blot analysis were: mouse anti-IN 8G4 obtained from the AIDS Research and Reference Reagent Program and anti-HIV-1 human sera generously supplied by Maurizio Federico. Secondary antibodies used for immunofluorescence were: anti-rabbit or anti mouse conjugated with Alexa-594, Alexa-633 and Alexa-647 (Molecular Probes, Eugene, OR) and anti-goat conjugated with Alexa-680 (Molecular Probes, Eugene, OR). Secondary antibodies used for western blot analysis were: anti-mouse and anti-human conjugated with HRP (Santa Cruz Biotechnology, Inc., Santa Cruz, CA).

EXPRESSION PLASMIDS

pVpr-IN-ECFP was constructed by cloning Vpr (PCR amplified from pNL4.3) in frame with the codon optimized IN (Limon et al., 2002a) into the pECFP-N1 vector (Clontech Laboratories, Inc., Saint-Germain-en-Laye, France). In addition an HIV-1 protease cleavage site (IRKVL), flanked at both C- and N- terminus by a flexible linker (KLRILQST and RDPPVAT, respectively), was introduced between Vpr and IN. pVpr-IN-EGFP was constructed by substituting the ECFP cDNA with EGFP.

p6xHis-tagged IN and IN-EGFP were constructed by cloning *wild-type* IN or IN-EGFP in frame with the plasmid pASK-IBA37plus.

The pD64E and pNL4-3.Luc.R-E- were obtained from the AIDS Reference and Reagent Program.

RECOMBINANT PROTEINS

N-terminal 6xHis-tagged IN and IN-EGFP proteins were expressed in *Escherichia Coli* BL21 and purified by metal ion affinity (BD TALON Metal Affinity Resin, BD Biosciences, Palo Alto, CA) according to the protocol reported in Bushman *et al.* (Bushman et al., 1993).

IN ACTIVITY ASSAY

Oligonucleotide substrates for IN reaction assays were as follows: 71 (5′-GTGTGGAAAATCTCTAGCA-3′) and 72 (5′-ACTGCTAGAGATTTTCCACAC-3′) (Parissi et al., 2001). 71 oligonucleotide was labeled with ^{32}P using polynucleotide kinase and annealed to the complementary 72 oligonucleotide. Strand transfer reaction was carried out in 20 mM Hepes, pH 7.2, 7.5 mM MnCl2, 0.05% NP-40 and 10 mM DTT, in the presence of the 71/72 substrate. [^{32}P]-labeled duplex DNA (1 pmol) was incubated in a final volume of 20 μl with 50 or 200 ng of 6xHis-IN or 6x-His-IN-EGFP proteins at 37 °C for 1h. The reaction products were separated by electrophoresis on a 15% polyacrylamide gel with 7M urea in Tris-Borate-EDTA buffer, pH 7.6, and then visualized by phosphoimaging (Cyclone).

VIRUS PRODUCTION AND INFECTION

HIV-IN-EGFP (-ECFP) virions were produced by transfecting $3x10^6$ 293T cells by calcium phosphate with 6 μg of pVpr-IN-EGFP (-ECFP), 6 μg of pD64E and 1 μg of pVSV-G. The control viruses were produced by transfecting $3X10^6$ 293T cells by calcium phosphate with 6 μg pNL4-3.Luc.R-E- or pD64E together with 1 μg pVSV-G. Supernatants were collected after 48 hrs, filtered through a 0.45 μm pore size filter and then concentrated by ultracentrifugation. For visualization experiments, luciferase assay and Alu-PCR ultracentrifugation was performed at 110.000 x g for 2 hrs at 4°C; for western blot analysis at 35,000 x g for 1.5 hrs at 4°C on a 20% sucrose cushion. Viral titers were quantified by RT assay or p24 ELISA (Innogenetics, Gent, Belgium). Infections for Alu-PCR and luciferase assays were performed using viral loads equivalent to 157.000 RT cpm on 400.000 cells. For immunofluorescence analysis viral loads equivalent to 1,5 μg or 3 μg of HIV-1-p24 were used to infect 40.000 cells; 2 hrs following infection cells were washed and

incubated for 1 min with 1x Trypsin (Sigma, Milan, Itlay) to eliminate un-entered virions absorbed onto cellular membrane.

Alu-PCR was performed as described in Cereseto *et al.* (Cereseto et al., 2005), treating the viral supernatants with 160U/ml Turbo DNase (Ambion, Austin, Texas) before infecting.

The synthesis of viral cDNA was analyzed in 293 T cells infected with viral loads equivalent to 157.000 RT cpm of NL4.3R-E-, D64E or HIV-IN-EGFP. Viral stocks used for the infections were treated with 160U/ml Turbo DNase (Ambion, Austin, Texas). In order to analyze viral cDNA from the moment of production up to the approximate time when the synthesis peaks, total genomic DNA was extracted at 2 h, 8 h, 24 and 36 h post-infection. The use of a specific set of primers allows the detection of viral cDNA at different stages of the synthesis. The early viral cDNA was monitored using the M667-AA55 (R/U5 specific) primer pair and the full length, or nearly complete viral cDNA (late), with M667-M661 (R/gag specific) set of primers (Zack et al., 1990).

IMMUNOFLUORESCENCE AND NERT FLUORESCENCE LABELING

Viral particles immunostaining was performed by adsorbing viral supernatants on chamber slides (BD Biosciences, Bedford, MA, USA) for 4hrs at 37°C with 10 μg/ml of polybrene, followed by rinsing with phosphate-buffered saline (PBS) and fixation with 2% paraformaldehyde in PBS for 15 minutes at room temperature. Intracellular immunostaining was performed in cells grown on chamber slides. Coverslips were then fixed with 2% paraformaldehyde in PBS for 15 minutes at room temperature followed by incubation for 5 minutes with glycine 100 mM in PBS and permeabilization with 0,1% Triton X-100 in PBS for 5 minutes. After treatment in blocking buffer (0,1% Tween and 1% BSA in PBS) for 30 minutes, primary antibodies were incubated for 1 hour at 37°C in blocking buffer followed by incubation for 1 hr at 37°C with secondary antibodies. Chamber slides were mounted with Vectashield before microscopy analysis (Vector Laboratories Inc., Burlingame, CA).

Virions containing fluorescently labeled cDNA by NERT activity were prepared by incubating 400 ng of p24 viral supernatants for 4 hrs at 37°C with an endogenous reverse transcription reaction buffer, as previously described (Zhang et al., 1996) and modified as follows: 10 mM Tris-HCl (pH7.4), 150 mM NaCl, 1mM MgCl2, 100 μM dATP, 100 μM dCTP, 100 μM dGTP, 25 μM dUTP, 10μM Alexa-594-dUTP (Molecular Probes, Eugene, OR).

IMAGE ACQUISITION AND ANALYSIS

Three-dimensional stacks of fixed cells were acquired with the TCS SL laser-scanning confocal microscope (Leica Microsystems, Milan, Italy) equipped with galvanometric stage using a 63×/1.4 NA HCX PL APO oil immersion objective. Z-step and y-step size was 0.3 μm. An Ar laser was used for ECFP (λ=458 nm), EGFP (λ=488 nm), EYFP (λ=514 nm) and Alexa-680 (λ=633 nm) excitation. Fluorescence emission was collected in the ranges 468-494, 495-525, 527-585 and 587-722 nm for ECFP, EGFP, EYFP and Alexa-680, respectively. For the two- and three-color analysis a sequential image acquisition was used to reduce crosstalk between different signals below 5%. Multi-channel images were contrast stretched (linearly) and assembled in ImageJ (NIH). H2B-EYFP fluorescence intensity among different cell images were normalized using the following procedure: for the acquisition the laser power was adjusted to maximize dynamic range and to avoid image saturation with the brightest value ranging between 220 and 250; the contrast range was then linearly expanded assigning the brightest value to 255. For cross analysis with 3MeK9H3 staining the H2B-EYFP fluorescence intensity was quantified in the 3MeK9H3 positive regions after rescaling with the above-described procedure.

Raw data (i.e. confocal z stacks) were deconvolved using the experimental PSF measured for each channel and imposing the optical parameters adopted during image acquisition. For each fluorescent channel the point spread function (PSF) of the microscope was calculated using PSF distilled function in Huygens Essential software (Scientific Volume Imaging BV. Hilversum, The Netherlands). There the lamin A/C Alexa-680 signal (blue) was linearly expanded between 30 and 250, while the PICs signal (green) between 2 and 50. The applied lookup table defines a grey background for values below the cutoff = 30.

CHAPTER 3

RESULTS

MOLECULAR ENGINEERING OF FLUORESCENT HIV-1 PARTICLES

Construction of fluorescently labeled IN proteins

Even though viral genome is restricted to 9 Kb, it has all the information for the transcription control elements and for coding 15 different proteins (Frankel and Young, 1998). Nonetheless, some viral proteins are the result of viral mRNA splicing, some other are translated as polyprotein, which, subsequently, are cleaved in specific regions by the HIV-1 protease. Therefore, altering the sequence of the provirus, by introducing or deleting sequences, can, in principle, impair the genome processing and the synthesis of viral proteins, leading to a block in the viral assembly and/or the viral replication cycle. Since our aim was to visualize the localization of HIV-1 IN in the nucleus of infected cells, we wanted to fuse IN viral protein to a fluorescent protein without disrupting the viral genome. Therefore, we exploited a technique known as *trans*-incorporation, which consists in the property of Vpr to interact with p6 region of Gag (Bachand et al., 1999; Paxton et al., 1993). As previously described (McDonald et al., 2002; Wu et al., 1995), exogenous proteins are shuttled in the viral particle by fusion with Vpr. In addition, it has been shown that *trans*-incorporated IN complements catalytically inactive IN of IN-mutant-HIV-1 molecular clones (*trans*-complementation), even though is less efficient (Fletcher et al., 1997). The introduction of a HIV-1 protease sensitive proteolytic cleavage site between Vpr and IN (Vpr-PC-IN) allows the separation of the two proteins, completely restoring the enzymatic activity of IN (Fletcher et al., 1997). Importantly, previous reports showed that the fusion of a protein at the C-terminus of Vpr-PC-IN does not affect viral assembly and infectivity (Holmes-Son and Chow, 2000; Tan et al., 2006).

Considering the above findings, we generated a plasmid construct carrying a HIV-1 sensitive proteolytic site (PC) in between Vpr and fluorescently labeled IN (IN-ECFP, IN-EGFP or IN-mCherry), as shown in Figure 3-1. The resulting sequence of the construct is Vpr-PC-IN-EGFP (hereafter, VIN-EGFP).

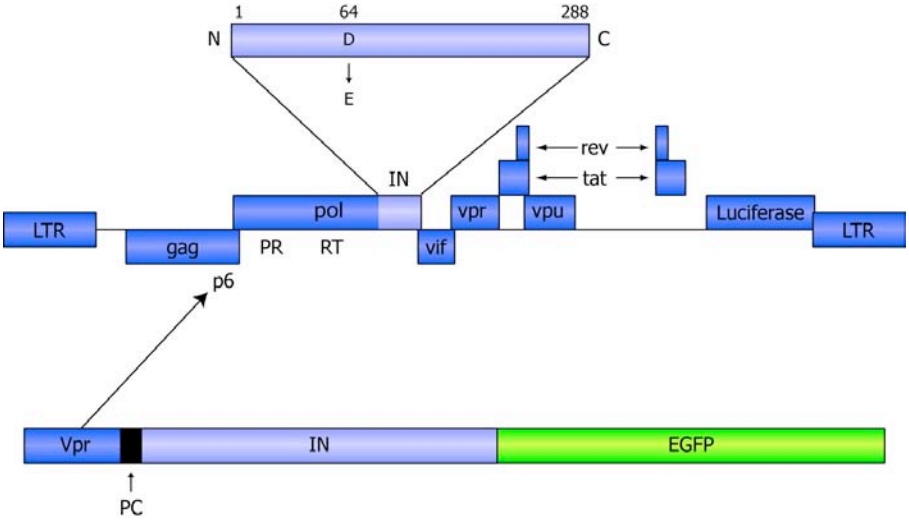

Figure 3-1. Vpr-IN-EGFP DNA construct. HIV-1 IN protein is fused at the N-terminus to Vpr and at the C-terminus to the fluorescent protein EGFP. Between Vpr and IN there is a proteolytic cleavage site (PC). HIV-1 protease recognize this site and cleave it, leaving the N-terminus of IN free from Vpr.

Initially, we analyzed the catalytic properties of IN following fusion with EGFP at the C-terminus. To this aim, recombinant wild-type IN or IN-EGFP proteins were expressed in *E. coli* with a 6xHis tag at the N-terminus, purified using nickel-chelate affinity chromatography and used in a strand transfer reaction. This experiment evaluates the capacity of IN to produce DNA fragments of different sizes (P), as a result of multiple integration events, when a short oligonucleotide is used as a substrate (S) (Marchand et al., 2001). The lengths of the 3'-end-joining products are heterogeneous because the site of joining is non-specific. As shown in Figure 1Bis, fusion of EGFP at the C terminus of IN did not change significantly the strand transfer activity with respect to the wild-type IN (Figure 3-2, lane 3 and 5, respectively). These results are in line with previous reports, proving that IN 3'-end-joining activity is not affected by the fusion of DNA binding protein at the C-terminus (Goulaouic and Chow, 1996; Tan et al., 2004).

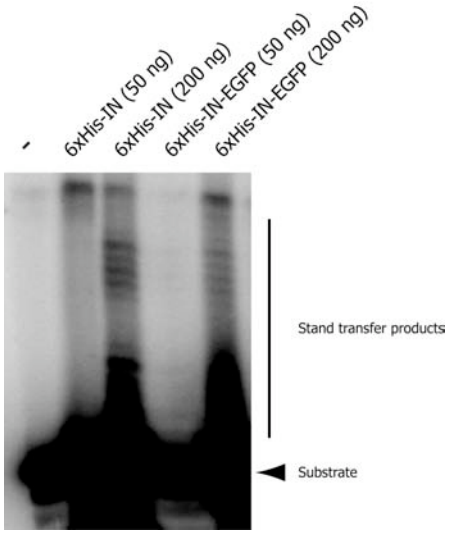

Figure 3-2. Catalytic activity of HIV-1 IN-EGFP fusione protein. The reaction was carried out with 50 or 200 ng of 6xHis-IN (Lanes 2 and 3) or 6xHis-IN-EGFP (Lanes 4 and 5). Lane 1 represents a reaction done in the absence of protein. The filled arrowhead denotes the position of the substrate (21-mer), while the bands that migrates above the substrate are the products of the strand transfer reaction.

IN-EGFP is *trans*-incorporated into the viral particles

In order to produce pseudotyped HIV-1 viral stock containing labeled IN (HIV-IN-EGFP), 293T cells were co-transfected with pVIN-EGFP, pVSV-G and the proviral construct pD64E. This HIV-1 molecular clone is derived from an *env*-deleted pNL4.3 provirus, expressing luciferase reporter gene and an IN mutated in the residue 64 (Svarovskaia et al., 2004). Since the substitution from Asp 64 to Glu results solely in a defect in integration and does not affect other critical stages of the virus life cycle, suppressed IN catalytic activity, the IN-EGFP fusion protein provided in *trans* exclusively mediates the integration of the recombinant HIV-1 fluorescent virus (hereafter, HIV-IN-EGFP).

To assess the incorporation in the viral particles and the protease cleavage of VIN-EGFP protein, supernatants containing *wild-type*, mutated or HIV-IN-EGFP virions were concentrated by ultracentrifugation (see Material and Methods) and analyzed by Western blot (WB). *Wild-type* and mutated viruses were produced by transfecting 293 T cells with pVSV-g and pNL4.3.Luc.R-E- (Connor et al., 1995; He et al., 1995) or with pD64E, respectively. Both wild-type and mutated viruses contain a luciferase reporter gene, but the former expresses a functional IN, while the latter

encodes a catalytically inactive IN. Using an anti-IN antibody, a band at the same size as IN (32 KDa) is detected in HIV-IN-EGFP virus, as well as in control NL4.3.Luc.R-E-, and D64E viruses (Figure 3-3A, lane 4, 2 and 3, respectively). In addition, two more bands, corresponding to Vpr-IN-EGFP and its proteolytic product IN-EGFP, are exclusively visible in the fluorescently labeled virions (Figure 3-3A, lane 4), proving that IN-EGFP is efficiently incorporated and subsequently digested by the viral protease. Notably, reproducible results showed that the amount of IN in both NL4.3.Luc.R-E- and D64E virions is comparable, while it decreases in HIV-IN-EGFP virions. Further investigations are needed to explain the different composition of the *trans*-incorporated viral particles.

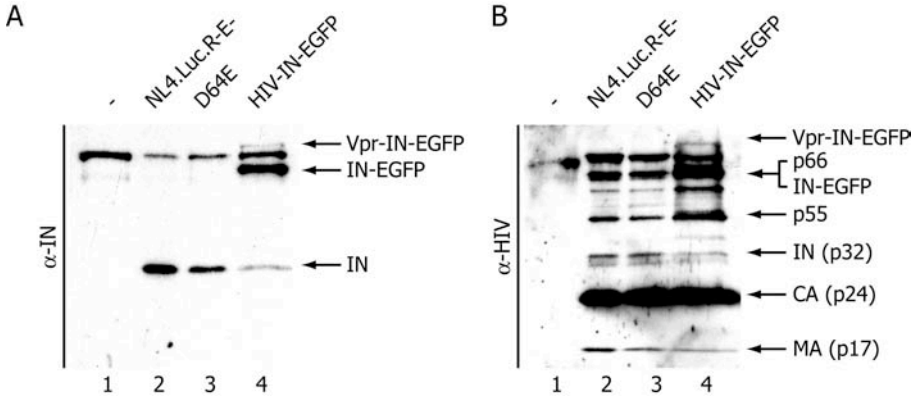

Figure 3-3. IN-EGFP is *trans*-incorporated into intact HIV-1 virions. Supernatant from un-transfected control cells (lane 1) or cells transfected with pVSV-G and pNL4-3.Luc.R-E- (lane 2), pD64E (lane 3) or pD64E together with pVpr-IN-EGFP (lane 4) were pelleted by ultra-centrifugation through a 20% sucrose cushion and analyzed by western blot using antibodies anti-IN (A) or with an anti-HIV-1 human serum (B).

In order to verify that the *trans*-incorporation of VIN-EGFP protein does not affect the regular assembly of HIV-IN-EGFP virions, we evaluated the correct synthesis of viral proteins and processing of Gag-Pol polyprotein by WB, using human anti-HIV serum. As shown in Figure 3-3B, HIV-IN-EGFP virions (lane 4) have same pattern and amounts of viral proteins and polyproteins as the two control viruses (lane 2 and 3), indicating that synthesis and maturation processes are not affected by *trans*-incorporation of VIN-EGFP. As expected, HIV-IN-EGFP virions (Figure 3-3B, lane 4) display two more bands, proving that Vpr-IN-EGFP is efficiently incorporated and is subsequently digested by the viral protease.

Visualized IN-EGFP particles are virions

Once assessed the regular HIV-IN-EGFP viral assembly and maturation, the fluorescence of these viral particles was observed with the confocal microscope, by directly spotting concentrated viral supernatant on a glass coverslip. As shown in Figure 3-4A, a high number of green fluorescent dots is visible. These dots appear heterogeneous in size, with a broad distribution of fluorescence intensity.

Indirect immunofluorescent staining of HIV-IN-EGFP virions bound to glass coverslip confirmed that virtually all the observed EGFP fluorescent dots were associated with matrix ($p17^{MA}$) (Figure 3-4C) or capsid viral proteins ($p24^{CA}$) (Figure 3-4D). These data prove that IN-EGFP fluorescent dots are indeed viral particles. The extensive colocalization between the EGFP spots and the two viral proteins (Figure 3-4E) is consistent with the findings of McDonald *et al*. (McDonald et al., 2002).

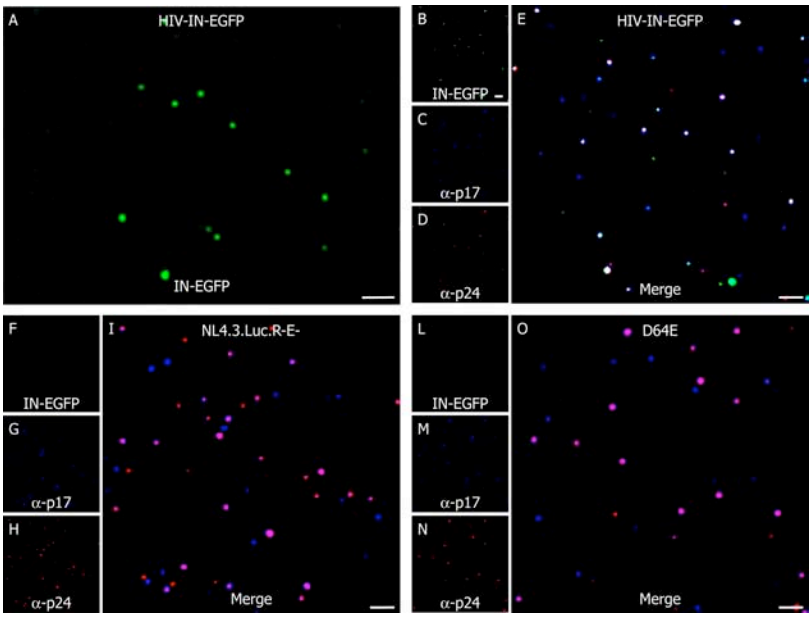

Figure 3-4. IN-EGFP colocalizes with HIV-1 viral proteins. (A) Supernatants from 293 T cells transfected with the pD64E, pVpr-IN-EGFP and pVSV-G plasmids were ultra-centrifuged through a 20% sucrose cushion, adhered to glass coverslips and visualized for EGFP fluorescente (green). (B-E) Harvested supernatant was fixed, immunostained with specific antibodies against viral proteins $p17^{MA}$ and $p24^{CA}$ and then visualized for EGFP fluorescence (B and E), $p17_{MA}$ (C and E) and $p24_{CA}$ (D and E). (F-I) sSme as in B-E with NL4.3-Luc.R-E-. (L-O) Same as in B-E with D64E. (E, I, O) Merged image, where white spots result from overlapping green, blue and red signals. Bars, 5 μm.

To ascertain that the green signal was exclusively due to the IN-EGFP protein the same immunostaining experiment was performed on both NL4.3.Luc.R-E- (Figure 3-4F, G, H and I) and D64E (Figure 3-4J, K, L and M) viral supernatants. The presence of $p17^{MA}$ and $p24^{CA}$ immunofluorescence signals in both *wild-type* and mutated viruses (Figure 3-4G and H, and Figure 3-4K and L, respectively) and the lack of green dots (Figure 3-4F and J) indicate that green fluorescence signals specifically originate from labeled IN of HIV-IN-EGFP virions. These results are a final demonstration that IN-EGFP is successfully and specifically *trans*-incorporated in the fluorescent virus.

Next, the amount of HIV-IN-EGFP viral particles colocalizing with $p17^{MA}$, $p24^{CA}$ or both was quantified. On average, 68% of the particles identified by α-$p17^{MA}$ antibody costain for IN-EGFP (see Table 3-1) and 63% of the virions detected by α-$p24^{CA}$ antibody colocalize with IN-EGFP. This indicates that a high percentage of virions identified by HIV-1 Gag protein is strongly labeled with IN-EGFP. Interestingly, 80% of the viral particles labeled with both α-$p17^{MA}$ and α-$p24^{CA}$ antibodies colocalize with IN-EGFP (see Table 3-1). These results indicate that IN-EGFP fusion protein allows the detection of all but a few virions by confocal microscopy.

Particles staining for	Colocalize with		
	$p17^{MA}$	$p24^{CA}$	VIN-EGFP
$p17^{MA}$	-	76% ± 7%	68% ± 2%
$p24^{CA}$	69% ± 3%	-	63% ± 11%
$p17^{MA}$ $p24^{CA}$	-	-	80% ± 9%

Table 3-1. Quantification of the colocalization between viral proteins and IN-EGFP particles.

VISUALIZATION OF HIV-IN-EGFP VIRIONS IN THE CYTOPLASM

IN-EGFP dots in the cell are viral particles

Previous structural and functional experiments revealed that HIV-IN-EGFP is a complete virion and behaves like a *wild-type* virus, showing that *trans*-incorporation of IN-EGFP does not affect any component or functionality of the viral particles.

Following, we focused on the visualization of fluorescently labeled virion in infected cells. To this aim, HIV-IN-EGFP virions were used to infect HeLa cells.

In order to visualize weather IN-EGFP interacts with the other viral proteins to form PICs in infected cells, we performed an immunostaining 6 hours post-infection, using antibody recognizing $p17^{MA}$ or $p24^{CA}$. It has been previously demonstrated that HIV-$p17^{MA}$ is detectable in PICs but $p24^{CA}$ is not (Miller et al., 1997). Conversely, McDonald *et al*. (McDonald et al., 2002) showed with visualization experiments that capsid structure remains intact during the initiation of reverse transcription in the cytoplasm. Our results, shown in Figure 3-5 are consistent with McDonaltd *et al*. (McDonald et al., 2002). Indeed, the majority of EGFP spots were positive for $p17^{MA}$ (Figure 3-5A) and $p24^{CA}$ (Figure 3-5B), indicating that IN-EGFP proteins form a complex with both the other two viral proteins in the cytoplasm of infected cells.

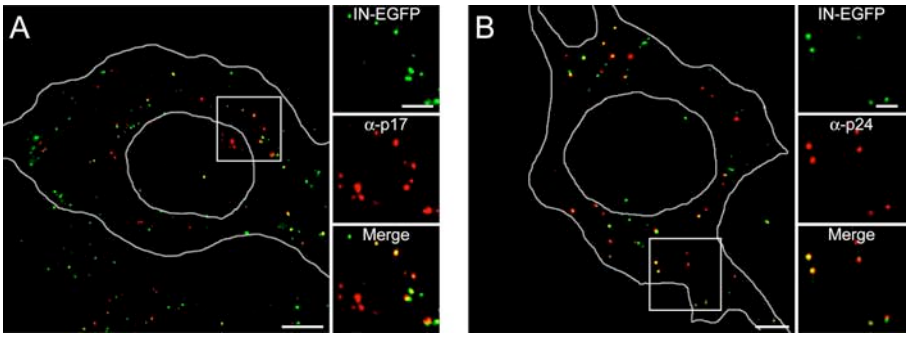

Figure 3-5. HIV-IN-EGFP virions can be visualized in infected cells. (A) Confocal visualization of HeLa cells infected with concentrated supernatants derived from cells transfected with the pD64E, pVpr-IN-EGFP and pVSV-G plasmids. Six hours post-infection cells were immunostained with antibodies against $p17^{MA}$ and visualized for EGFP fluorescence (green) or $p17^{MA}$ staining (red). In the merged image, where cell and nuclear shapes are outlined in white, yellow spots indicate full overlapping of green and red signals. Bar, 5 μm. Enlargements of the boxed region show individual color and merged images. Bar, 2 μm. (B) Same as in (A) using antibodies against $p24^{CA}$.

Visualization of IN-EGFP retrotranscription complexes: IN-EGFP PICs

PICs are defined as integration-competent complexes (Lehmann-Che and Saib, 2004), since they complete the reverse transcription of the viral genome, translocate into the nucleus of the infected cell and integrate viral cDNA. Therefore, the colocalization of IN-EGFP with $p17^{MA}$ or $p24^{CA}$ is not enough to show that

cytoplasmic fluorescent spots are indeed PICs. In order to visualize that IN-EGFP particles are able to reverse transcribe the viral genome, natural endogenous reverse transcription (NERT) activity was exploited. It has been shown that reverse transcription starts during viral particle formation and can be promoted by adding deoxynucleotides, divalent cations, and polyamines to extracellular viral supernatant (Zhang et al., 1996). This approach has been previously used for visualization purposes (Turelli et al., 2001) by incubating viral supernatant in presence of fluorescent dUTPs (Alexa-594 dUTPs). Similarly, this labeling was performed on supernatant containing NL4.3.LucR-E- virions, HIV-IN-EGFP virions, or 293 T cells not producing viruses (mock) for 4 hours at 37°C. Following, each supernatant was used to infect HeLa cells. Four hours post-infection cells were fixed and imaged at the confocal microscope. As shown by the presence of red dots in Figure 3-6B, *wild-type* virions incorporate fluorescent dUTPs in the retrotranscribed viral DNA during NERT, allowing the visualization of NL4.3.Luc.R-E- PICs in the infected HeLa cells. Similarly, red fluorescent dots (Figure 3-6E) are visualized in HeLa cells infected with HIV-IN-EGFP virions labeled with fluorescent dUTPs. Moreover, no fluorescence has been detected in the cells treated with mock supernatant, indicating that the fluorescent signal is specific for the labeling of retrotranscribed viral cDNA and does not gives unspecific signal. Notably, this experiment also shows that reverse transcription is not impaired.

Next, colocalization between HIV-IN-EGFP viral particles and fluorescent dUTPs was evaluated. As shown in Figure 3-6D, IN-EGFP viral particles are visualized in infected HeLa cells and two of them colocalize with the fluorescently labeled retrotranscribed viral cDNA (Figure 3-6F and Figure 3-6F insets). This result demonstrates that IN-EGFP particles are indeed PICs. However, Figure 3-6F shows only a minority of IN-EGFP spots overlapping with fluorescently labeled cDNA. The reduced number of positive PICs can be explained by the rather low efficiency of the NERT assay and to the reported observation that only a limited number of entered viral particles is actually infectious (Thomas et al., 2007).

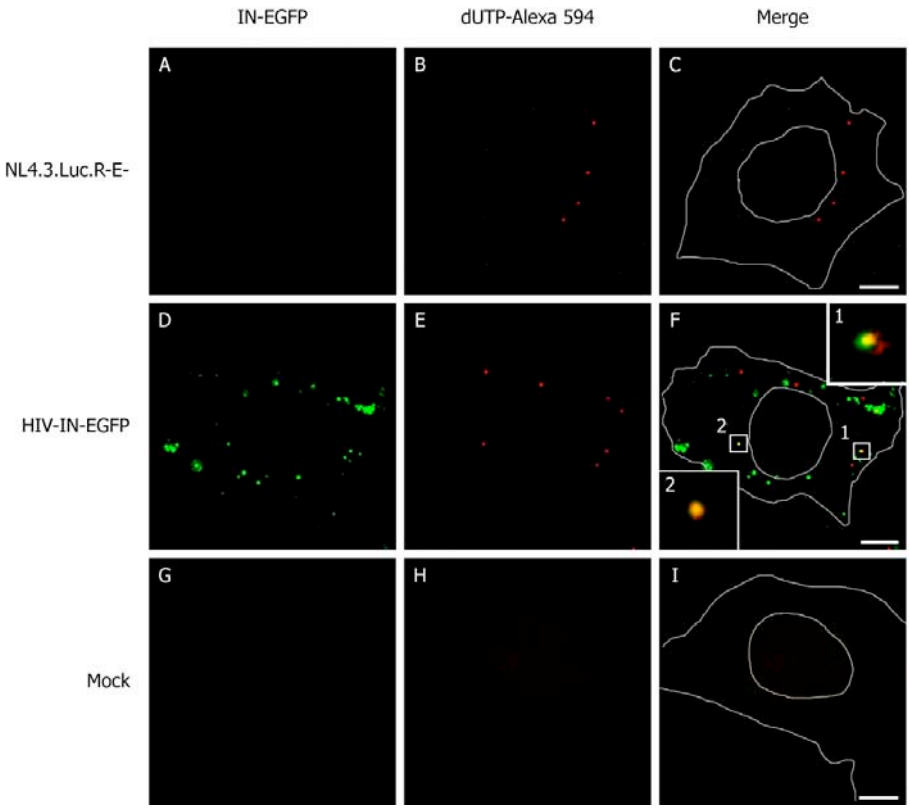

Figure 3-6. HIV-IN-EGFP virions containing neo-synthesized viral cDNA can be visualized in infected cells. (A-C)) Confocal visualization of a HeLa cell at 6 hours after infection with NL4.3.Luc.R-E- viral supernatant (A) incubated with deoxynucleotides Alexa-594-dUTP (B). Merged image is represented in (C). (D-F) Same as in A-C. (1 and 2) Enlargements of two IN-EGFP viral particles colocalizing with neo-synthesized viral cDNA. (G-I) Same as in A-C with supernatant costaining no virus. Cell and nuclear shapes are outlined in white. Bar, 5 μm.

FUNCTIONAL IN-EGFP PICS TRANSLOCATE IN THE NUCLEUS

Are IN-EGFP viral particles really visualized in the nucleus?

As demonstrated, IN-EGFP particles in infected cells are functionally active PICs and integrate like *wild-type* viruses in the host cell genome. Therefore, next step was to visualize the nuclear level of IN-EGFP PICs in target cells. To this aim, HeLa cells, constitutively expressing histone H2B fused to EYFP (HeLa H2B-EYFP) (Weidemann et al., 2003), were infected with HIV-IN-ECFP virions. ECFP labeled virions were used in place of HIV-IN-EGFP to allow better spectral separation.

H2B-EYFP has been used to visualize the nuclear compartment in order to distinguish cytoplasmatic PICs (cPICs) from nuclear PICs (nPICs). Initial analysis revealed that several PICs located in the close proximity or juxtaposed to the nuclear membrane. To circumvent the misleading signals deriving from these outer PICs a bi-directional scanning was employed.

Usually, the laser beam of confocal microscope scans the specimen along the XY plane (see Figure 8A), giving an image as result (Minsky, 1988). Acquisition of adjacent images of the sample along the *z*-axis allows the 3D reconstruction of the specimen. In addition, specimen can be acquired also along the XZ axes (see Figure 3-7B), giving as result an image that is orthogonal to the previous one. Taking advantage from these 2 different acquisition modes, we were able to clearly distinguish PICs located into the nuclear compartment from those that were not.

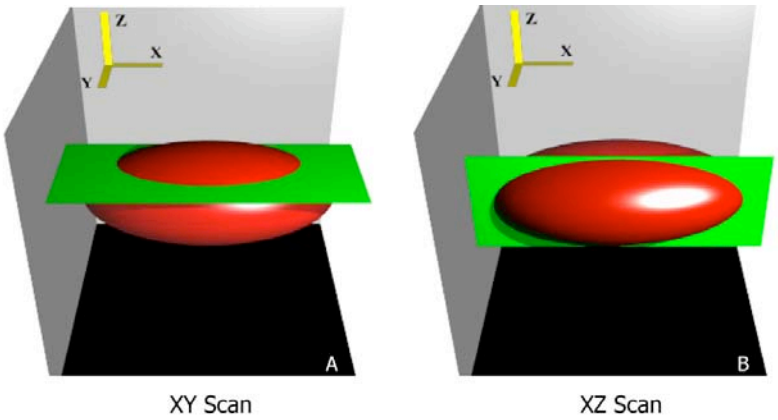

Figure 3-7. Confocal scan modes. 3-dimensional illustration showing the XY scan mode (A) or the XZ scan mode (B) of the confocal microscope.

Figure 3-8 shows the result of three XY-XZ double scans of putative nuclear PICs. For each cell, the three upper panels correspond to images acquired with XY scan in the IN-ECFP channel, H2B-EYFP channel or the merge of the two channels, respectively. Subsequently, on these cells an XZ scan was performed (vertical scan) in correspondence of a putative nuclear PIC. The position where we performed this vertical scan is reported for each cell as a white line at both sides of the XY merge image. The XZ scans in the IN-ECFP channel, H2B-EYFP channel or the merge of the two channels are in the lower panels. A white line at both sides of XZ merge

images indicates the height at which the XY image has been acquired. As demonstrated from these images nuclear localization might be interpreted in all cells here reported (cell 1, 2 and 3) (see Figure 3-8 C, I, P). However, due to the irregular shape of the nucleus, the comparison of the XZ scans reveals that exclusively cell 3 (Figure 3-8S) contains a nuclear PIC, while cells 1 (Figure 3-8F and 2 (Figure 3-8L) show PICs trapped in nuclear invagination, outside the envelope.

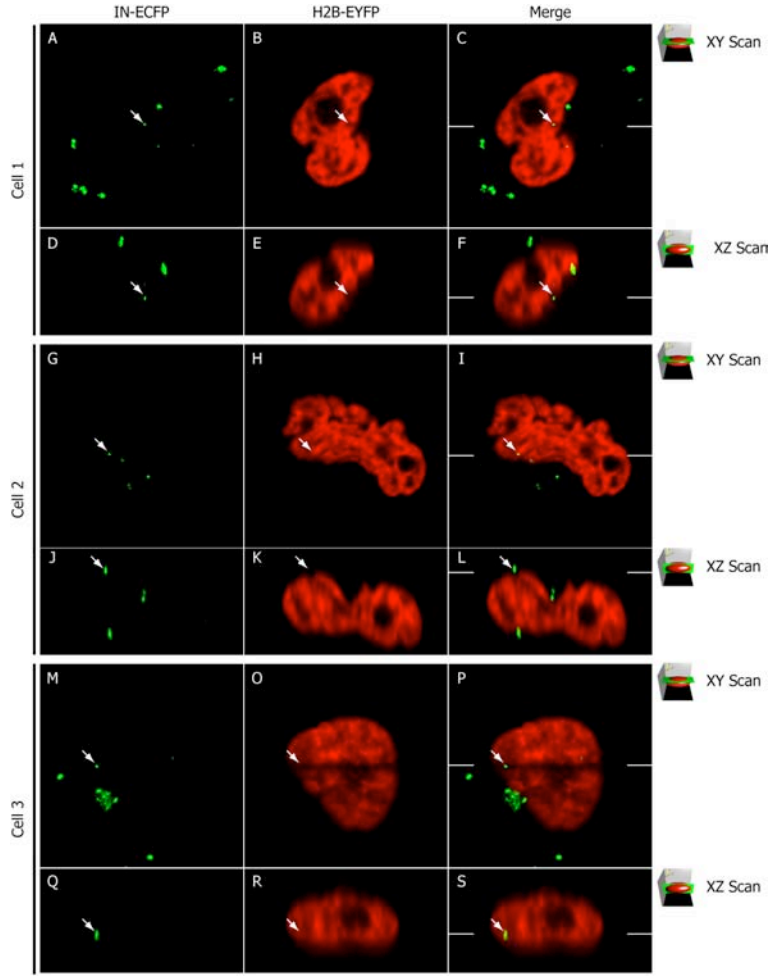

Figure 3-8. Cytoplasmic or nuclear localization of PICs. (A-C) XY scan of HeLa H2B-EYFP nucleus (B, red) infected with HIV-IN-EGFP virions (A, green). Merged image is shown in C. (D-E) XZ scan of the nucleus in B. White lines in C and F represent where XZ and XY images were acquired, respectively. (G-L) same as in A-F. (M-S) same as in A-F. Cell 1 (A-F) and cell 2 (G-L) show PICs in the close proximity or juxtaposed to the nucleus, while cell 3 (M-S) displays a nuclear PIC.

The XZ scan of an infected cell showed in Figure 3-9 further demonstrates that the irregularity of the nuclear membranes in which PICs are trapped might induce the misinterpretation of the results.

Therefore these experiments clearly demonstrate that the H2B-EYFP used to label the nucleus cannot allow to detect nuclear invagination or whole nuclear 3D structure, thus misleading to wrong PICs intranuclear localization.

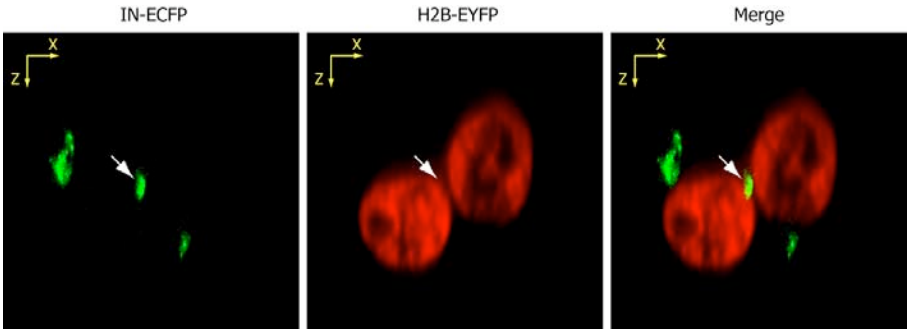

Figure 3-9. PIC trapped in the irregularity of the nuclea membrane. The nucleus of HeLa H2B-EYFP (mid panel) infected with HIV-IN-EGFP virions (left panel) shows an IN-EGFP PIC trapped in the irregularity of the nuclear membrane (right panel).

To better define the nuclear border, we decided to stain the internal boundary of the nucleus, occupied by the nuclear lamin. To this aim, we performed an immunofluorescence staining of nuclear lamin with antibody α-Lamin A/C. Subsequently we acquired a series of XY stacks every 0.3 μm, starting from the top of the nucleus towards the bottom. This approach leads to the acquisition of a sufficient number of *z*-stack images of the nuclear lamina, covering the whole nuclear compartment, which allowed us to make a 3D reconstruction of the nuclear boundaries. The antibody α-Lamin A/C specifically stains the nuclear periphery, so that the final 3D reconstruction gives a hollow sphere as result (see Figure 3-10A). This approach allowed a clear definition of the nuclear lamina, which in turn enables the visualization of the nuclear envelope irregularity (see Figure 3-10B).

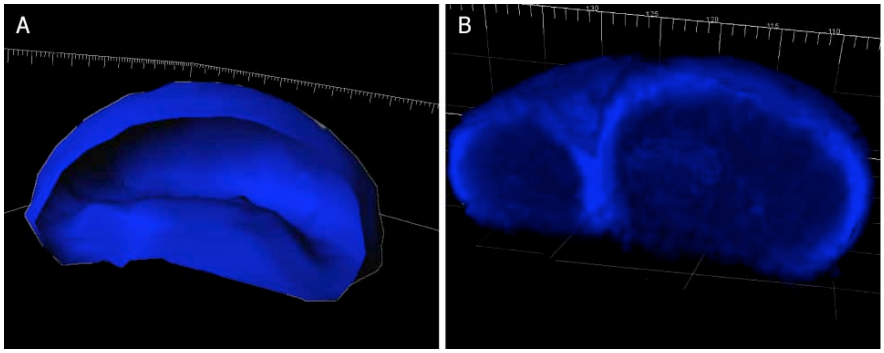

Figure 3-10. Nuclear lamin A/C staining. (A and B) two different visualization modes of a 3-dimensional reconstraction of a HeLa cell nucleus immunostained with antibody anti-Lamin A/C.

The staining with nuclear lamin antibody was then performed on HeLa cells infected with HIV-IN-EGFP. XY images of nuclear PICs were acquired in the channel of IN-EGFP and in that of the Lamin A/C (Figure 3-11A). Following, XZ scan in both channels (represented by the red lines at both sides of Figure 3-11A) was performed exactly in correspondence of the identified nPIC (Figure 3-11B). A 3D reconstruction of Figure 3-11A and B was carried out (Figure 3-11C-H) to better visualize PICs localization with respect to the nuclear volume.

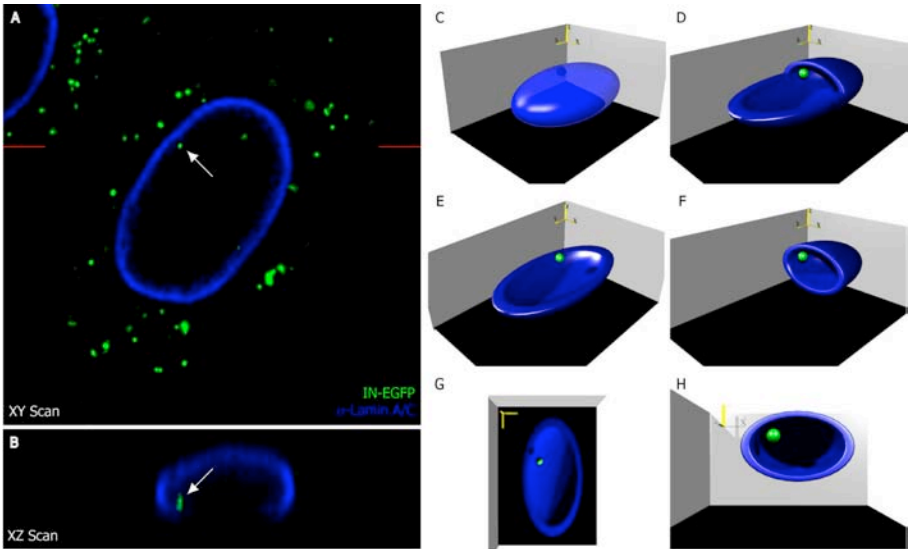

Figure 3-11. Nuclear visualization of the HIV-IN-EGFP virus. Nucleus of a HeLa cell infected with the HIV-IN-ECFP virus (green) and immunostained with lamin A/C (blue). (A) XY section of the nucleus of the infected cell. (B) XZ section of the nucleus in A performed in correspondence of the red lines represented in A. (C-H) 3-dimensional reconstructions of the nucleus in A.

Next, the infected cell shown in Figure 3-11 was sectioned every 0.3 μm along the *z*-axis or the *y*-axis by acquiring confocal images of IN-EGFP and LaminA/C signals with the XY (Figure 3-12B) or XZ (Figure 3-12C) scan mode, respectively. in the spectral channels corresponding to IN-EGFP and lamin A/C staining (Figure 3-12).

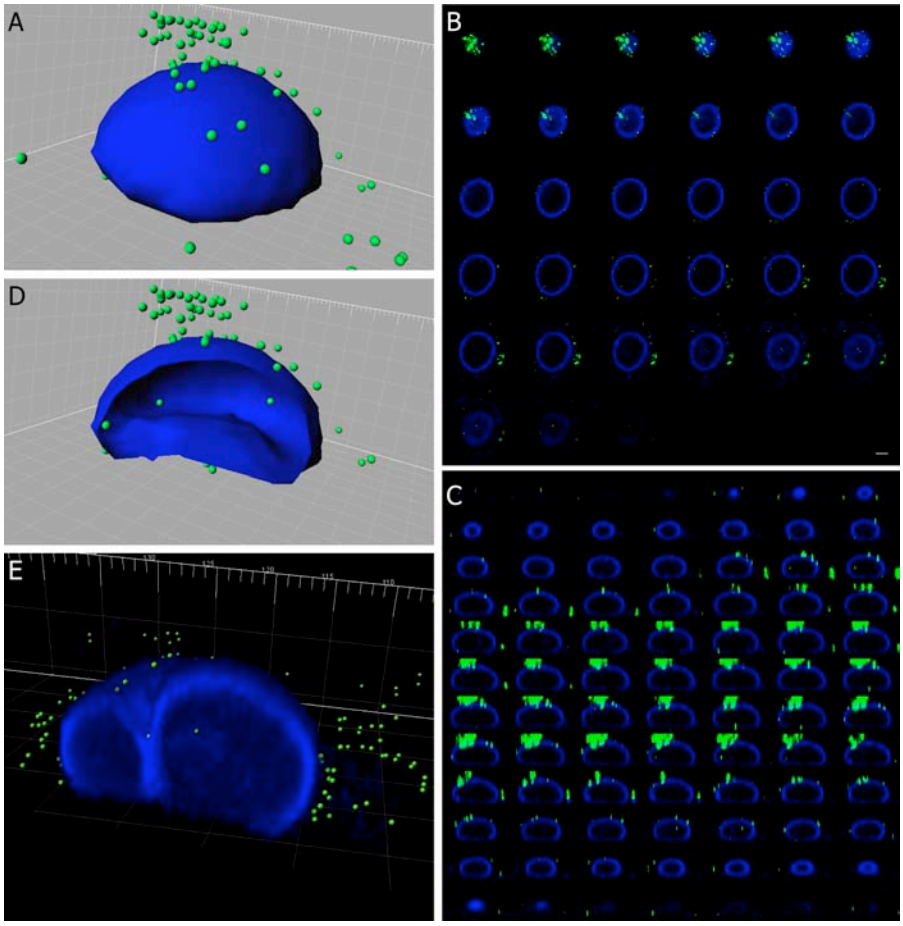

Figure 3-12. Visualization of HIV-IN-EGFP in the nucleus of infected cell. Nucleus of a HeLa cell infected with the HIV-IN-ECFP virus (green) and immunostained with lamin A/C (blue). Acquisition of confocal images was performed as *z*-stack (B) with a z step size of 0.3 μm and was followed by deconvolution based on experimentally determined PSF (see Experimental Procedure) and 3-dimensional reconstruction (A and D). (C) Adjacent xz section of the nucleus in B acquired every 0.301 μm. Bars, 5 μm. (E) HeLa cells were infected with HIV-IN-EGFP virions, fixed 6 hours after infection and immunostained with antibody anti-lamin A/C. The image shows an IN-EGFP PIC trapped in the irregularity of the nuclear membranes and a PIC in the nuclear compartment.

This approach allowed the detection of all the PICs present in the different focal planes of the whole cell. Notably, since images are acquired every 0.3 μm along *z*-axis and PICs are not planar but occupy a 3D volume, fluorescence coming from IN-EGFP PICs is detectable in more than one stack, typically in three stacks.

Comparing Figure 3-12B with Figure 3-12C the number of nuclear PICs is the same, proving that combining the staining of nuclear lamin A/C with the acquisition of confocal images along the *z*-axis of the nucleus is the best system to accurately define nuclear PICs. The 3D reconstruction of these *z*-stack images allowed a better visualization of these data (Figure 3-12D). In addition, this approach identifies nuclear invaginations, avoiding misinterpretation of PICs localization, as shown in Figure 3-12E.

Summarizing, our approach consists in plating HeLa cells on a chamber slide, infecting with HIV-IN-EGFP virions and fixing typically 6 hours post-infection to perform an immunofluorescence using Ab α-Lamin A/C. Following, XY scan mode of the confocal microscope is used to acquire images of infected cells every 0.3 μm along the *z*-axis, starting from the top to the bottom of the nucleus. The combination of lamin staining together with the acquisition of 3D images are the necessary criteria to establish the nuclear localization of PICs.

Translocation of HIV-IN-EGFP in the nucleus follows CA disassembly

It is known that CA shells disassemble is a necessary event before viral DNA translocation through the nuclear pore (Arhel et al., 2007; Forshey et al., 2002; Miller et al., 1997). Therefore, as a better indication that PICs identified in the nucleus are functionally active virions, an immunofluorescence was performed on HeLa cells infected with HIV-IN-EGFP using antibody α-Lamin A/C and α-$p24^{CA}$. This experimental set up allows to visualize at the same time the position of IN-EGFP PICs with respect to nuclear lamin and the capsid protein. To discriminate cPICs from nPICs, images were acquired with the confocal microscope every 0.3 μm with the XY scan mode. Figure 3-13A shows IN-EGFP virions colocalizing heterogeneously with p24. Figure 3-13B displays two cPICs costaining with $p24^{CA}$:

one is few microns far from the nuclear envelope, while the other is very close to it. In Figure 3-13C a nPIC is observed and it does not costain with $p24^{CA}$.

This analysis has been performed on 10 different cells, obtaining a colocalization between IN-EGFP signal and $p24^{CA}$ signal of 50% in the cytoplasm and of 0% in the nucleus, where we found a total of 12 nPICs. The analysis with Student's t-test revealed that these results are statistically significant different, with $P<0.01$. Therefore, these data further prove the functional integrity of the nuclear HIV-IN-EGFP virions.

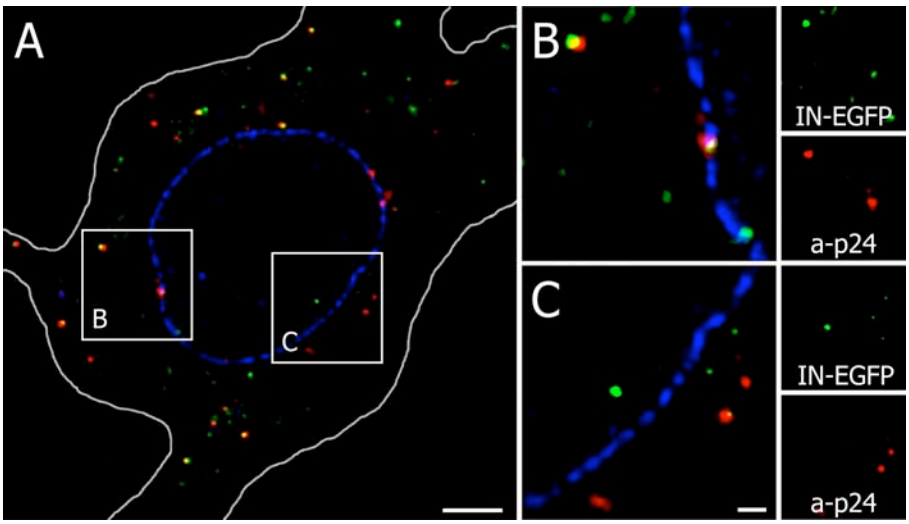

Figure 3-13. Nuclear translocation of HIV-IN-EGFP virions follows capsid disassembly. (A) Merged image of a confocal section obtained from HeLa cells infected with HIV-IN-EGFP supernatants (green) and immunostained with antibodies anti-$p24^{CA}$ (red) and lamin A/C (blue). Yellow indicates full overlapping of EGFP and anti-p24CA signals. Cell and nuclear shapes are outlined in white. Enlargements of frames B and C are shown in the right panels along with the individual color images. Bars, 5 μm and 1 μm in the whole frame and enlarged boxes, respectively.

Nuclear IN-EGFP particles bind viral cDNA

As shown previously, cytoplasmic IN-EGFP PICs are functionally active, since they bind retrotranscribed viral cDNA. In order to verify that their functional integrity is preserved at the nuclear level, we wondered weather nuclear IN-EGFP PICs still bind viral cDNA. To this aim, NERT approach was exploited to incorporate fluorescent dUTPs in retrotranscribed viral cDNA of HIV-IN-ECFP virions. The dUTPs labeled supernatant was used to infect HeLa expressing H2B-EYFP histones

and after 6h cells were fixed and imaged at the confocal microscope. A *z*-scan of the nucleus was performed, by recording separately the three spectral channels corresponding to IN-ECFP PICs (Figure 3-14A, green), H2B-EYFP (Figure 3-14A, blue) and Alexa-594-dUTPs (Figure 3-14A, red). Figure 3-14A shows a nuclear IN-ECFP PIC colocalizing with fluorescent dUTPs, indicating that nPIC is indeed bound to retrotranscribed viral cDNA and suggesting its integrity and functionality.

To further prove the intranuclear localization of PICs associated with neosynthesized cDNA, the same experiment was also performed in HeLa cells that have been subsequently immunostained with Lamin A/C antibody (Figure 3-14B). Cells were imaged at the confocal microscope, acquiring pictures with the XY-scan mode and sectioning the whole nucleus every 0.3 μm. Figure 3-14B (white arrow) shows a cytoplasmic IN-EGFP PIC (green) colocalizing with Alexa-dUTPs (red) very close to the nucleus (blue). More interesting, a PIC colocalizing with retrotranscribed viral DNA is observed within the nuclear boundaries.

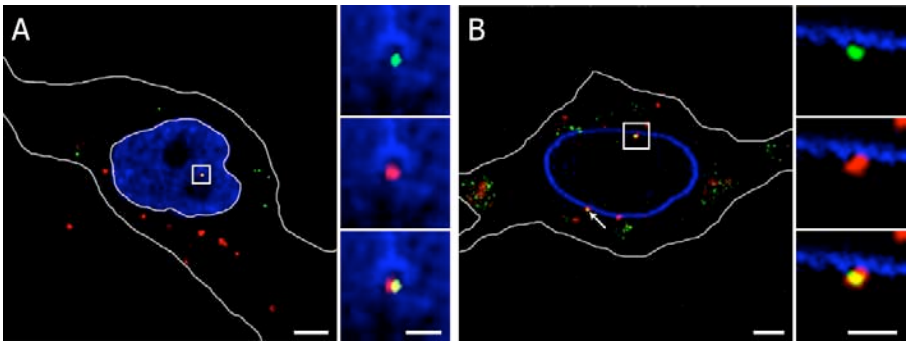

Figure 3-14. Nuclear IN-EGFP virions colocalize with viral cDNA. (A) Merged image of a confocal section obtained from H2B-EYFP HeLa cell infected with HIV-IN-EGFP supernatant incubated with deoxynucleotides Alexa-594-dUTP. Cell and nuclear shapes are outlined in white. (B) Merged image of a confocal section obtained from HeLa cell infected with HIV-IN-EGFP supernatant incubated with deoxynucleotides Alexa-594-dUTP and immunostained with antibody anti-LaminA/C. Cell shape is outlined in white. Yellow indicates full overlapping of EGFP and Alexa-594-dUTP signals. Bars, 5 μm and 1 μm in the whole frame and inset box, respectively.

Taken together, these results show the functional integrity of nuclear IN-EGFP PICs, validating HIV-IN-EGFP virus as a tool in visualization experiments.

HIV-IN-EGFP nuclear translocation kinetic

The visualization of functionally active HIV-IN-EGFP virions in the nuclear compartment allowed to investigate the kinetic of nuclear translocation. It has been estimated that proviral DNA is detectable almost 8 hours after HIV-1 entry (Kim et al., 1989). We have thus quantified the number of viral PICs at different time points from 3 to 24 hours after infection. HeLa cells were plated on six different chamber slides and infected with HIV-IN-EGFP virions. Next, cells were fixed at different time points (3h, 6h, 9h, 12h, 16h and 24h) and immunostained with antibody α-Lamin A/C.

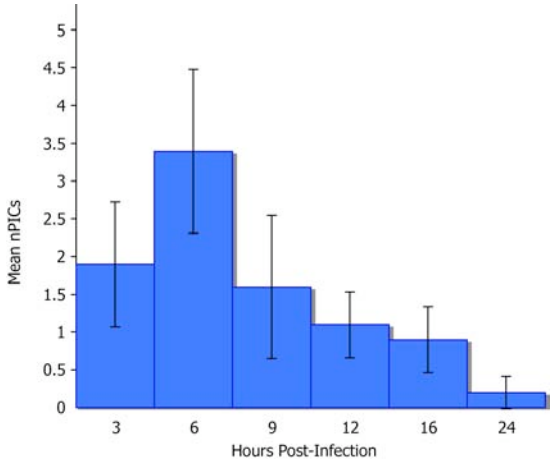

Figure 3-15. Nuclear translocation kinetic of HIV-IN-EGFP virions. HeLa cells infected with HIV-IN-EGFP virions were fixed and the mean number of intranuclear viral particles per cell was quantified at 3 hrs, 6 hrs, 9 hrs, 12 hrs, 16 hrs and 24 hrs. At each time point an average of 30 cells was analyzed and SD represented as error bars.

Images were acquired with the XY scan mode along the *z*-axis of the whole nucleus, as previously described. The amount of IN-EGFP PICs in infected cells was quantified automatically using the function "Analyze particles" of the software ImageJ (NIH). Automated quantification could not be used for nuclear PICs due to multiple parameters required for the analysis. Therefore, nPICs were counted one by one, screening each cell stack by stack. Thirty cells per each time point were analyzed, finding the highest number of nPICs at 6 hours post-infection (Figure 3-14), with a mean of 3.5±1.1 (mean±SD, Standard Deviation). From 6 hours to 9 hours post infection the number of nPICs decreases steeply while after this time

point the number of nuclear PICs decreases gradually up to 24 hours when no PICs are detectable anymore.

Finally, 6 hours post-infection the ratio of nuclear-to-cytoplasmic PICs was evaluated. Compared to the total average amount of PICs per cell (167.5±33.4; mean±SD, 30 cells), only a small fraction (2.0±0.8%; mean±SD) was found in the nucleus.

DISTRIBUTION OF IN-EGFP PARTICLES IN THE NUCLEUS

Peripheral distribution of HIV-IN-EGFP

Analyzing HeLa cells infected with HIV-IN-EGFP we noticed that PICs were preferentially detected at the nuclear periphery. In order to quantify this preliminary observation at 6 hours post-infection, cells were immunostained with α-Lamin A/C antibody and the distance of nPICs from the nuclear boundaries was evaluated. Interestingly, our results, showed in Figure 3-16, reveal a preferential distribution of nuclear pre-integration complexes in the nuclear periphery. In fact, HIV-IN-EGFP nPICs localize at distances ranging from 0.4 to 2.0 μm from the nuclear border, with a mean of 0.9±0.4 nPICs, while the frequency of nPICs decreases dramatically toward the centre of the nuclei.

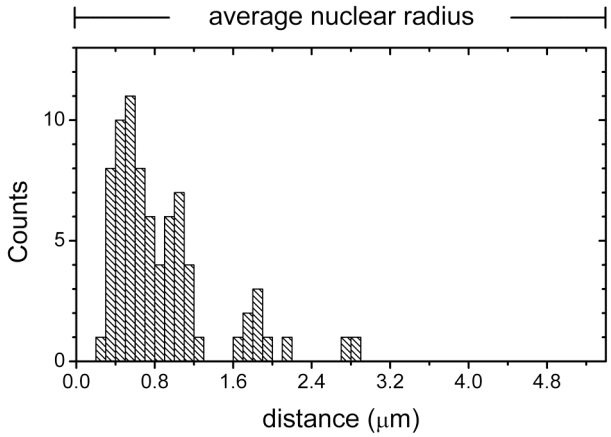

Figure 3-16. HIV-IN-EGFP virions preferentially localize in the periphery of the nucleus. Distribution of intranuclear PICs distances from the lamin A/C staining.

Characterization of heterochromatin in HeLa H2B-EYFP cells

The peculiar distribution of IN-EGFP PICs at the periphery of the nucleus arises the question weather chromatin organization may influence their localization. Indeed, recent studies revealed that chromatin has different levels of accessibility, depending on histone acetylation (Gorisch et al., 2005). This allowed the description of the dynamic accessibility of different chromatin states in response to histone acetylation with an apparent pore diameter, which defines the maximal size of complexes capable to penetrate these regions.

In order to verify weather different chromatin condensation states may affect PICs accessibility, HeLa cells expressing histone H2B fused to EYFP fluorescent protein were used. Since H2B is part of the nucleosomes, the fluorescent signal coming form EYFP correlates with chromatin condensation, with brighter and darker areas indicating heterochromatin and euchromatin, respectively (Bhattacharya et al., 2006; Kanda et al., 1998; Kimura and Cook, 2001). However, the correspondence between fluorescence intensity and chromatin condensation state is merely arbitrary. In fact, we wondered weather it was possible to associate euchromatin and heterochromatin to the H2B-EYFP fluorescence intensity, so as to correctly identify those areas within the regions occupied by nPICs. Therefore, we needed to verify the correlation of these two forms of chromatin with H2B-EYFP fluorescence intensity. It has been shown that different histone posttranslational modifications are related to highly condensed, transcriptionally inactive and late replicating heterochromatin (Allis et al., 2007; Dimitrova and Gilbert, 1999; Wu et al., 2005). Therefore, HeLa H2B-EYFP cells (Figure 3-17A) were immunostained with an antibody specific for the tri-methylated lysine 9 of histone 3 (3MeK9H3) (Figure 3-17B and C). We acquired images at the confocal microscope, by recording separately the channels corresponding to H2B-EYFP (Figure 3-17A, red) and 3MeK9H3 staining (Alexa-647) (Figure 3-17B, green). The cross analysis of fluorescence related to H2B-EYFP and the 3MeK9H3 immunostaining (Figure 3-17B, green bars) allowed us to precisely and rigorously correlate heterochromatin with a range of fluorescence intensity of H2B-EYFP. This analysis revealed that the average H2B fluorescence intensity of the overlapping regions is equal to 195 arbitrary units (a.u.) and its distribution width at half-height ranges from 140 to 230 a.u. as indicated by the

arrow in Figure 3-17D. Therefore, these data not only demonstrate that the high intensity H2B-EYFP fluorescence regions are indeed occupied by silenced heterochromatin but, more important, we can assign them precise values.

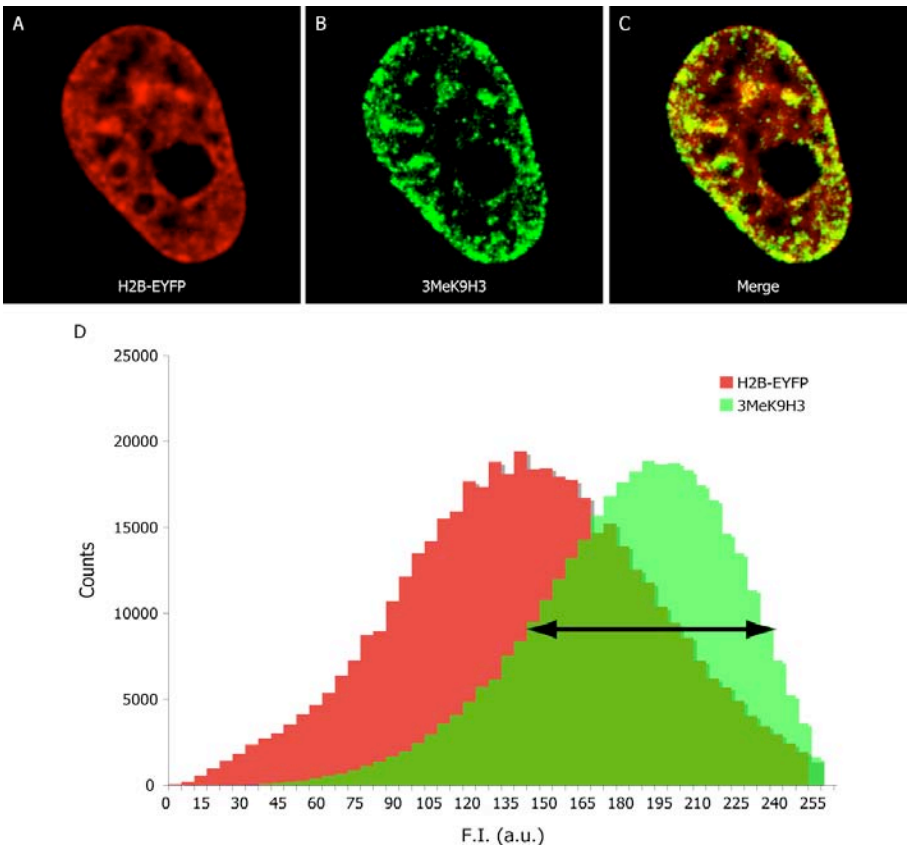

Figure 3-17. Correlation between H2B-EYFP fluorescence intensity and heterochromatin. HeLa cells constitutively expressing H2B-EYFP histones (A) were immunostained with the antibody anti-tri-methylated lysine 9of histone 3 (B), which is a heterochromatin marker. Merged image (C) shows that only high intensity H2B-EYFP fluorescent regions costain (shown in yellow) with silenced heterochromatin. (D) Fluorescence intensity distribution frequency for H2B-EYFP (red bars) and for H2B-EYFP in the 3MeK9H3 positive regions (green bars) of the nucleus represented in A. The arrow represents the width at half-height of the H2B-EYFP fluorescence intensity distribution derived by cross analyzing with the 3MeK9H3 heterochromatin marker.

IN-EGFP viral particles localize in less condensed chromatin

In order to identify weather heterochromatin or euchromatin could influence the localization of PICs within intact nuclei, HeLa-EYFP cells were infected with HIV-IN-EFCP virions and fixed 6 hours post-infection. ECFP labeled virions were used in place of HIV-IN-EGFP to allow better spectral separation. Cells were acquired at

the confocal microscope, by recording separately the spectral channels of IN-ECFP and H2B-EYFP. The presence of a chromatin condensation marker, such as H2B-EYFP, allowed to identify the fluorescence intensity signal precisely in the regions of nuclear IN-ECFP PICs. In order to quantify this signal, a linescan was performed in the channel of H2B-EYFP (see Figure 3-18). For each image containing a nPIC three lines were drawn. Two were in the highest (blue line) and lowest (green line) intensity regions, respectively. A third line was drawn in correspondences of IN-ECFP PICs, allowing to detect both the H2B-EYFP (white line) and the IN-ECFP signals (cyan line). As shown in Figure 3-18, in correspondence of peak of the IN-ECFP nPIC fluorescence signal the linescan of H2B-EYFP display values comparable to those relative to the linescan drawn in the lower fluorescence intensity areas, reflecting a decondensed and highly accessible chromatin.

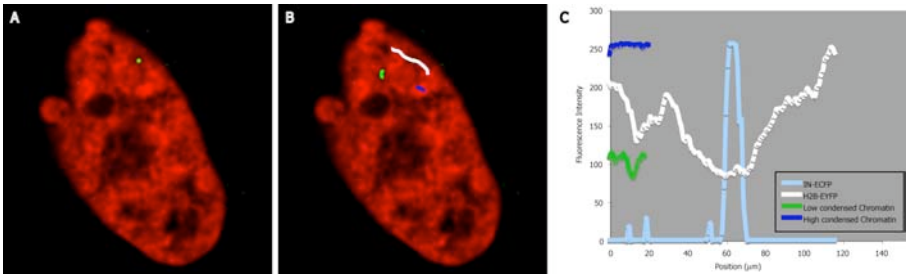

Figure 3-18. IN-EGFP virions localize in less condensed chromatin. (A) H2B-EYFP (red) HeLa cells were infected with HIV-IN-EGFP virions (green). (B and C) Linescans of the H2B-EYFP fluorescent signal were drawn in correspondence of condensed and decondensed chromatin (blue and green, respecitvely), and IN-ECFP PIC (white). (C) Cyan line identifies HIV-PIC. It represents how IN-ECFP fluorescence signal change along the white linescan. In correspondence of IN-ECFP peak the H2B-EYFP fluorescent signal is comparable to that of decondensed chromatin regions.

Next, an automated approach was required for a broad screening. Since the expression of histone H2B fused to EYFP is not equal among different cells, comparable normalized values were required. To this aim the H2B-EYFP fluorescence intensity was linearly rescaled over the 8-bit range (0-255 arbitrary units, a.u.), as described in Material and Methods. Then, a region of interest (ROI) was drawn around each IN-ECFP nPIC and the mean fluorescence intensity in the EYFP channel has been measured (see white circles in Figure 3-19A, and Table 3-2). In parallel, in the same picture, the mean fluorescence intensity was recorded in three ROIs drawn in the brightest regions (Figure 3-19B, blue circles) and three more ROIs drawn in the darkest regions (excluding nucleolar regions) (Figure

3-19B, green circles). Then, the mean value and the standard deviation relative to the highest and lowest fluorescence intensity were calculated (see Table 3-2) and displayed in the graph of Figure 3-19C. Since acquired images have 8-bit, each channel has a depth of 256 colors. This means that darkest regions have a value of zero, while brightest regions correspond to 255. Figure 3-19C shows in red the counts of fluorescence intensity relative to H2B-EYFP, starting from the lowest value (zero) to 255. The resulting graph is a Gaussian curve, where the counts represent the number of pixels that have the same intensity value. The averages and standard deviations of the less condensed and more condensed regions are represented with a green bar and a blue bar, respectively. The two green bars in the Gaussian curve of Figure 3-19C represent the mean value of the fluorescence intensity of the regions occupied by the two IN-ECFP nPICs visualized in Figure 3-19A. Therefore, both nPICs are located in the less condensed regions. Following this procedure, 48 different cells were analyzed (see Figure 3-19D and Table 3-3): 60 PICs were in the less condensed regions, 8 in the more condensed regions and 11 in the region in between these two, that we called intermediate region. Therefore, this analysis revealed that the vast majority of nuclear PICs are in more accessible and less condensed regions, while only the 3% of them are in the tightly condensed chromatin (see Figure 3-19E and Table 3-3). These results show thus a bias of nPICs for less condensed chromatin.

	Mean F.I. (a.u.)	SD
Less condensed regions	88	20
Tightly condensed regions	215	27
IN-ECFP nPICs regions	93	24

Table 3-2.

Total cells	PICs in less condensed regions	PICs in an intermediate status	PICs in tightly condensed regions
48	62	16	2

Table 3-3.

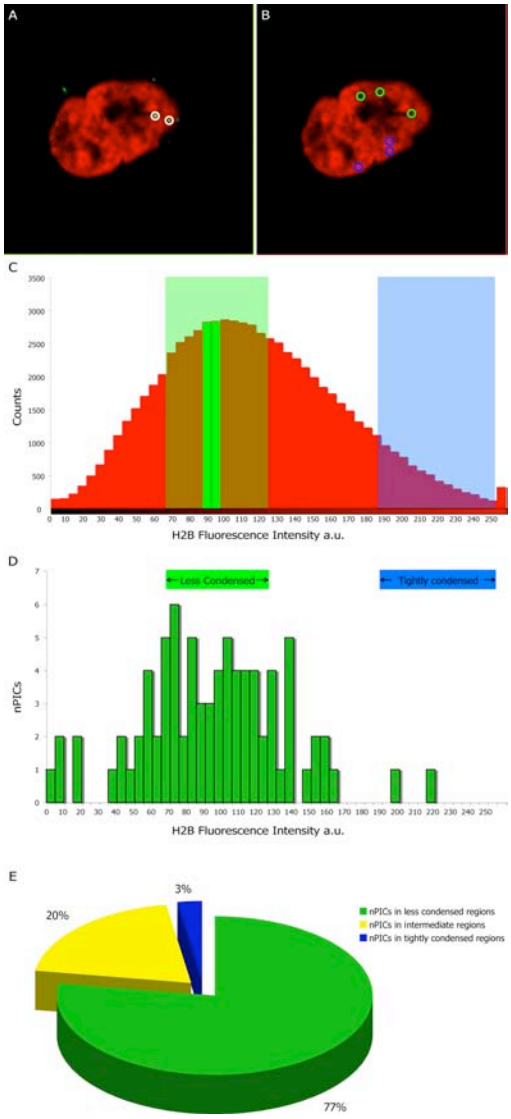

Figure 3-19. IN-EGFP PICs localize in less condensed chromatin regions. (A) H2B-EYFP (red) HeLa cells were infected with HIV-IN-EGFP virions (green). A circular ROI was drawn around each nuclear PIC and the mean fluorescence intensity in the EYFP channel has been measured and reported as green bar in the graph represented in C. (B) The mean fluorescence intensity was recorded in three ROIs drawn in the brightest regions (blue circles) and three more ROIs drawn in the darkest regions (green circles). Mean values and the standard deviations were calculated and plotted in C as light blue area and light green area, respectively. (C) Graph representing the counts of fluorescence intensity relative to H2B-EYFP, starting from the lowest value (zero) to 255. The resulting graph is a Gaussian curve, where the counts represent the number of pixels that have the same intensity value. The two green bars represent the mean value of the fluorescence intensity of the regions occupied by the two IN-ECFP nPICs visualized in A. (D) Histogram representing the number of PICs in the different regions of chromatin. (E) Pie graph showing the percentage of PICs in the less condensed regions, in the more condensed regione or in region in betweeen these two.

IN-EGFP viral particles selectively target euchromatin

The establishment of values of H2B-EYFP fluorescence intensity corresponding to heterochromatin allowed to set up a new and more rigorous method to analyze the condensation of the chromatin in the regions occupied by nPICs and to correlate it with either euchromatin or heterochromatin. However, this analysis method needed still an improvement. In fact, drawing a ROI around each nPICs includes also pixels that are not really occupied by them. Therefore, it was analyzed the condensation of the chromatin only in the pixels of H2B-EYFP images overlapping with IN-ECFP nPICs fluorescence signal. To this aim, 70 randomly chosen HeLa H2B-EYFP cells infected with HIV-IN-ECFP virions were analyzed, fixed 6 hours post-infection and immunostained with antibody α-Lamin A/C. As explained above, a *z*-stack of the whole nucleus of each cell was acquired by recording separately the three spectral channels corresponding to IN-ECFP, H2B-EYFP and Lamin A/C staining (Alexa-680). Figure 3-20A shows four representative HeLa H2B-EYFP nuclei (red) delimited by the nuclear lamin immunostaining (blue) and containing individual IN-ECFP viral PICs (green). A total of 103 IN-ECFP nPICs was identified in the nuclei of the 70 randomly chosen cells and a ROI was defined exactly in the pixels occupied by each nPIC (PIC ROIs). In addition, the same number of ROIs was randomly chosen within the same nuclear planes (Random ROIs). Subsequently, in order to see if there was a preferential distribution of IN-ECFP nPICs, H2B-EYFP fluorescence intensity was measured in the PIC ROIs (Figure 3-20B, red bars) and compared to the H2B-EYFP fluorescence intensity in the Random ROIs (Figure 3-20B, grey bars). As explained above and in Material and Methods, in order to obtain comparable values among different cells, the H2B-EYFP fluorescence intensity was rescaled over the entire 8-bit range (0-255 a.u.). As a result of this analysis the average H2B-EYFP fluorescence intensity was equal to 104.5±11 (mean±SD) and 132.6±15 (mean±SD) for PIC ROIs and Random ROIs, respectively. In order to understand weather the two distributions were similar, we compared them by using the non-parametric two-tailed Kolmogorov-Smirnov test, which yielded a statistically significant difference among them ($P<0.001$) (Figure 3-20B, inset). These results clearly demonstrate that IN-ECFP nPICs are non-randomly distributed in the nuclei, showing a preferential localization in low H2B-

EYFP fluorescence intensity areas. Moreover, since our previous experiments showed that H2B-EYFP fluorescence intensity ranging from 140 a.u. to 230 a.u. correlate with heterochromatin (indicated with an arrow in Figure 3-20B), and since nPICs occupy areas with a fluorescence intensity equal to 104.5±11, we can conclude that IN-ECFP nPICs avoid heterochromatic regions and selectively target euchromatin.

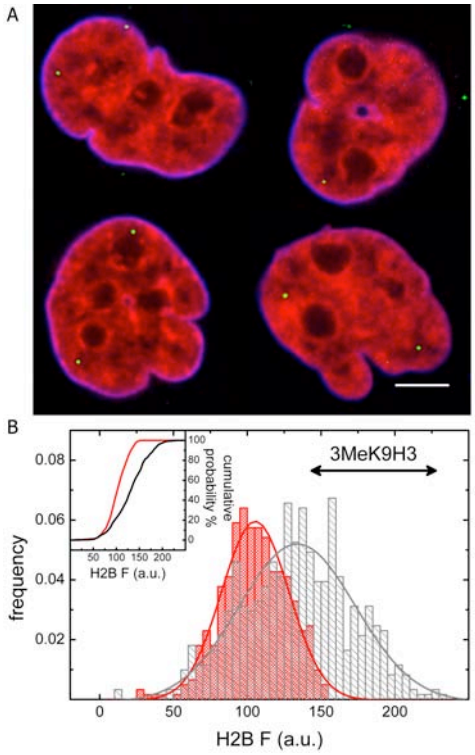

Figure 3-20. HIV-IN-ECFP virions preferentially localize in the periphery of the nucleus and outside heterochromatin regions. (A) Confocal images of HIV-IN-ECFP virions (green) in nuclei of HeLa cells expressing H2B-EYFP (red) and immunostained with antibody against lamin A/C (blue). Bar, 5 mm. (B) H2B-EYFP fluorescence intensità distribution frequency for PIC ROIs (defined by the HIV-IN-ECFP virions, red bars) and for Random ROIs (selected randomly in the same planes, grey bars) (n = 103). Solid lines are obtained by Gaussian fitting. The 3MeK9H3 labeled arrow represents the width at half-height of the H2BEYFP fluorescence intensity distribution derived by cross analyzing with this heterochromatin marker (see Experimental Procedures). In the inset the distribution cumulative probabilities are plotted for PIC ROIs (red) and Random ROIs (grey) (P,0.001, Kolmogorov–Smirnov test).

HIV-IN-EGFP AS NUCLEAR IMPORT ASSAY

Influences of drugs in nuclear import

In the past few years, many drugs have been developed to block different steps of HIV-1 replication cycle. For example, 3'azido-3'deoxythymidine (AZT) specifically blocks reverse transcription process, while MK-518 (Vandegraaff and Engelman, 2007) inhibits strand transfer activity of IN. Treatment of infected cells with these drugs differently affects the fate of PICs.

In order to investigate which step of the viral infectivity process is hampered, these drugs were tested in combination with HIV-IN-EGFP virus. First of all, different concentrations of AZT or MK-518 (1x, 10x, 100x, with respect to their IC50) were tested in order to completely impair viral replication cycle. Treated and untreated HeLa cells were infected with *wild-type* virus and luciferase activity was monitored 2 days post-infection. As shown in Figure 3-21A (green histogram), an IC50 of AZT results in a moderate decrease of luciferase activity. Increasing the concentration of two orders of magnitude almost no luciferase activity is detected, indicating that retrotranscription process is completely blocked. To exclude that luciferase activity was related to transcription of non-integrated viral DNA, the IN catalytically inactive viral clone D64E was used instead of NL4.3.Luc.R-E- (Figure 3-21A, red histogram). Similar results are observed in Figure 3-21B, indicating MK-518 completely blocks integration at a dosage of 100x with respect to its IC50. To monitor cells viability with the increasing concentration of AZT or MK-518, similar experiments were performed in uninfected cells, showing no cytopathic effects (Figure 3-21A and Figure 3-21B blue histogram, respectively).

Next, the effect of AZT and MK-518 on PICs nuclear import was monitored. To this aim, HeLa cells were treated with either AZT 100x or MK-518 100x and infected with HIV-IN-EGFP virions. As control, similar experiments were preformed on untreated HeLa cells. Since the amount of IN-EGFP PICs in the nucleus reaches its peak 6 hours post-infection, cells were fixed at this time point and immunostained with antibody α-Lamin A/C. Following, *z*-stacks of these cells were acquired and the amount of total and nuclear PICs was evaluated. Representative images of mock,

MK-518, and AZT treated cell are showed in Figure 3-22A, B and C, respectively.

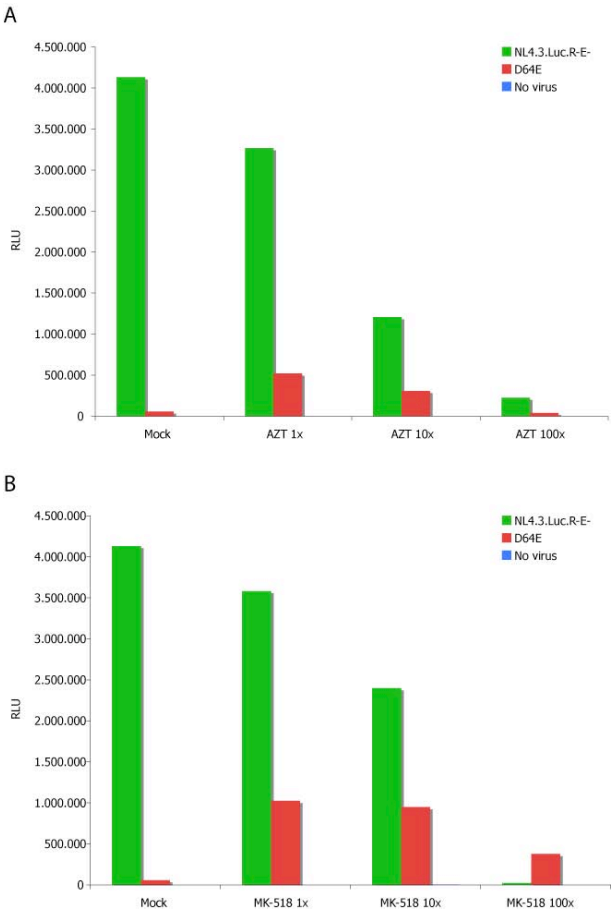

Figure 3-21. AZT and MK-518 impair HIV-1 viral replication. (A) HeLa cells non-treated (blue bar) or treated with different concentration (1x, 10x or 100x) of AZT were infected with *wild-type* (green bar) or D64E (red bar) viruses and luciferase activity was monitored 2 days post-infection. (B) Same as in A with MK-518 intstead of AZT.

In these experiments no major effects of the drugs on the fluorescence signal or cell morphology could be revealed, as shown in Figure 3-22D and E. The treatment with AZT or MK-518 does not alter the total amount of PICs in the cell (Figure 3-22D). Indeed, the average of PICs in mock cells is 176±7 (mean±SD), which is comparable with that of AZT or MK-518 treated cells, 182±3 and 173±12, respectively. However, the treatment with AZT 100x showed a drastic decrease of nuclear PICs (Figure 3-22E). In particular, no nPICs could be detected in 30 cells analyzed in two different experiments. These results suggest that the presence of

AZT influences the nuclear translocation of PICs. Previous data, based on molecular biology assays, indicate that AZT blocks retrotranscription of viral genome. The visualization of HIV-IN-EGFP trafficking in the infected cells treated with AZT showed that viral particles do not reach the nuclear compartment. Therefore, the accomplishment of the retrotranscription is required for the nuclear translocation. The number of nuclear PICs in MK-518 treated cells is slightly lower than mock, 2.4±0.2 compared to 3.2±0.3 (Figure 3-22B). This led us to hypothesize a putative role for MK-518 in destabilizing nPICs.

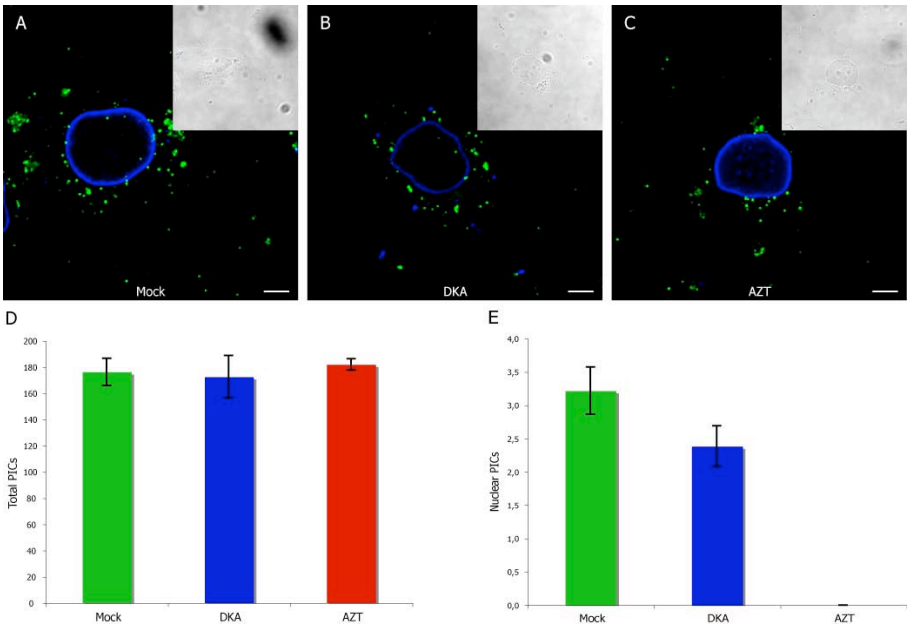

Figure 3-22. AZT blocks PICs nuclear import. HeLa cells non-treated (green bar), treated with DKA (MK-518, blue bar) or with AZT (red bar) were infected with HIV-IN-EGFP virions, fixed 6 hours post-infection and immunostained with antibody anti-Lamin A/C. Confocal *z*-stacks of these cells were acquired and representative images of mock, MK-518, and AZT treated cell are shown in A, B and C, respectively. The total and nuclear amount of PICs was evaluated and plotted in the graphs D and E, respectively. An average of 30 cells in two independent experiments was analyzed for each treatment and SD is represented as error bar.

In order to investigate on such hypothesis a time laps experiment was performed on HeLa cells treated with MK-518 and infected with HIV-IN-EGFP. Infected cells were fixed at different time points (3, 6, 9, 12, 16 and 24 hours post infection), immunostained with antibody α-Lamin A/C and then *z*-stack images were acquired at the confocal microscope. The results of total PICs and nuclear PICs at each time

point are shown in Figure 3-23A and B, respectively. The total amount of PICs in treated and not treated cells starts decreasing 9 hours post-infection and no significant differences are observed in the presence of MK-518. As shown in Figure 3-23B, the number of nuclear PICs in treated cells is lower at 6 hours post infection, at 3, 9 and 12 hours post infection the reduction is slightly lower with respect to the mock and at 16 and 24 hours post infection there are no differences. However, if any, the reductions are not significant and the histograms of mock and MK-518 treated cells are quite similar, suggesting that the drug does not influence either nuclear translocation, or nPICs stability.

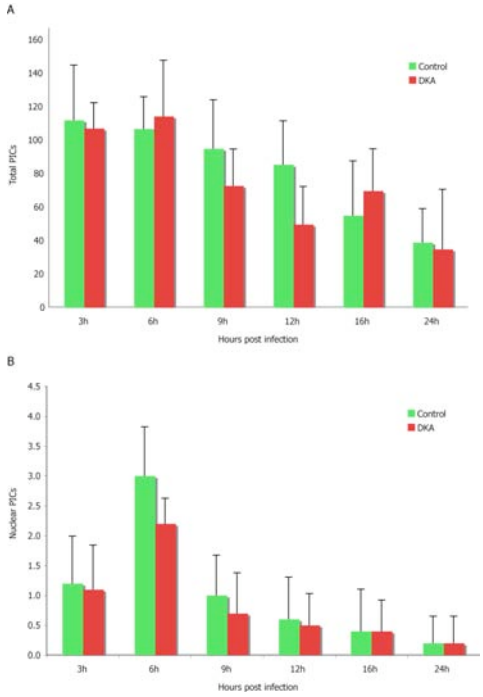

Figure 3-23. DKA does not affect the kinetic of nuclear import either the PIC stability in the nucleus. HeLa cells untreated or treated with DKA (MK-518) were infected with HIV-IN-EGFP virions, fixed and the mean number of total and intranuclear viral particles per cell was quantified at 3h, 6h, 9h, 12h, 16h and 24h. At each time point an average of 30 cells in two independent experiments was analyzed and the SD is represented as error bar.

Transportin SR2 imports PICs into the nucleus

Recently, it has been shown that the depletion of the cellular protein transportin SR2 (TRN-SR2) produces a lentiviral specific pre-integration block (Brass et al., 2008). Simultaneously, Debyser group revealed by two hybrid screening the interaction

between the same factor, transportin SR2, and integrase (Christ et al., 2008). Since transportin SR2 is involved in nuclear transportation, it was necessary to design experiments to address the role of this factor in HIV-1 nuclear entry. One of the most used nuclear import assay is an *in vitro* transport system, in which recombinant transport factors and their potential cargos are added to digitonin-premeabilized cells (Liu et al., 1999b). However, this import assay lacks the use of intact cells and intact nuclei. The use of a HIV-IN-EGFP virus allows to overcome this problem. In fact, as shown in the previous sections, visualization experiments with this fluorescently labeled virion revealed to be an accurate system to monitor the nuclear import of PICs.

The expression of transportin SR2 on HeLaP4 cells by selectively targeting its mRNA with a siRNA. In order to analyze at the confocal microscope only silenced cells, TR-siRNA was conjugated to the fluorescent probe Alexa-568 (siTRN-SR_2 Alexa-568). In parallel as a control, mismatch siRNA (siTRN-SR_2MM Alexa-568) was transfected in HeLaP4 cells. The day after these cells were infected with HIV-IN-EGFP virions, fixed six hours post-infection and immunostained with antibody anti-Lamin A/C, so as to clearly identify nuclear boundaries. As explained in detail above, a *z*-stack of the whole nucleus of each cell was acquired, by recording separately the three spectral channels corresponding to IN-EGFP, siTRN-SR_2MM Alexa-568 (Figure 3-24A and B) or siTRN-SR_2 Alexa-568 (Figure 3-24C and D), and Lamin A/C staining (Alexa-680). HeLaP4 cells positive for the fluorescently labeled siRNA-Alexa568 were analyzed with the confocal microscope in order to evaluate the ratio of nuclear over cytoplasmatic PICs. The number of nuclear and cytoplasmatic PICs was evaluated for each cell, and the derived ratio distribution plotted in Figure 3-24E. The average nuclear/cytoplasmatic ratio results equal to 0.4±0.1% and 2.1±0.1 (mean±SD; n=55) for the TRN-SR2 knocked down and control cells, respectively. The two distributions were then compared using the non-parametric two-tailed Kolmogorov-Smirnov test yielding a statistically significant difference ($P<0.001$) between the two cell populations. This analysis clearly demonstrates a decrease in the number of viral PICs in the nucleus upon TRN-SR2 depletion and demonstrates a primary role of this import factor in PIC nuclear translocation. This results in a strong defect in the integration with a consequent

block of viral replication. Therefore, the identification of small molecules that inhibit the interaction between IN and TRN-SR2 could open new strategies in the fight against HIV-1/AIDS.

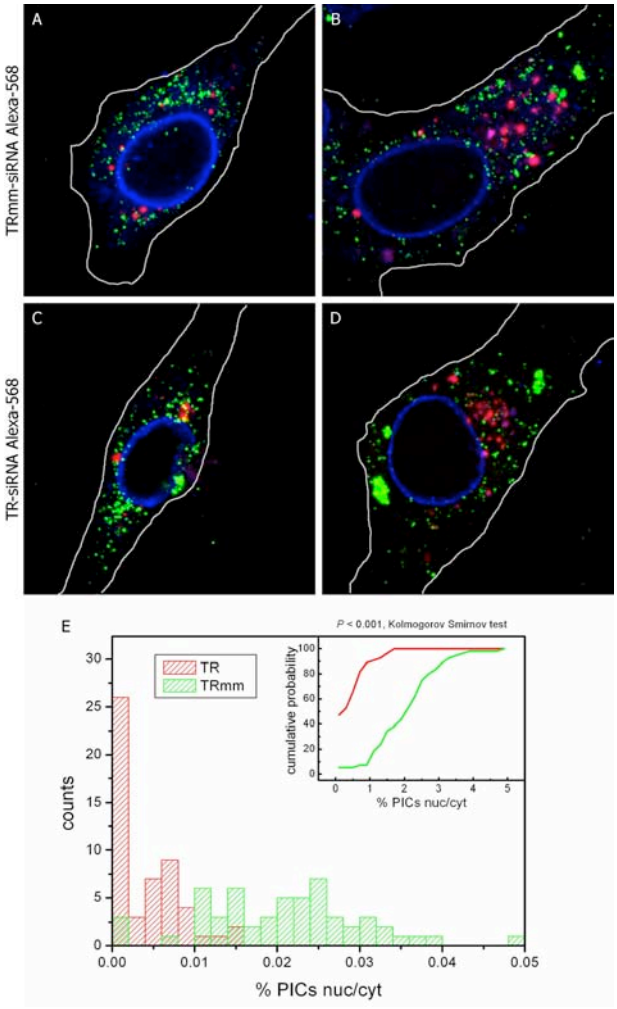

Figure 3-24. Nuclear Translocation of PICs in HeLaP4 TRN-SR2 Knockdown Cells (A-D) Representative images of cells treated with Alexa-568 (red)-labeled siTRN-SR_2MM (A and B) and siTRN-SR_2 (C and D). Cells were infected with HIV-IN-EGFP (green) and immunostained with lamin A/C (blue). Six hours after infection, cells were fixed and analyzed by laser-scanning confocal microscopy. Images are derived from confocal *z*-stacks with the maximum projection of 3-µm-thick slices centered in the middle of the nucleus. Cell shapes are outlined in white. (E) Percentage of PICs in the nucleus versus cytoplasmic PICs in cells treated with siTRN-SR_2 (red bars, n = 100) and siTRN-SR_2MM (green bars, n = 100). Nearly half of the cells treated with siTRN-SR_2 did not contain any PIC in the nucleus, whereas in the mismatched control cells, on average 2.2% of the PICs had been imported into the nucleus. In the inset, the distribution of cumulative probabilities is plotted for TRN-SR2 siRNA-treated cells (red) and mismatched siRNA-treated cells (gray) ($p < 0.001$, Kolmogorov-Smirnov test).

CHAPTER 4

DISCUSSION

Technology developed in the past 10 years has dramatically increased the ability of researchers to directly visualize and measure various stages of the HIV-1 life cycle. In many cases, the generation of a great variety of fluorescent viruses together with the use of imaging based approaches allowed to answer many previously unsolved issues, and to investigate new aspects of the viral replication cycle (Arhel et al., 2006a; Brandenburg and Zhuang, 2007; Campbell et al., 2007b; Damm et al., 2005; del Rio et al., 2005b; Jouvenet et al., 2008; Lakadamyali et al., 2003; Lampe et al., 2007; Lehmann et al., 2005; McDonald et al., 2002; McDonald et al., 2003; Muller et al., 2004; Nicola and Straus, 2004; Rudner et al., 2005; Rust et al., 2004). In addition, live cell imaging has allowed a better understanding of dynamic, transient events that occur during HIV-1 during HIV-1 replication, including the steps involved in viral fusion, trafficking of the viral nucleoprotein complex in the cytoplasm and the formation of new virions from an infected cell.

In this study we have engineered viral particles containing IN fused to EGFP. We have obtained this by the *trans*-incorporation system (Bachand et al., 1999; Paxton et al., 1993), allowing the preservation of viral activity. The resulting recombinant fluorescent virus enabled the visualization of pre-integration complexes in the nucleus of infected cells. We, thus, exploited HIV-IN-EGFP virions to study the infection process at the nuclear level. Our results show a prevalence of PICs in the nucleus 6 hours post-infection, which localize close to the nuclear periphery, specifically in euchromatin regions. Moreover, visualization experiments with IN-EGFP virions allowed to identify that PICs cannot reach the nuclear compartment in AZT treated cells, while MK-518 has no effect in the nuclear import or nuclear PIC stability. In addition, IN-EGFP virions revealed that the cellular protein TNPO3 is essential for the nuclear import of PICs. This last result arises the possibility to use such fluorescent virus as a tool in nuclear import assays.

MOLECULAR ENGINEERING OF FLUORESCENT HIV-1 PARTICLES

The work described in this thesis shows the development, the characterization and the exploitation of fluorescently labeled HIV-1 virus.

We produced a fluorescent HIV-1 virus by labeling with either EGFP or ECFP the viral protein IN. However, we could not insert the sequence of the fluorescent protein at the C-terminus of IN in the context of infectious molecular clones of HIV-1. In fact, previous attempts to produce retroviruses that contained integrase fusion proteins were unsuccessful due to loss of virus infectivity after transfection (Bushman and Miller, 1997) or loss of fusion protein expression during viral replication owing to reversion (Katz et al., 1996). Each of these attempts encoded the integrase fusion protein as part of the viral genome, inserting the DNA sequence of the sequence-specific DNA-binding protein at the 3' end of the integrase gene. The difficulty in encoding the fusion protein in the viral genome is probably due to the overlapping coding region of 3' IN with *vif* and to the splice acceptor site (Purcell and Martin, 1993). To avoid interfering with crucial elements in the integrase gene, we decided to incorporate IN-EGFP fusion protein into HIV-1 viral particles in *trans*. This approach, exploits the Vpr property to interact with p6 region of gag (Bachand et al., 1999; Paxton et al., 1993) to shuttle fused exogenous proteins inside the viral particles (Fletcher et al., 1997; Liu et al., 1997; Liu et al., 1999a; Wu et al., 1999; Wu et al., 1997; Wu et al., 1995). For example, the *trans*-incorporation system has been successfully used to incorporate IN-LexA (Holmes-Son and Chow, 2000) or IN-E2C (Tan et al., 2006). Importantly, the presence of Vpr at the N terminus of *trans*-incorporated IN does not complement efficiently the proviral D64E catalytically inactive IN unless it is cleaved from its fusion partner by the viral protease (Fletcher et al., 1997). Therefore, in order to restore its catalytic activity, we introduced a proteolytic cleavage site to remove Vpr from the IN-EGFP protein after packaging. The successful cleavage of the *trans*-incorporated construct Vpr-IN-EGFP by the HIV-1 protease shown in Figure 3-1 was verified by western blot in Figure 3-3A and B.

We evaluated the capacity of IN to perform the 3'-end-joining with the strand transfer assay (Figure 3-2), revealing that the introduction of EGFP protein at the C-terminus of IN does not affect its catalytic activity *in vitro*. Our data are in agreement with previous reports (Holmes-Son and Chow, 2000; Tan et al., 2006), showing that the fusion of different proteins at the C terminus of IN does not decrease strand transfer activity.

The HIV-IN-EGFP virions we produced are structurally intact. In fact, we confirmed by different criteria that EGFP signal marks genuine HIV-1 *trans*-incorporated complexes: WB (Figure 3-3), colocalization with $p17^{MA}$ and $p24^{CA}$ in extracellular (Figure 3-4) and intracellular complexes (Figure 3-5), and association with retrotranscribed viral DNA in the cytoplasm (Figure 3-6) and in the nucleus (Figure 3-14). WB analyses revealed that the *trans*-incorporation of Vpr-IN-EGFP protein does not alter the structural composition of the virions. Indeed, the composition of fluorescently labeled virions is consistent with that of *bona fide* viral particles. As observed in Figure 3-3, it is noteworthy that HIV-IN-EGFP virions have a greater amount of IN-EGFP compared to the amount of IN in *wild type* and mutated virions. This can be explained by the fact that IN-EGFP is *trans*-incorporated. Notably, visualization experiments on viral particles confirms WB analysis on complete viral assembly. In fact, colocalization with HIV-1 viral proteins in extracellular viral particles revealed that $p17^{MA}$ and $p24^{CA}$ are virtually always associated with the extracellular HIV-IN-EGFP virions as is expected for *wild type* and mutated viruses. An important consideration is that 80% of the viral particles double labeled with both α-$p17^{MA}$ and α-$p24^{CA}$ antibodies colocalize with IN-EGFP, indicating that our labeling system allows the detection of almost all virions by confocal microscopy.

Another interesting observation is that viral particles appear heterogeneous in size in the immunofluorescence with a broad distribution of fluorescence intensity (Figure 3-4). This is in accordance with previous data (Lampe et al., 2007) and is not surprising since HIV-1 particles display a flexible architecture with a broad rage of diameters and are composed of variable amounts of Gag polyproteins (Briggs et al., 2004; Briggs et al., 2003; Wilk et al., 2001).

VISUALIZATION OF HIV-IN-EGFP VIRIONS IN THE CYTOPLASM

The direct observation of individual virions in target cells increased our understanding of HIV-1 infection process (Arhel et al., 2006a; Campbell et al., 2007b; Jouvenet et al., 2008; Lampe et al., 2007; McDonald et al., 2002; Muller et al., 2004; Rudner et al., 2005), which had been difficult to study using classical

molecular and cellular biology techniques. This is because many of the virions that enter a target cell are non-specifically endocytosed and never enter the cytoplasm by envelope-mediated fusion, making the activity of the small population of relevant viral cores difficult to assay. Moreover, biologically important events might only occur in the context of intact viral cores, which are unstable and difficult to purify biochemically. The ability to fluorescently label HIV-1 viral particles with Vpr-IN-EGFP fusion protein allowed us to overcome this obstacle. In fact, IN remains associated with the viral genome until the viral complex enters the nucleus and integrates. Therefore, the labeling of IN allows the direct observation of both cytoplasmic and nuclear behaviour of individual PICs, as we showed in this thesis.

The first step for the virus during infection process is the binding to the plasma membrane. HIV-1 is considered to be relatively inefficient at infecting cells (Andreadis et al., 2000; Kimpton and Emerman, 1992; Piatak et al., 1993). Our studies have benefited from the ability to pseudotype HIV-1 virions with the pH-dependent envelope glycoprotein of vesicular stomatitis virus (VSV-g), which allows a majority of virions to productively enter the host cell, compared with the small percentage of virions that achieve productive entry using the HIV-1 envelope protein. In addition, we were interested in studying virions within the cell. Therefore, in order to distinguish between productive and non-productive entry, infected cells were treated with trypsin 1x. Recently, Campbell *et al.* (Campbell et al., 2007b) developed an elegant system based on a dual-fluorescent virus to clearly identify virions that have productively entered the target cells in a more elegant way. However, since our aim was to visualize IN-EGFP PICs within the nuclear compartment we did not implement the HIV-IN-EGFP virions with the double labeling system.

Following the entry, HIV-1 releases the capsid in the cytoplasm. There has been much speculation about the cytoplasmic fate of the capsid that contains the HIV genome inside virions. In some models, it dissolves immediately after membrane fusion (Bukrinsky et al., 1993b; Fassati and Goff, 2001; Miller et al., 1997). Others propose that it remains intact until the genome reaches a nuclear pore (Arhel et al., 2007; Forshey et al., 2002). Capsid is a relatively unstable complex that is sensitive

to all but the mildest detergent treatment. Therefore the way in which it is isolated and purified from infected cells could explain this discrepancy. Our results showed that the majority of IN-EGFP spots within the cell are positive for both $p17^{MA}$ and $p24^{CA}$ (Figure 3-5), and those within the nuclear compartment does not colocalize with $p24^{CA}$ (Figure 3-13), confirming that capsid shells disassemble before entering the nucleus. These data are in accordance with Foreshey *et al.* (Forshey et al., 2002), where they show that the stability of the viral core in the cytoplasm of infected cells is a prerequisite for efficient HIV-1 retrotranscription and infection. Moreover, our data are consistent with McDonald *et al.* (McDonald et al., 2002), where they demonstrate that capsid structure remains intact during the initiation of reverse transcription in the cytoplasm. The combination of fluorescent probes and confocal microscopy enabled to circumvent the problems related to the isolation and purification of cores, allowing us to investigate the real structure of the PICs within intact target cells without altering their structure and composition. This confirms the great powerful of the fluorescence approach in addressing issues without the artefacts related to other techniques.

Even though IN-EGFP particles in the cytoplasm colocalize with the viral proteins $p17^{MA}$ and $p24^{CA}$, it does not indicate they are pre-integration complexes. Indeed, PICs are usually defined as integration competent complexes, whereas complexes where reverse transcription process is incomplete are named reverse transcription complexes (RTCs) (Lehmann-Che and Saib, 2004; McDonald et al., 2002). The presence of EGFP fused to IN within the context of intracellular viral complexes might interfere with reverse transcription process, leading to the formation of RTCs and not of PICs. In order to visualize reverse transcription associated with the internalized viral particle, Hope's lab (McDonald et al., 2002) injected a fluorescently labeled deoxynucleotide into the cells before infection. This is an elegant approach to show the retrotranscribed viral DNA in the cytoplasm, although fluorescently labeled dUTPs are also incorporated in the nucleus of the target cells as a consequence of the microinjection during cellular DNA replication. Therefore the high background signal prevents the visualization of retrotranscribed viral cDNA within the nuclear compartment. To circumvent the problem we took advantage of the natural endogenous reverse transcription activity of the HIV-1 viral particles.

Following this procedure neo-synthesized viral cDNA was visualized both in the cytoplasm (Figure 3-6) and in the nuclear compartment (Figure 3-14)., associated to the IN-EGFP particles. It has been shown that virions subjected to NERT are about twice infectious as untreated controls (Naldini et al., 1996). However, we detected only a minority of IN-EGFP particles colocalizing with the fluorescently labeled viral DNA. This reduced number of positive PICs can be explained by the reported observation that only a limited number of entered viral particles is actually infective (Thomas et al., 2007). Alternatively, this discrepancy could be explained with the lack of poliamines in our reaction mixture during natural endogenous reverse transcription, which have been shown to remarkably enhance HIV-1 reverse transcription (Zhang et al., 1996). Another important consideration to take into account is the steric hindrance of the fluorescently moiety of Alexa-dUTPs, which could lead to abortive or non-infectious viral particles. However, the observation of HIV-IN-EGFP reverse transcribed viral particles within the nuclear compartment (Figure 3-14) shows that the fluorescent label of dUTPs does not impair neither the accomplishment of the retrotranscription process nor the nuclear import. Finally, our results prove that IN-EGFP complexes are indeed functional PICs.

FUNCTIONAL IN-EGFP PICS TRANSLOCATE IN THE NUCLEUS

The main scope of this study was the nuclear visualization of HIV-1 PICs. Our great effort was to clearly identify the nuclear boundaries, so as to precisely distinguish nuclear PICs from cytoplasmic PICs. To this aim we labeled nuclear lamin, which stains the inner membrane of the nucleus. This approach resulted to be the best solution in order to avoid misinterpretations (see Figure 3-8, Figure 3-9, Figure 3-11 and Figure 3-12). The combination of multidirectional imaging and accurate image processing allowed us to unambiguously identify the viral particles located inside the nuclear envelope and distinguish them from those located in its outer proximity. In fact, we infected cells with HIV-IN-EGFP and we immunostained them with antibody anti-Lamin A/C. Our results (Figure 3-11 and Figure 3-12) show a high number of fluorescent PICs very close or juxtaposed to the nuclear membrane, thus an accurate analysis is necessary to establish the nuclear nature of viral PICs. The acquisition of a cell with both the XYZ and XZY scan modes (Figure 3-12) revealed

the same amount of PICs in the nucleus, validating therefore our experimental set up and acquisition system.

Notably, we observed a high frequency of PICs adherent to the borders of the nuclei (Figure 3-12). Our results are in agreement with previous reports, where they showed that a significant proportion of the signal accumulated in the perinuclear region (McDonald et al., 2002). These data suggests that the transition through the nuclear membrane is a strong limiting factor during viral replication. This observation is also supported by the disproportionate number of nuclear versus cytoplasmic viral particles (1/50 ratio). Similarly, Thomas *et al.* (Thomas et al., 2007) showed a predominance of virions that do not accomplish reverse transcription with respect to those that successfully integrate. In addition, our data are consistent with Iordanskiy *et al.* (Iordanskiy et al., 2006); in fact, they exploited quantitative real time PCR to reveal a ratio of nuclear to cytoplasmic complexes of 1:60. Therefore, results obtained with the multidirectional confocal microscopy we set up are in agreement with data coming from a molecular biology approach, further confirming the powerful of the HIV-IN-EGFP fluorescent virus as a reliable tool to study HIV-1 biology.

It has been estimated that proviral DNA is detectable almost 8 hours after HIV-1 entry (Kim et al., 1989). We have thus quantified the number of viral PICs at different time points from 3 to 24 hours after infection. We found that the maximum nuber of intranuclear HIV-IN-EGFP PICs was observed at 6 hours post-infection (Figure 15). The observation of PICs in the nuclear compartment few hours post-infection (3 and 6 hours) is confirmed by previous studies, where they revealed PICs containing retrotranscribed viral DNA in nuclear extracts four hours after infection (Fassati and Goff, 2001). At subsequent time points we detected that the number of PICs rapidly declined and virtually none was detected 24 hours post-infection (Figure 15). Our kinetic data are at odds with previous studies (Arhel et al., 2006a). In fact, very recently Arhel *et al.* developed a fluorescent virus based on Flash labeling of IN, allowing HIV-1 nuclear visualization. This system has the enormous advantage of exploiting a very little tag, and thus it does not lead to disruption of viral functions and loss of infectivity (Engelman et al., 1995; Muller et al., 2004).

However, they reported to detect only occasionally Flash-labeled HIV-1 complexes within nuclear compartment 24 hours after infection. This discrepancy could be explained by a lower sensitivity of the tetracystein labeling approach coupled to an analyses performed 24 hours post-infection instead of 6 hours (Figure 3-15).

HIV-1 is able to replicate in interphasic cells (Weinberg et al., 1991), indicating that PICs are able to actively cross the nuclear membrane (Bukrinsky et al., 1992). In contrast, it has been shown that PICs from most retroviruses are unable to enter intact nuclei and are believed to wait until nuclear membrane breakdown during mitosis (Lehmann-Che and Saib, 2004; Lewis and Emerman, 1994; Roe et al., 1993). Completion of the reverse transcription correlates with changes in protein composition of the PICs, which may contribute to the ability of complexes to translocate through the nuclear pore complexes. Recently, it has been shown that disassembly of nuclear membrane during mitosis allows cytoplasmic viral complexes to get access to the nuclear compartment (Iordanskiy et al., 2006). Among these, there are two populations: complexes containing incomplete reverse transcription products (RTCs) and integration-competent complexes (PICs). Iordanskiy *et al.* showed that these nuclear immature RTCs, contain RT and incomplete DNA, can accomplish reverse transcription, but are defective for integration (Iordanskiy et al., 2006). Therefore, one could infer that IN-EGFP PICs we visualized in the nucleus belong to this population, getting access to the nuclear compartment during mitosis. However, we showed that the nuclear IN-EGFP PICs we observed did not translocate in the nucleus as a consequence of nuclear membrane breakdown. As a matter of fact, we did not detect any IN-EGFP PICS in the nucleus of cells treated with AZT (Figure 3-22). In fact, blocking reverse transcription process, AZT impedes the intracytoplasmic maturation of RTCs in functional PICs. We showed that incomplete reverse transcription results in a block of PICs nuclear import (Figure 3-22). Consequently, IN-EGFP particles in cells treated with AZT can get access to the nucleus only during mitosis. However, the complete absence of nuclear PICs in 60 different treated cells suggests that this phenomenon is negligible with our experimental set up.

DISTRIBUTION OF IN-EGFP PARTICLES IN THE NUCLEUS

Integration of the viral cDNA into the host cellular genome is a necessary and deeply investigated event in retroviral replication, particularly as concerns the identification of the preferred integration sites. To date, however, no specific genomic sequences have been associated to such sites. Yet, unraveling the mechanisms of integration-site selection for HIV-1 is important not only to better understand the biology of retroviruses but also because of its impact on other fields as retrovirus-based technology. For instance, retroviral vectors have been extensively developed for gene therapy applications, however their use is limited by the uncontrollable integration site, a situation that may eventually cause disruption of normal cellular proliferation (Cereseto and Giacca, 2004; Hacein-Bey-Abina et al., 2003b). In fact, it is now clear that integration of therapeutic retroviral vectors can activate proto-oncogenes in patients (Bushman, 2002; Hacein-Bey-Abina et al., 2003a; Hacein-Bey-Abina et al., 2003b; Williams and Baum, 2003). In recent years, wide genome and transcriptome surveys revealed that retroviral integration is favoured near transcriptionally active genes (Crise et al., 2005; Kang et al., 2006; Lewinski et al., 2006; Mitchell et al., 2004; Schroder et al., 2002; Wu et al., 2003). Mounting evidence suggest that the cellular lens epithelium-derived growth factor (LEDGF/p75), a IN-interacting factor (Cherepanov et al., 2003; Emiliani et al., 2005; Turlure et al., 2004), may direct viral integration into transcription units (Ciuffi et al., 2005; Shun et al., 2007b). It has been speculated that LEDGF/p75 may tether PICs at specific sites by interacting through its PWWP domain with specific histone modifications associated with transcriptional elongation. Indeed, the role of the chromatin structure and of higher order nuclear organization in retroviral integration has not been yet investigated.

In order to visualize the distribution of PICs with respect to the chromatin organization,we exploited the fluorescently labeled histone H2B (H2B-EYFP). In fact, it is part of the nucleosomes, which are localized in the nucleus. Many different groups have already used this nuclear marker, since it allows the identification of the nucleus both in fixed and in living cells (Kanda et al., 1998; Kimura and Cook, 2001; Weidemann et al., 2003). Therefore, we reasoned that the visualization with

confocal microscopy of the fluorescent signal coming from the labeled H2B could precisely identify the nuclear structure and organization. In fact, the ability of the confocal microscope to create sharp optical sections allows the 3D image reconstruction of nucleus. Thus, we infected HeLa cells constitutively expressing H2B-EYFP with HIV-IN-ECFP virions and we immunostained them with antibody anti-Lamin A/C, in order to accurately distinguish cytoplasmic PICs from nuclear PICs. By using HeLa H2B-EYFP cells as an experimental system to distinguish different chromatin structure regions (Bhattacharya et al., 2006; Kanda et al., 1998; Kimura and Cook, 2001), this study demonstrates that the vast majority of PICs localize in decondensed regions of the chromatin, as compared to more condensed areas (Figure 3-20). To better correlate chromatin condensation forms observed in these cells with functionally distinct regions of euchromatin or heterochromatin, we exploited antibodies against post-translational modification of histone H3 (K9 tri-methylated) specific for transcriptionally silenced regions of heterochromatin (Kouzarides, 2007) (Figure 22 and Figure 23). Localization in euchromatin regions is in accordance with a recent report showing that proviral integration sites are characterized by specific epigenetic codes (Wang et al., 2007). The association with definite regions of the chromatin marked by specific post-translational modifications might also suggest that chromatin modification factor/s might tether HIV-1 to specific sites. We have recently demonstrated that cellular histone-acetyltransferase, p300, acetylates IN and enhances viral integration (Cereseto et al., 2005). This cellular enzyme, which determines chromatin decondensation through histones acetylation, may favour integration by both acetylating IN and by tethering the virus to acetylated/decondensed regions of the chromatin. Further study must be carried out to address these hypotheses (Cereseto and Giacca, 2004). In addition, another factor has been shown to be involved in tethering HIV-1 PICs to the cellular genomic transcription units: LEDGF/p75 (Ciuffi et al., 2005; Shun et al., 2007a). LEDGF/p75 is predominantly localized in the nucleus, where it is intimately associated with the chromosomes (Nishizawa et al., 2001), and it is implicated in gene expression (Fatma et al., 2001; Ge et al., 1998; Singh et al., 2001). The PWWP domain of LEDGF/p75 interacts specifically with histone modifications associated with transcriptional elongation. Therefore, it has been suggested that LEDGF might tether PICs at specific sites in the nucleus (De Rijck et al., 2007;

Van Maele et al., 2006). Taking into account all these data, what does really address PICs in transcriptionally active regions? Is it the histone-acetyltransferase p300, which binds IN and tethers PICs to acetylated regions of the chromatin? Is it the binding of LEDGF at the cytoplasmic level, which tether PICs to transcriptionally active units and increase the affinity of IN for DNA? Is it the structure of the chromatin, which allows PICs to easily move in euchromatin, while it blocks their entry in the tightly condensed heterochromatin? It is not easy to answer these questions, however we can speculate on it taking into account our current knowledge in this field. Interestingly, it has been shown that heterochromatin is characterized by an apparent pore size of 16–20 nm (Gorisch et al., 2005). This means that molecules or complexes higher than this value are excluded from heterochromatin. Notably, PICs are characterized by the presence of many proteins and the retrotranscribed viral genome. Therefore, they are enormous complexes, with a size estimated around 28 nm (Miller et al., 1997). This means that they can easily enter into the nucleus through the nuclear pore complexes, which are able to transport macromolecules up to 39 nm (Pante and Kann, 2002). On the contrary, they are excluded by the tightly packed chromatin, since they find a physical barrier of 16-20 nm.

Interestingly, we found that IN-EGFP PICs displays a clear preferential position at the nuclear periphery (Figure 3-16). This result, together with the observation that PICs distribute in euchromatic regions, suggests a role for chromatin structure in addressing the viral complexes towards preferential genome domains. This perspective arises by the fact that DNA-related metabolic processes including transcription, recombination, DNA repair and replication, are coordinated by functionally distinct chromatin domains spatially arranged within a precisely defined nuclear architecture (Misteli, 2007). It is known that chromosomes, genome regions and single genes are nonrandomly arranged within the nucleus (Casolari et al., 2004; Taddei et al., 2006; van Steensel et al., 2001). Interestingly, recent advances highlight the role of nuclear envelope components in the control of gene expression (Akhtar and Gasser, 2007). Indeed, it has been showed that the peripheral localization of genome regions might occur directly via interactions between lamin A and core histones (Gruenbaum et al., 2005). In addition, the position of single genes relative to the nuclear periphery is non random, but rather linked to their

functional status (Chambeyron and Bickmore, 2004; Kim et al., 2004). Moreover, very recently Taddei *et al.* (Taddei et al., 2006) demonstrated that genes repositioned to the nuclear periphery interact with the nuclear pore components when they are activated. As a consequence, there is a specific chromatin architecture very close to the nuclear periphery, which may dictate or influence the position of pre-integration complexes within the nuclear compartment. Therefore, once nPICs translocate into the nucleus, they get in contact with less condensed and more accessible euchromatin, which favours the integration process (Bushman et al., 2005). Bushman lab (Schroder et al., 2002) showed that genes activated by infection are favoured integration targets. Consequently, activation process itself may promote formation of regional hotspots. Therefore, one could speculate that following infection some genes are activated and repositioned towards the nuclear periphery. As a consequence of activation these genes are in a more open chromatin structure, thus favouring integration process (Bushman et al., 2005).

Taking into account the above observations and our results, we can hypothesize that once accomplished reverse transcription process, PICs loose $p24^{CA}$ and translocate in the nucleus through the nuclear pores. As soon as they pass the nuclear pores and arrive in the nuclear compartment they are already in euchromatin regions, since transcriptionally active genes are associated with nuclear pore complexes (Gruenbaum et al., 2005; Taddei et al., 2006). At this stage, PICs can move only in the less condensed chromatin regions, since they are physically excluded from the heterochromatin (Gorisch et al., 2005). Therefore chromatin would act as a determinant element for PICs distribution. Subsequently, other proteins such as p300 and/or LEDGF/p75 might act by bridging PICs to specific regions of the cellular euchromatin.

HIV-IN-EGFP AS NUCLEAR IMPORT ASSAY

Lentiviruses are capable of infecting non-dividing cells, such as terminally differentiated macrophages (Lewis et al., 1992), due to their capacity to translocate in the nuclear compartment through the nuclear pore complexes. Once reached the nucleus the integration process takes place. Therefore, one very interesting target of anti-retroviral therapy is blocking the nuclear entry, which, in turn, abolishes the integration and the subsequent viral replication and spreading.

As described in the introduction, it has to be considered that nuclear import is not accompanied by a measurable enzymatic activity (De Rijck et al., 2007). To date, different techniques have been used such as fractionation assays (Mannioui et al., 2005), southern blot (Petit et al., 2000), digitonin-permeabilized cells (Adam et al., 1990). PICs nuclear import can be also indirectly measured quantifying the integrated proviruses. However, it can happen that retrotranscribed viral genome can translocate in the nuclear compartment without being integrated. To circumvent this problem, 2-LTR circles have been used as an indirect measure for the nuclear import of PICs. In fact, once in the nucleus, viral DNA can be integrated or forms 1-LTR and 2-LTR circles, which are dead-end by-products of viral replication (Coffin et al., 1997). For example, a reduction in the 2-LTR formation and a subsequent block of integration suggest that the block of HIV-1 replication is at the nuclear entry step.

Since the fluorescent virus we developed can be detected at the nuclear level, we reasoned that it could be used as direct assay to measure nuclear import. To assess such role we exploited two different drugs: 3'azido-3'deoxythymidine (AZT) and MK-518. While the former specifically blocks reverse transcription process, the latter inhibits strand transfer activity of IN. We reasoned to test the fluorescently labeled virus with these drugs because they differently affect the fate of PICs. In fact, while the block of retrotranscription hampers nuclear import, inhibition of IN activity does not prevent PICs from reaching the nucleus. As we showed (Figure 16 and Figure 17) AZT completely inhibit the nuclear translocation. In fact, as recently reported, the block in reverse transcription is determinant for the nuclear import (Iordanskiy et al., 2006). On the contrary, MK-518 did not hamper PICs to reach the nucleus, even if it blocked retroviral integration. In addition, our results revealed only a slightly decrease of PICs nuclear import, which is not statistically significative, suggesting that this drug acts exclusively through its two strand-transfer-specific IN inhibition activity and does not affect PICs stability of kinetic of nuclear translocation. These results confirmed the specificity of HIV-IN-EGFP in combination with nuclear lamin staining as experimental tool to monitor nuclear import

To date many viral and cellular nuclear import factors have been investigated: MA (Bukrinsky et al., 1993a), Vpr (Heinzinger et al., 1994), the DNA Flap (De Rijck and Debyser, 2006), IN (Depienne et al., 2000; Limon et al., 2002b; Pluymers et al., 1999; Tsurutani et al., 2000), LEDGF/p75 (Llano et al., 2004; Maertens et al., 2004). Despite the great efforts in finding a putative factor involved, no one of the proposed can be put forward as the dominant nuclear import factor. Moreover, some factors are actually involved in steps before or after nuclear import; therefore mutations on these proteins can lead to only an apparent nuclear import defect. In addition, it might be that HIV-1 has adopted several redundant pathways to ensure that the PICs can pass the critical step of nuclear import. Very recently, Debyser lab discovered a cellular co-factor, known as transportin TRN-SR2 (Christ et al., 2008). This factor has been identified as HIV-1 IN co-factor with yeast two-hybrid screen system. They showed that its depletion interferes with HIV-1 replication. The reduction in the 2-LTR circles formation together with the block of integration suggested that nuclear import of PICs was hampered. However, a direct assay to reveal such block was missing. Therefore, we exploited HIV-IN-EGFP virus as an *in vivo* nuclear import assay to demonstrate the defect in PICs nuclear translocation after depletion of TRN-SR2 (Figure 3-24). This method allowed to conclude that the great majority of siRNA-treated cells did not contain any PIC in the nucleus as opposed to control cell lines. Very recently, Brass *et al.* (Brass et al., 2008) published an extensive siRNA screen to identify host factors of HIV-1 IIIb replication. Two hundred and seventy three siRNAs that decreased HIV replication at least 2-fold were identified. Interestingly, the *tnpo3* gene, encoding for TRN-SR2 was identified as a hit. However, they did not pinpoint IN as the viral partner of interaction, nor could they validate TRN-SR2 as the nuclear import factor of HIV. Therefore, this is the first time that a HIV-1 cellular co-factor has been put forward as dominant nuclear import factor.

To productively infect host cells, HIV needs to perform two entry steps. First the virus has to attach cellular membrane receptors and co-receptors in order to enter the cytoplasm. Once the pre-integration complex is formed, it needs to dock onto nuclear-import receptors to cross the second physical barrier against infection: the nuclear membrane. Cell fusion inhibitors like maraviroc and enfuvirtide have

successfully entered the clinic (Flexner, 2007). Because nuclear import is still poorly understood in comparison, it has remained a yet unexplored target in anti-HIV therapy. The strong replication defect provoked by silencing of TRN-SR2 provides a rationale for the identification of small-molecule protein-protein interaction inhibitors to obstruct loading of the PIC onto its nuclear import factor. Subsequently, the use of HIV-IN-EGFP together with lamin staining could be exploited as a tool to identify or validate such inhibitors. This shows great promise for HIV-IN-EGFP as s novel tool to study anti-HIV drugs.

FUTURE PERSPECTIVES

In the absence of an effective vaccine against human immunodeficiency virus type 1 (HIV-1), small molecule inhibitors that target essential steps in the viral life cycle represent the best strategy for suppressing HIV-1 replication and controlling the spread of AIDS. There are currently four classes of drugs approved for use with AIDS patients: fusion inhibitors that block virus entry; nucleoside reverse transcriptase inhibitors (NRTIs) that mimic natural nucleotide substrates; non-nucleoside reverse transcriptase inhibitors (NNRTIs) that allosterically inhibit reverse transcriptase; and protease inhibitors (PIs). Highly active antiretroviral therapy (HAART), typically consisting of a PI or NNRTI and two NRTIs, is in most cases sufficient to reduce and/or maintain HIV-1 RNA levels within patient blood to below levels of detection. However, the relatively low fidelity of the reverse transcriptase enzyme in combination with the enormous population of circulating virus particles at steady-state replication leads to resistance to single as well as multiple drug classes (Brenner et al., 2002; Wensing and Boucher, 2003). Furthermore, cessation of HAART in patients with undetectable viral RNA loads for periods up to 2 years invariably results in viral rebound, indicating the presence of ongoing residual replication in the presence of therapy and/or the persistence of latent virus capable of reactivation in response to environmental triggers (Chun et al., 1997; Finzi et al., 1999; Wong et al., 1997). Considering the toxicity associated with many of the available treatments (Carr et al., 1998; Lewis et al., 2003) and difficulties in adhering to complex treatment regimens, there is an urgent need to identify and develop new drug targets. As we showed in the last part of this thesis,

hampering nuclear import of PICs is perhaps one of the most interesting perspectives, since it impede the PIC to enter in the nuclear compartment and, in turn, it would block viral integration.

Therefore, the ability of HIV-1 labeled virus as nuclear import tool could be exploited in the development of such new compounds. However, usually a great number of drugs need to be tested. To this aim, the combination of HIV-IN-EGFP virions with the lamina labeling might be improved and implemented in an automated high throughput system, so as to screen a huge number of putative drugs that block the PICs nuclear import. The resulting system could lead to the development of new compounds to treat AIDS.

CHAPTER 5

REFERENCES

Abruzzi, K.C., Belostotsky, D.A., Chekanova, J.A., Dower, K. and Rosbash, M. (2006) 3'-end formation signals modulate the association of genes with the nuclear periphery as well as mRNP dot formation. *Embo J*, **25**, 4253-4262.

Adam, S.A., Marr, R.S. and Gerace, L. (1990) Nuclear protein import in permeabilized mammalian cells requires soluble cytoplasmic factors. *J Cell Biol*, **111**, 807-816.

Adams, S.R., Campbell, R.E., Gross, L.A., Martin, B.R., Walkup, G.K., Yao, Y., Llopis, J. and Tsien, R.Y. (2002) New biarsenical ligands and tetracysteine motifs for protein labeling in vitro and in vivo: synthesis and biological applications. *J Am Chem Soc*, **124**, 6063-6076.

Aiyar, A., Hindmarsh, P., Skalka, A.M. and Leis, J. (1996) Concerted integration of linear retroviral DNA by the avian sarcoma virus integrase in vitro: dependence on both long terminal repeat termini. *J Virol*, **70**, 3571-3580.

Akhtar, A. and Gasser, S.M. (2007) The nuclear envelope and transcriptional control. *Nat Rev Genet*, **8**, 507-517.

Albanese, A., Arosio, D., Terreni, M. and Cereseto, A. (2008) HIV-1 pre-integration complexes selectively target decondensed chromatin in the nuclear periphery. *PLoS ONE*, **3**, e2413.

Alberts, B., Johnson, A., Lewis, J., Raff, M., Roberts, K. and Walter, P. (2002) *Molecular biology of the cell*. Garland Science, New York.

Allis, C.D., Jenuwein, T. and Reinberg, D. (2007) *Epigenetics*. Cold Spring Harbor Laboratory Press, Cold Spring Harbor, N.Y.

Amos, W.B. and White, J.G. (2003) How the confocal laser scanning microscope entered biological research. *Biol Cell*, **95**, 335-342.

Andreadis, S., Lavery, T., Davis, H.E., Le Doux, J.M., Yarmush, M.L. and Morgan, J.R. (2000) Toward a more accurate quantitation of the activity of recombinant retroviruses: alternatives to titer and multiplicity of infection. *J Virol*, **74**, 1258-1266.

Ao, Z., Fowke, K.R., Cohen, E.A. and Yao, X. (2005) Contribution of the C-terminal tri-lysine regions of human immunodeficiency virus type 1 integrase for efficient reverse transcription and viral DNA nuclear import. *Retrovirology*, **2**, 62.

Apolonia, L., Waddington, S.N., Fernandes, C., Ward, N.J., Bouma, G., Blundell, M.P., Thrasher, A.J., Collins, M.K. and Philpott, N.J. (2007)

Stable gene transfer to muscle using non-integrating lentiviral vectors. *Mol Ther*, **15**, 1947-1954.

Arhel, N., Genovesio, A., Kim, K.A., Miko, S., Perret, E., Olivo-Marin, J.C., Shorte, S. and Charneau, P. (2006a) Quantitative four-dimensional tracking of cytoplasmic and nuclear HIV-1 complexes. *Nat Methods*, **3**, 817-824.

Arhel, N.J., Souquere-Besse, S. and Charneau, P. (2006b) Wild-type and central DNA flap defective HIV-1 lentiviral vector genomes: intracellular visualization at ultrastructural resolution levels. *Retrovirology*, **3**, 38.

Arhel, N.J., Souquere-Besse, S., Munier, S., Souque, P., Guadagnini, S., Rutherford, S., Prevost, M.C., Allen, T.D. and Charneau, P. (2007) HIV-1 DNA Flap formation promotes uncoating of the pre-integration complex at the nuclear pore. *Embo J*, **26**, 3025-3037.

Asante-Appiah, E. and Skalka, A.M. (1999) HIV-1 integrase: structural organization, conformational changes, and catalysis. *Adv Virus Res*, **52**, 351-369.

Axelrod, D. (2001) Total internal reflection fluorescence microscopy in cell biology. *Traffic*, **2**, 764-774.

Babcock, H.P., Chen, C. and Zhuang, X. (2004) Using single-particle tracking to study nuclear trafficking of viral genes. *Biophys J*, **87**, 2749-2758.

Bachand, F., Yao, X.J., Hrimech, M., Rougeau, N. and Cohen, E.A. (1999) Incorporation of Vpr into human immunodeficiency virus type 1 requires a direct interaction with the p6 domain of the p55 gag precursor. *J Biol Chem*, **274**, 9083-9091.

Barr, S.D., Ciuffi, A., Leipzig, J., Shinn, P., Ecker, J.R. and Bushman, F.D. (2006) HIV integration site selection: targeting in macrophages and the effects of different routes of viral entry. *Mol Ther*, **14**, 218-225.

Barr, S.D., Leipzig, J., Shinn, P., Ecker, J.R. and Bushman, F.D. (2005) Integration targeting by avian sarcoma-leukosis virus and human immunodeficiency virus in the chicken genome. *J Virol*, **79**, 12035-12044.

Bartz, S.R., Rogel, M.E. and Emerman, M. (1996) Human immunodeficiency virus type 1 cell cycle control: Vpr is cytostatic and mediates G2 accumulation by a mechanism which differs from DNA damage checkpoint control. *J Virol*, **70**, 2324-2331.

Beitzel, B. and Bushman, F. (2003) Construction and analysis of cells lacking the HMGA gene family. *Nucleic Acids Res*, **31**, 5025-5032.

Belmont, A.S. (2002) Mitotic chromosome scaffold structure: new approaches to an old controversy. *Proc Natl Acad Sci U S A*, **99**, 15855-15857.

Belmont, A.S. and Bruce, K. (1994) Visualization of G1 chromosomes: a folded, twisted, supercoiled chromonema model of interphase chromatid structure. *J Cell Biol*, **127**, 287-302.

Bernstein, B.E., Meissner, A. and Lander, E.S. (2007) The mammalian epigenome. *Cell*, **128**, 669-681.

Berthoux, L., Sebastian, S., Sokolskaja, E. and Luban, J. (2005) Cyclophilin A is required for TRIM5{alpha}-mediated resistance to HIV-1 in Old World monkey cells. *Proc Natl Acad Sci U S A*, **102**, 14849-14853.

Bhattacharya, D., Mazumder, A., Miriam, S.A. and Shivashankar, G.V. (2006) EGFP-tagged core and linker histones diffuse via distinct mechanisms within living cells. *Biophys J*, **91**, 2326-2336.

Bieniasz, P.D. (2004) Intrinsic immunity: a front-line defense against viral attack. *Nat Immunol*, **5**, 1109-1115.

Bieniasz, P.D., Grdina, T.A., Bogerd, H.P. and Cullen, B.R. (1998) Recruitment of a protein complex containing Tat and cyclin T1 to TAR governs the species specificity of HIV-1 Tat. *Embo J*, **17**, 7056-7065.

Bor, Y.C., Bushman, F.D. and Orgel, L.E. (1995) In vitro integration of human immunodeficiency virus type 1 cDNA into targets containing protein-induced bends. *Proc Natl Acad Sci U S A*, **92**, 10334-10338.

Bor, Y.C., Miller, M.D., Bushman, F.D. and Orgel, L.E. (1996) Target-sequence preferences of HIV-1 integration complexes in vitro. *Virology*, **222**, 283-288.

Bosco, D.A., Eisenmesser, E.Z., Pochapsky, S., Sundquist, W.I. and Kern, D. (2002) Catalysis of cis/trans isomerization in native HIV-1 capsid by human cyclophilin A. *Proc Natl Acad Sci U S A*, **99**, 5247-5252.

Bosco, D.A. and Kern, D. (2004) Catalysis and binding of cyclophilin A with different HIV-1 capsid constructs. *Biochemistry*, **43**, 6110-6119.

BouHamdan, M., Xue, Y., Baudat, Y., Hu, B., Sire, J., Pomerantz, R.J. and Duan, L.X. (1998) Diversity of HIV-1 Vpr interactions involves usage of the WXXF motif of host cell proteins. *J Biol Chem*, **273**, 8009-8016.

Bour, S. and Strebel, K. (2003) The HIV-1 Vpu protein: a multifunctional enhancer of viral particle release. *Microbes Infect*, **5**, 1029-1039.

Brandenburg, B. and Zhuang, X. (2007) Virus trafficking - learning from single-virus tracking. *Nat Rev Microbiol*, **5**, 197-208.

Brass, A.L., Dykxhoorn, D.M., Benita, Y., Yan, N., Engelman, A., Xavier, R.J., Lieberman, J. and Elledge, S.J. (2008) Identification of host proteins required for HIV infection through a functional genomic screen. *Science*, **319**, 921-926.

Brenner, B.G., Turner, D. and Wainberg, M.A. (2002) HIV-1 drug resistance: can we overcome? *Expert Opin Biol Ther*, **2**, 751-761.

Briggs, J.A., Simon, M.N., Gross, I., Krausslich, H.G., Fuller, S.D., Vogt, V.M. and Johnson, M.C. (2004) The stoichiometry of Gag protein in HIV-1. *Nat Struct Mol Biol*, **11**, 672-675.

Briggs, J.A., Wilk, T., Welker, R., Krausslich, H.G. and Fuller, S.D. (2003) Structural organization of authentic, mature HIV-1 virions and cores. *Embo J*, **22**, 1707-1715.

Bukrinsky, M.I., Haggerty, S., Dempsey, M.P., Sharova, N., Adzhubel, A., Spitz, L., Lewis, P., Goldfarb, D., Emerman, M. and Stevenson, M. (1993a) A nuclear localization signal within HIV-1 matrix protein that governs infection of non-dividing cells. *Nature*, **365**, 666-669.

Bukrinsky, M.I., Sharova, N., Dempsey, M.P., Stanwick, T.L., Bukrinskaya, A.G., Haggerty, S. and Stevenson, M. (1992) Active nuclear import of human immunodeficiency virus type 1 preintegration complexes. *Proc Natl Acad Sci U S A*, **89**, 6580-6584.

Bukrinsky, M.I., Sharova, N., McDonald, T.L., Pushkarskaya, T., Tarpley, W.G. and Stevenson, M. (1993b) Association of integrase, matrix, and reverse transcriptase antigens of human immunodeficiency virus type 1 with viral nucleic acids following acute infection. *Proc Natl Acad Sci U S A*, **90**, 6125-6129.

Bushman, F. (2002) *Lateral DNA transfer : mechanisms and consequences*. Cold Spring Harbor Laboratory Press, Cold Spring Harbor, N.Y.

Bushman, F., Lewinski, M., Ciuffi, A., Barr, S., Leipzig, J., Hannenhalli, S. and Hoffmann, C. (2005) Genome-wide analysis of retroviral DNA integration. *Nat Rev Microbiol*, **3**, 848-858.

Bushman, F.D. (1994) Tethering human immunodeficiency virus 1 integrase to a DNA site directs integration to nearby sequences. *Proc Natl Acad Sci U S A*, **91**, 9233-9237.

Bushman, F.D., Engelman, A., Palmer, I., Wingfield, P. and Craigie, R. (1993) Domains of the integrase protein of human immunodeficiency virus type 1 responsible for polynucleotidyl transfer and zinc binding. *Proc Natl Acad Sci U S A*, **90**, 3428-3432.

Bushman, F.D. and Miller, M.D. (1997) Tethering human immunodeficiency virus type 1 preintegration complexes to target DNA promotes integration at nearby sites. *J Virol*, **71**, 458-464.

Busschots, K., Vercammen, J., Emiliani, S., Benarous, R., Engelborghs, Y., Christ, F. and Debyser, Z. (2005) The interaction of LEDGF/p75 with integrase is lentivirus-specific and promotes DNA binding. *J Biol Chem*, **280**, 17841-17847.

Campbell, E.M., Dodding, M.P., Yap, M.W., Wu, X., Gallois-Montbrun, S., Malim, M.H., Stoye, J.P. and Hope, T.J. (2007a) TRIM5 alpha cytoplasmic bodies are highly dynamic structures. *Mol Biol Cell*, **18**, 2102-2111.

Campbell, E.M., Nunez, R. and Hope, T.J. (2004) Disruption of the actin cytoskeleton can complement the ability of Nef to enhance human immunodeficiency virus type 1 infectivity. *J Virol*, **78**, 5745-5755.

Campbell, E.M., Perez, O., Anderson, J.L. and Hope, T.J. (2008) Visualization of a proteasome-independent intermediate during restriction of HIV-1 by rhesus TRIM5alpha. *J Cell Biol*, **180**, 549-561.

Campbell, E.M., Perez, O., Melar, M. and Hope, T.J. (2007b) Labeling HIV-1 virions with two fluorescent proteins allows identification of virions that have productively entered the target cell. *Virology*, **360**, 286-293.

Carlson, M. and Laurent, B.C. (1994) The SNF/SWI family of global transcriptional activators. *Curr Opin Cell Biol*, **6**, 396-402.

Carr, A., Samaras, K., Chisholm, D.J. and Cooper, D.A. (1998) Pathogenesis of HIV-1-protease inhibitor-associated peripheral lipodystrophy, hyperlipidaemia, and insulin resistance. *Lancet*, **351**, 1881-1883.

Carteau, S., Hoffmann, C. and Bushman, F. (1998) Chromosome structure and human immunodeficiency virus type 1 cDNA integration: centromeric alphoid repeats are a disfavored target. *J Virol*, **72**, 4005-4014.

Casolari, J.M., Brown, C.R., Komili, S., West, J., Hieronymus, H. and Silver, P.A. (2004) Genome-wide localization of the nuclear transport machinery couples transcriptional status and nuclear organization. *Cell*, **117**, 427-439.

Cereseto, A. and Giacca, M. (2004) Integration site selection by retroviruses. *AIDS Rev*, **6**, 13-21.

Cereseto, A., Manganaro, L., Gutierrez, M.I., Terreni, M., Fittipaldi, A., Lusic, M., Marcello, A. and Giacca, M. (2005) Acetylation of HIV-1 integrase by p300 regulates viral integration. *Embo J*, **24**, 3070-3081.

Chalfie, M., Tu, Y., Euskirchen, G., Ward, W.W. and Prasher, D.C. (1994) Green fluorescent protein as a marker for gene expression. *Science*, **263**, 802-805.

Chambeyron, S. and Bickmore, W.A. (2004) Chromatin decondensation and nuclear reorganization of the HoxB locus upon induction of transcription. *Genes Dev*, **18**, 1119-1130.

Champoux, J.J. (1977) Strand breakage by the DNA untwisting enzyme results in covalent attachment of the enzyme to DNA. *Proc Natl Acad Sci U S A*, **74**, 3800-3804.

Charneau, P., Alizon, M. and Clavel, F. (1992) A second origin of DNA plus-strand synthesis is required for optimal human immunodeficiency virus replication. *J Virol*, **66**, 2814-2820.

Charneau, P., Mirambeau, G., Roux, P., Paulous, S., Buc, H. and Clavel, F. (1994) HIV-1 reverse transcription. A termination step at the center of the genome. *J Mol Biol*, **241**, 651-662.

Chen, P., Hubner, W., Spinelli, M.A. and Chen, B.K. (2007) Predominant mode of human immunodeficiency virus transfer between T cells is mediated by sustained Env-dependent neutralization-resistant virological synapses. *J Virol*, **81**, 12582-12595.

Cherepanov, P., Devroe, E., Silver, P.A. and Engelman, A. (2004) Identification of an evolutionarily conserved domain in human lens epithelium-derived growth factor/transcriptional co-activator p75 (LEDGF/p75) that binds HIV-1 integrase. *J Biol Chem*, **279**, 48883-48892.

Cherepanov, P., Maertens, G., Proost, P., Devreese, B., Van Beeumen, J., Engelborghs, Y., De Clercq, E. and Debyser, Z. (2003) HIV-1 integrase forms stable tetramers and associates with LEDGF/p75 protein in human cells. *J Biol Chem*, **278**, 372-381.

Choe, H., Farzan, M., Sun, Y., Sullivan, N., Rollins, B., Ponath, P.D., Wu, L., Mackay, C.R., LaRosa, G., Newman, W., Gerard, N., Gerard, C. and Sodroski, J. (1996) The beta-chemokine receptors CCR3 and CCR5 facilitate infection by primary HIV-1 isolates. *Cell*, **85**, 1135-1148.

Chowers, M.Y., Spina, C.A., Kwoh, T.J., Fitch, N.J., Richman, D.D. and Guatelli, J.C. (1994) Optimal infectivity in vitro of human

immunodeficiency virus type 1 requires an intact nef gene. *J Virol*, **68**, 2906-2914.

Christ, F., Thys, W., De Rijck, J., Gijsbers, R., Albanese, A., Arosio, D., Emiliani, S., Rain, J.C., Benarous, R., Cereseto, A. and Debyser, Z. (2008) Transportin-SR2 Imports HIV into the Nucleus. *Curr Biol*, **18**, 1192-1202.

Chun, T.W., Stuyver, L., Mizell, S.B., Ehler, L.A., Mican, J.A., Baseler, M., Lloyd, A.L., Nowak, M.A. and Fauci, A.S. (1997) Presence of an inducible HIV-1 latent reservoir during highly active antiretroviral therapy. *Proc Natl Acad Sci U S A*, **94**, 13193-13197.

Ciuffi, A., Llano, M., Poeschla, E., Hoffmann, C., Leipzig, J., Shinn, P., Ecker, J.R. and Bushman, F. (2005) A role for LEDGF/p75 in targeting HIV DNA integration. *Nat Med*, **11**, 1287-1289.

Cody, C.W., Prasher, D.C., Westler, W.M., Prendergast, F.G. and Ward, W.W. (1993) Chemical structure of the hexapeptide chromophore of the Aequorea green-fluorescent protein. *Biochemistry*, **32**, 1212-1218.

Coelho, P.A., Queiroz-Machado, J. and Sunkel, C.E. (2004) Could condensin scaffold the mitotic chromosome? *Cell Cycle*, **3**, 538-540.

Coffin, J.M. (1979) Structure, replication, and recombination of retrovirus genomes: some unifying hypotheses. *J Gen Virol*, **42**, 1-26.

Coffin, J.M., Hughes, S.H. and Varmus, H. (1997) *Retroviruses*. Cold Spring Harbor Laboratory Press, Plainview, N.Y.

Cohen, E.A., Dehni, G., Sodroski, J.G. and Haseltine, W.A. (1990) Human immunodeficiency virus vpr product is a virion-associated regulatory protein. *J Virol*, **64**, 3097-3099.

Connor, R.I., Chen, B.K., Choe, S. and Landau, N.R. (1995) Vpr is required for efficient replication of human immunodeficiency virus type-1 in mononuclear phagocytes. *Virology*, **206**, 935-944.

Corbeil, J., Sheeter, D., Genini, D., Rought, S., Leoni, L., Du, P., Ferguson, M., Masys, D.R., Welsh, J.B., Fink, J.L., Sasik, R., Huang, D., Drenkow, J., Richman, D.D. and Gingeras, T. (2001) Temporal gene regulation during HIV-1 infection of human CD4+ T cells. *Genome Res*, **11**, 1198-1204.

Crameri, A., Whitehorn, E.A., Tate, E. and Stemmer, W.P. (1996) Improved green fluorescent protein by molecular evolution using DNA shuffling. *Nat Biotechnol*, **14**, 315-319.

Crise, B., Li, Y., Yuan, C., Morcock, D.R., Whitby, D., Munroe, D.J., Arthur, L.O. and Wu, X. (2005) Simian immunodeficiency virus integration preference is similar to that of human immunodeficiency virus type 1. *J Virol*, **79**, 12199-12204.

Cubitt, A.B., Heim, R., Adams, S.R., Boyd, A.E., Gross, L.A. and Tsien, R.Y. (1995) Understanding, improving and using green fluorescent proteins. *Trends Biochem Sci*, **20**, 448-455.

Cullen, B.R. (1998) Retroviruses as model systems for the study of nuclear RNA export pathways. *Virology*, **249**, 203-210.

Dalgleish, A.G., Beverley, P.C., Clapham, P.R., Crawford, D.H., Greaves, M.F. and Weiss, R.A. (1984) The CD4 (T4) antigen is an essential component of the receptor for the AIDS retrovirus. *Nature*, **312**, 763-767.

Damm, E.M., Pelkmans, L., Kartenbeck, J., Mezzacasa, A., Kurzchalia, T. and Helenius, A. (2005) Clathrin- and caveolin-1-independent endocytosis: entry of simian virus 40 into cells devoid of caveolae. *J Cell Biol*, **168**, 477-488.

De Rijck, J. and Debyser, Z. (2006) The central DNA flap of the human immunodeficiency virus type 1 is important for viral replication. *Biochem Biophys Res Commun*, **349**, 1100-1110.

De Rijck, J., Vandekerckhove, L., Christ, F. and Debyser, Z. (2007) Lentiviral nuclear import: a complex interplay between virus and host. *Bioessays*, **29**, 441-451.

De Rijck, J., Vandekerckhove, L., Gijsbers, R., Hombrouck, A., Hendrix, J., Vercammen, J., Engelborghs, Y., Christ, F. and Debyser, Z. (2006) Overexpression of the lens epithelium-derived growth factor/p75 integrase binding domain inhibits human immunodeficiency virus replication. *J Virol*, **80**, 11498-11509.

del Rio, T., Ch'ng, T.H., Flood, E.A., Gross, S.P. and Enquist, L.W. (2005a) Heterogeneity of a fluorescent tegument component in single pseudorabies virus virions and enveloped axonal assemblies. *J Virol*, **79**, 3903-3919.

del Rio, T., DeCoste, C.J. and Enquist, L.W. (2005b) Actin is a component of the compensation mechanism in pseudorabies virus virions lacking the major tegument protein VP22. *J Virol*, **79**, 8614-8619.

DelPiero, G., Albanese, R., Albanese, G. and Albanese, A. (2009) Aiorte DNA Rganu ie Sote Sere Canna. *J Str On Z A*, **10**, 19-77.

Demirov, D.G., Orenstein, J.M. and Freed, E.O. (2002) The late domain of human immunodeficiency virus type 1 p6 promotes virus release in a cell type-dependent manner. *J Virol*, **76**, 105-117.

Deng, H., Liu, R., Ellmeier, W., Choe, S., Unutmaz, D., Burkhart, M., Di Marzio, P., Marmon, S., Sutton, R.E., Hill, C.M., Davis, C.B., Peiper, S.C., Schall, T.J., Littman, D.R. and Landau, N.R. (1996) Identification of a major co-receptor for primary isolates of HIV-1. *Nature*, **381**, 661-666.

Depienne, C., Mousnier, A., Leh, H., Le Rouzic, E., Dormont, D., Benichou, S. and Dargemont, C. (2001) Characterization of the nuclear import pathway for HIV-1 integrase. *J Biol Chem*, **276**, 18102-18107.

Depienne, C., Roques, P., Creminon, C., Fritsch, L., Casseron, R., Dormont, D., Dargemont, C. and Benichou, S. (2000) Cellular distribution and karyophilic properties of matrix, integrase, and Vpr proteins from the human and simian immunodeficiency viruses. *Exp Cell Res*, **260**, 387-395.

Derdowski, A., Ding, L. and Spearman, P. (2004) A novel fluorescence resonance energy transfer assay demonstrates that the human immunodeficiency virus type 1 Pr55Gag I domain mediates Gag-Gag interactions. *J Virol*, **78**, 1230-1242.

Dhalluin, C., Carlson, J.E., Zeng, L., He, C., Aggarwal, A.K. and Zhou, M.M. (1999) Structure and ligand of a histone acetyltransferase bromodomain. *Nature*, **399**, 491-496.

Di Marzio, P., Choe, S., Ebright, M., Knoblauch, R. and Landau, N.R. (1995) Mutational analysis of cell cycle arrest, nuclear localization and virion packaging of human immunodeficiency virus type 1 Vpr. *J Virol*, **69**, 7909-7916.

Dimitrova, D.S. and Gilbert, D.M. (1999) The spatial position and replication timing of chromosomal domains are both established in early G1 phase. *Mol Cell*, **4**, 983-993.

Dohner, K., Wolfstein, A., Prank, U., Echeverri, C., Dujardin, D., Vallee, R. and Sodeik, B. (2002) Function of dynein and dynactin in herpes simplex virus capsid transport. *Mol Biol Cell*, **13**, 2795-2809.

Dou, Y. and Gorovsky, M.A. (2002) Regulation of transcription by H1 phosphorylation in Tetrahymena is position independent and requires clustered sites. *Proc Natl Acad Sci U S A*, **99**, 6142-6146.

Dvorin, J.D., Bell, P., Maul, G.G., Yamashita, M., Emerman, M. and Malim, M.H. (2002) Reassessment of the roles of integrase and the central DNA

flap in human immunodeficiency virus type 1 nuclear import. *J Virol*, **76**, 12087-12096.

Ebina, H., Aoki, J., Hatta, S., Yoshida, T. and Koyanagi, Y. (2004) Role of Nup98 in nuclear entry of human immunodeficiency virus type 1 cDNA. *Microbes Infect*, **6**, 715-724.

Eckstein, D.A., Sherman, M.P., Penn, M.L., Chin, P.S., De Noronha, C.M., Greene, W.C. and Goldsmith, M.A. (2001) HIV-1 Vpr enhances viral burden by facilitating infection of tissue macrophages but not nondividing CD4+ T cells. *J Exp Med*, **194**, 1407-1419.

Ehrlich, M., Boll, W., Van Oijen, A., Hariharan, R., Chandran, K., Nibert, M.L. and Kirchhausen, T. (2004) Endocytosis by random initiation and stabilization of clathrin-coated pits. *Cell*, **118**, 591-605.

Elphick, G.F., Querbes, W., Jordan, J.A., Gee, G.V., Eash, S., Manley, K., Dugan, A., Stanifer, M., Bhatnagar, A., Kroeze, W.K., Roth, B.L. and Atwood, W.J. (2004) The human polyomavirus, JCV, uses serotonin receptors to infect cells. *Science*, **306**, 1380-1383.

Emiliani, S., Mousnier, A., Busschots, K., Maroun, M., Van Maele, B., Tempe, D., Vandekerckhove, L., Moisant, F., Ben-Slama, L., Witvrouw, M., Christ, F., Rain, J.C., Dargemont, C., Debyser, Z. and Benarous, R. (2005) Integrase mutants defective for interaction with LEDGF/p75 are impaired in chromosome tethering and HIV-1 replication. *J Biol Chem*, **280**, 25517-25523.

Engelman, A. (1999) In vivo analysis of retroviral integrase structure and function. *Adv. Virus. Res.*, **52**, 411-426.

Engelman, A., Englund, G., Orenstein, J.M., Martin, M.A. and Craigie, R. (1995) Multiple effects of mutations in human immunodeficiency virus type 1 integrase on viral replication. *J Virol*, **69**, 2729-2736.

Engelman, A., Hickman, A.B. and Craigie, R. (1994) The core and carboxyl-terminal domains of the integrase protein of human immunodeficiency virus type 1 each contribute to nonspecific DNA binding. *J Virol*, **68**, 5911-5917.

Engelman, A., Mizuuchi, K. and Craigie, R. (1991) HIV-1 DNA integration: mechanism of viral DNA cleavage and DNA strand transfer. *Cell*, **67**, 1211-1221.

Ewers, H., Smith, A.E., Sbalzarini, I.F., Lilie, H., Koumoutsakos, P. and Helenius, A. (2005) Single-particle tracking of murine polyoma virus-like

particles on live cells and artificial membranes. *Proc Natl Acad Sci U S A*, **102**, 15110-15115.

Farnet, C.M. and Bushman, F.D. (1997) HIV-1 cDNA integration: requirement of HMG I(Y) protein for function of preintegration complexes in vitro. *Cell*, **88**, 483-492.

Fassati, A. and Goff, S.P. (2001) Characterization of intracellular reverse transcription complexes of human immunodeficiency virus type 1. *J Virol*, **75**, 3626-3635.

Fatma, N., Singh, D.P., Shinohara, T. and Chylack, L.T., Jr. (2001) Transcriptional regulation of the antioxidant protein 2 gene, a thiol-specific antioxidant, by lens epithelium-derived growth factor to protect cells from oxidative stress. *J Biol Chem*, **276**, 48899-48907.

Felsenfeld, G. and Groudine, M. (2003) Controlling the double helix. *Nature*, **421**, 448-453.

Finzi, D., Blankson, J., Siliciano, J.D., Margolick, J.B., Chadwick, K., Pierson, T., Smith, K., Lisziewicz, J., Lori, F., Flexner, C., Quinn, T.C., Chaisson, R.E., Rosenberg, E., Walker, B., Gange, S., Gallant, J. and Siliciano, R.F. (1999) Latent infection of CD4+ T cells provides a mechanism for lifelong persistence of HIV-1, even in patients on effective combination therapy. *Nat Med*, **5**, 512-517.

Fischle, W., Tseng, B.S., Dormann, H.L., Ueberheide, B.M., Garcia, B.A., Shabanowitz, J., Hunt, D.F., Funabiki, H. and Allis, C.D. (2005) Regulation of HP1-chromatin binding by histone H3 methylation and phosphorylation. *Nature*, **438**, 1116-1122.

Fitzgerald, M.L. and Grandgenett, D.P. (1994) Retroviral integration: in vitro host site selection by avian integrase. *J Virol*, **68**, 4314-4321.

Fletcher, T.M., 3rd, Soares, M.A., McPhearson, S., Hui, H., Wiskerchen, M., Muesing, M.A., Shaw, G.M., Leavitt, A.D., Boeke, J.D. and Hahn, B.H. (1997) Complementation of integrase function in HIV-1 virions. *Embo J*, **16**, 5123-5138.

Flexner, C. (2007) HIV drug development: the next 25 years. *Nat Rev Drug Discov*, **6**, 959-966.

Flint, S.J., Enquist, L.W., Krug, R.M., R., R.V. and Skalka, A.M. (2004) *Principles of virology : molecular biology, pathogenesis, and control of animal viruses*. ASM Press, Washington, D.C.

Forshey, B.M., von Schwedler, U., Sundquist, W.I. and Aiken, C. (2002) Formation of a human immunodeficiency virus type 1 core of optimal stability is crucial for viral replication. *J Virol*, **76**, 5667-5677.

Fouchier, R.A., Meyer, B.E., Simon, J.H., Fischer, U. and Malim, M.H. (1997) HIV-1 infection of non-dividing cells: evidence that the amino-terminal basic region of the viral matrix protein is important for Gag processing but not for post-entry nuclear import. *Embo J*, **16**, 4531-4539.

Francastel, C., Schubeler, D., Martin, D.I. and Groudine, M. (2000) Nuclear compartmentalization and gene activity. *Nat Rev Mol Cell Biol*, **1**, 137-143.

Franke, E.K., Yuan, H.E. and Luban, J. (1994) Specific incorporation of cyclophilin A into HIV-1 virions. *Nature*, **372**, 359-362.

Frankel, A.D. and Young, J.A. (1998) HIV-1: fifteen proteins and an RNA. *Annu Rev Biochem*, **67**, 1-25.

Freed, E.O. (2004) HIV-1 and the host cell: an intimate association. *Trends Microbiol*, **12**, 170-177.

Furukawa, K. (1999) LAP2 binding protein 1 (L2BP1/BAF) is a candidate mediator of LAP2-chromatin interaction. *J Cell Sci*, **112 (Pt 15)**, 2485-2492.

Gallay, P., Hope, T., Chin, D. and Trono, D. (1997) HIV-1 infection of nondividing cells through the recognition of integrase by the importin/karyopherin pathway. *Proc Natl Acad Sci U S A*, **94**, 9825-9830.

Gallay, P., Stitt, V., Mundy, C., Oettinger, M. and Trono, D. (1996) Role of the karyopherin pathway in human immunodeficiency virus type 1 nuclear import. *J Virol*, **70**, 1027-1032.

Gallay, P., Swingler, S., Song, J., Bushman, F. and Trono, D. (1995) HIV nuclear import is governed by the phosphotyrosine-mediated binding of matrix to the core domain of integrase. *Cell*, **83**, 569-576.

Garcia, J.V. and Miller, A.D. (1991) Serine phosphorylation-independent downregulation of cell-surface CD4 by nef. *Nature*, **350**, 508-511.

Garrus, J.E., von Schwedler, U.K., Pornillos, O.W., Morham, S.G., Zavitz, K.H., Wang, H.E., Wettstein, D.A., Stray, K.M., Cote, M., Rich, R.L., Myszka, D.G. and Sundquist, W.I. (2001) Tsg101 and the vacuolar protein sorting pathway are essential for HIV-1 budding. *Cell*, **107**, 55-65.

Ge, H., Si, Y. and Roeder, R.G. (1998) Isolation of cDNAs encoding novel transcription coactivators p52 and p75 reveals an alternate regulatory mechanism of transcriptional activation. *Embo J*, **17**, 6723-6729.

Georgi, A., Mottola-Hartshorn, C., Warner, A., Fields, B. and Chen, L.B. (1990) Detection of individual fluorescently labeled reovirions in living cells. *Proc Natl Acad Sci U S A*, **87**, 6579-6583.

Glozak, M.A., Sengupta, N., Zhang, X. and Seto, E. (2005) Acetylation and deacetylation of non-histone proteins. *Gene*, **363**, 15-23.

Goff, S.P. (2007) Host factors exploited by retroviruses. *Nat Rev Microbiol*, **5**, 253-263.

Goh, W.C., Rogel, M.E., Kinsey, C.M., Michael, S.F., Fultz, P.N., Nowak, M.A., Hahn, B.H. and Emerman, M. (1998) HIV-1 Vpr increases viral expression by manipulation of the cell cycle: a mechanism for selection of Vpr in vivo. *Nat Med*, **4**, 65-71.

Goldberg, A.D., Allis, C.D. and Bernstein, E. (2007) Epigenetics: a landscape takes shape. *Cell*, **128**, 635-638.

Goll, M.G. and Bestor, T.H. (2005) Eukaryotic cytosine methyltransferases. *Annu Rev Biochem*, **74**, 481-514.

Gomez, C.Y. and Hope, T.J. (2006) Mobility of human immunodeficiency virus type 1 Pr55Gag in living cells. *J Virol*, **80**, 8796-8806.

Goodarzi, G., Chiu, R., Brackmann, K., Kohn, K., Pommier, Y. and Grandgenett, D.P. (1997) Host site selection for concerted integration by human immunodeficiency virus type-1 virions in vitro. *Virology*, **231**, 210-217.

Goodenow, M.M. and Hayward, W.S. (1987) 5' long terminal repeats of myc-associated proviruses appear structurally intact but are functionally impaired in tumors induced by avian leukosis viruses. *J Virol*, **61**, 2489-2498.

Gorisch, S.M., Wachsmuth, M., Toth, K.F., Lichter, P. and Rippe, K. (2005) Histone acetylation increases chromatin accessibility. *J Cell Sci*, **118**, 5825-5834.

Gottlinger, H.G., Sodroski, J.G. and Haseltine, W.A. (1989) Role of capsid precursor processing and myristoylation in morphogenesis and infectivity of human immunodeficiency virus type 1. *Proc Natl Acad Sci U S A*, **86**, 5781-5785.

Goulaouic, H. and Chow, S.A. (1996) Directed integration of viral DNA mediated by fusion proteins consisting of human immunodeficiency virus type 1 integrase and Escherichia coli LexA protein. *J Virol*, **70**, 37-46.

Gousset, K., Ablan, S.D., Coren, L.V., Ono, A., Soheilian, F., Nagashima, K., Ott, D.E. and Freed, E.O. (2008) Real-time visualization of HIV-1 GAG trafficking in infected macrophages. *PLoS Pathog*, **4**, e1000015.

Greber, U.F. and Way, M. (2006) A superhighway to virus infection. *Cell*, **124**, 741-754.

Griffin, B.A., Adams, S.R. and Tsien, R.Y. (1998) Specific covalent labeling of recombinant protein molecules inside live cells. *Science*, **281**, 269-272.

Gruenbaum, Y., Margalit, A., Goldman, R.D., Shumaker, D.K. and Wilson, K.L. (2005) The nuclear lamina comes of age. *Nat Rev Mol Cell Biol*, **6**, 21-31.

Hacein-Bey-Abina, S., von Kalle, C., Schmidt, M., Le Deist, F., Wulffraat, N., McIntyre, E., Radford, I., Villeval, J.L., Fraser, C.C., Cavazzana-Calvo, M. and Fischer, A. (2003a) A serious adverse event after successful gene therapy for X-linked severe combined immunodeficiency. *N Engl J Med*, **348**, 255-256.

Hacein-Bey-Abina, S., Von Kalle, C., Schmidt, M., McCormack, M.P., Wulffraat, N., Leboulch, P., Lim, A., Osborne, C.S., Pawliuk, R., Morillon, E., Sorensen, R., Forster, A., Fraser, P., Cohen, J.I., de Saint Basile, G., Alexander, I., Wintergerst, U., Frebourg, T., Aurias, A., Stoppa-Lyonnet, D., Romana, S., Radford-Weiss, I., Gross, F., Valensi, F., Delabesse, E., Macintyre, E., Sigaux, F., Soulier, J., Leiva, L.E., Wissler, M., Prinz, C., Rabbitts, T.H., Le Deist, F., Fischer, A. and Cavazzana-Calvo, M. (2003b) LMO2-associated clonal T cell proliferation in two patients after gene therapy for SCID-X1. *Science*, **302**, 415-419.

Haffar, O.K., Popov, S., Dubrovsky, L., Agostini, I., Tang, H., Pushkarsky, T., Nadler, S.G. and Bukrinsky, M. (2000) Two nuclear localization signals in the HIV-1 matrix protein regulate nuclear import of the HIV-1 pre-integration complex. *J Mol Biol*, **299**, 359-368.

Harris, D. and Engelman, A. (2000) Both the structure and DNA binding function of the barrier-to-autointegration factor contribute to reconstitution of HIV type 1 integration in vitro. *J Biol Chem*, **275**, 39671-39677.

Harris, R.S., Bishop, K.N., Sheehy, A.M., Craig, H.M., Petersen-Mahrt, S.K., Watt, I.N., Neuberger, M.S. and Malim, M.H. (2003) DNA deamination mediates innate immunity to retroviral infection. *Cell*, **113**, 803-809.

Harris, R.S., Petersen-Mahrt, S.K. and Neuberger, M.S. (2002) RNA editing enzyme APOBEC1 and some of its homologs can act as DNA mutators. *Mol Cell*, **10**, 1247-1253.

Hassan, A.H., Prochasson, P., Neely, K.E., Galasinski, S.C., Chandy, M., Carrozza, M.J. and Workman, J.L. (2002) Function and selectivity of bromodomains in anchoring chromatin-modifying complexes to promoter nucleosomes. *Cell*, **111**, 369-379.

He, J., Choe, S., Walker, R., Di Marzio, P., Morgan, D.O. and Landau, N.R. (1995) Human immunodeficiency virus type 1 viral protein R (Vpr) arrests cells in the G2 phase of the cell cycle by inhibiting p34cdc2 activity. *J Virol*, **69**, 6705-6711.

Hearps, A.C. and Jans, D.A. (2006) HIV-1 integrase is capable of targeting DNA to the nucleus via an importin alpha/beta-dependent mechanism. *Biochem J*, **398**, 475-484.

Hebbes, T.R., Clayton, A.L., Thorne, A.W. and Crane-Robinson, C. (1994) Core histone hyperacetylation co-maps with generalized DNase I sensitivity in the chicken beta-globin chromosomal domain. *Embo J*, **13**, 1823-1830.

Heim, R., Prasher, D.C. and Tsien, R.Y. (1994) Wavelength mutations and posttranslational autoxidation of green fluorescent protein. *Proc Natl Acad Sci U S A*, **91**, 12501-12504.

Heinzinger, N.K., Bukinsky, M.I., Haggerty, S.A., Ragland, A.M., Kewalramani, V., Lee, M.A., Gendelman, H.E., Ratner, L., Stevenson, M. and Emerman, M. (1994) The Vpr protein of human immunodeficiency virus type 1 influences nuclear localization of viral nucleic acids in nondividing host cells. *Proc Natl Acad Sci U S A*, **91**, 7311-7315.

Hermida-Matsumoto, L. and Resh, M.D. (2000) Localization of human immunodeficiency virus type 1 Gag and Env at the plasma membrane by confocal imaging. *J Virol*, **74**, 8670-8679.

Herrero-Martinez, E., Roberts, K.L., Hollinshead, M. and Smith, G.L. (2005) Vaccinia virus intracellular enveloped virions move to the cell periphery on microtubules in the absence of the A36R protein. *J Gen Virol*, **86**, 2961-2968.

Hindmarsh, P. and Leis, J. (1999) Retroviral DNA integration. *Microbiol Mol Biol Rev*, **63**, 836-843, table of contents.

Hirota, T., Lipp, J.J., Toh, B.H. and Peters, J.M. (2005) Histone H3 serine 10 phosphorylation by Aurora B causes HP1 dissociation from heterochromatin. *Nature*, **438**, 1176-1180.

Hizi, A. and Levin, H.L. (2005) The integrase of the long terminal repeat-retrotransposon tf1 has a chromodomain that modulates integrase activities. *J Biol Chem*, **280**, 39086-39094.

Hollinshead, M., Rodger, G., Van Eijl, H., Law, M., Hollinshead, R., Vaux, D.J. and Smith, G.L. (2001) Vaccinia virus utilizes microtubules for movement to the cell surface. *J Cell Biol*, **154**, 389-402.

Holmes-Son, M.L. and Chow, S.A. (2000) Integrase-lexA fusion proteins incorporated into human immunodeficiency virus type 1 that contains a catalytically inactive integrase gene are functional to mediate integration. *J Virol*, **74**, 11548-11556.

Howard, M.T. and Griffith, J.D. (1993) A cluster of strong topoisomerase II cleavage sites is located near an integrated human immunodeficiency virus. *J Mol Biol*, **232**, 1060-1068.

Hsu, K., Seharaseyon, J., Dong, P., Bour, S. and Marban, E. (2004) Mutual functional destruction of HIV-1 Vpu and host TASK-1 channel. *Mol Cell*, **14**, 259-267.

Huang, M., Orenstein, J.M., Martin, M.A. and Freed, E.O. (1995) p6Gag is required for particle production from full-length human immunodeficiency virus type 1 molecular clones expressing protease. *J Virol*, **69**, 6810-6818.

Hubner, W., Chen, P., Del Portillo, A., Liu, Y., Gordon, R.E. and Chen, B.K. (2007) Sequence of human immunodeficiency virus type 1 (HIV-1) Gag localization and oligomerization monitored with live confocal imaging of a replication-competent, fluorescently tagged HIV-1. *J Virol*, **81**, 12596-12607.

Hungnes, O., Tjotta, E. and Grinde, B. (1992) Mutations in the central polypurine tract of HIV-1 result in delayed replication. *Virology*, **190**, 440-442.

Inouye, S. and Tsuji, F.I. (1994) Evidence for redox forms of the Aequorea green fluorescent protein. *FEBS Lett*, **351**, 211-214.

International Committee on Taxonomy of Viruses (6th), Murphy, F.A. and International Union of Microbiological Societies. Virology Division. (1995) *Virus taxonomy : classification and nomenclature of viruses : sixth report of the International Committee on Taxonomy of Viruses*. Springer-Verlag, Wien ; New York.

Iordanskiy, S., Berro, R., Altieri, M., Kashanchi, F. and Bukrinsky, M. (2006) Intracytoplasmic maturation of the human immunodeficiency virus type 1 reverse transcription complexes determines their capacity to integrate into chromatin. *Retrovirology*, **3**, 4.

Jarmuz, A., Chester, A., Bayliss, J., Gisbourne, J., Dunham, I., Scott, J. and Navaratnam, N. (2002) An anthropoid-specific locus of orphan C to U RNA-editing enzymes on chromosome 22. *Genomics*, **79**, 285-296.

Jolly, C., Kashefi, K., Hollinshead, M. and Sattentau, Q.J. (2004) HIV-1 cell to cell transfer across an Env-induced, actin-dependent synapse. *J Exp Med*, **199**, 283-293.

Jolly, C., Mitar, I. and Sattentau, Q.J. (2007) Requirement for an intact T-cell actin and tubulin cytoskeleton for efficient assembly and spread of human immunodeficiency virus type 1. *J Virol*, **81**, 5547-5560.

Jordan, A., Defechereux, P. and Verdin, E. (2001) The site of HIV-1 integration in the human genome determines basal transcriptional activity and response to Tat transactivation. *Embo J*, **20**, 1726-1738.

Jouvenet, N., Bieniasz, P.D. and Simon, S.M. (2008) Imaging the biogenesis of individual HIV-1 virions in live cells. *Nature*.

Jouvenet, N., Monaghan, P., Way, M. and Wileman, T. (2004) Transport of African swine fever virus from assembly sites to the plasma membrane is dependent on microtubules and conventional kinesin. *J Virol*, **78**, 7990-8001.

Jouvenet, N., Windsor, M., Rietdorf, J., Hawes, P., Monaghan, P., Way, M. and Wileman, T. (2006) African swine fever virus induces filopodia-like projections at the plasma membrane. *Cell Microbiol*, **8**, 1803-1811.

Kalpana, G.V., Marmon, S., Wang, W., Crabtree, G.R. and Goff, S.P. (1994) Binding and stimulation of HIV-1 integrase by a human homolog of yeast transcription factor SNF5. *Science*, **266**, 2002-2006.

Kanda, T., Sullivan, K.F. and Wahl, G.M. (1998) Histone-GFP fusion protein enables sensitive analysis of chromosome dynamics in living mammalian cells. *Curr Biol*, **8**, 377-385.

Kang, Y., Moressi, C.J., Scheetz, T.E., Xie, L., Tran, D.T., Casavant, T.L., Ak, P., Benham, C.J., Davidson, B.L. and McCray, P.B., Jr. (2006) Integration site choice of a feline immunodeficiency virus vector. *J Virol*, **80**, 8820-8823.

Kar, A.K., Iwatani, N. and Roy, P. (2005) Assembly and intracellular localization of the bluetongue virus core protein VP3. *J Virol*, **79**, 11487-11495.

Kataoka, N., Bachorik, J.L. and Dreyfuss, G. (1999) Transportin-SR, a nuclear import receptor for SR proteins. *J Cell Biol*, **145**, 1145-1152.

Katz, R.A., Gravuer, K. and Skalka, A.M. (1998) A preferred target DNA structure for retroviral integrase in vitro. *J Biol Chem*, **273**, 24190-24195.

Katz, R.A., Merkel, G. and Skalka, A.M. (1996) Targeting of retroviral integrase by fusion to a heterologous DNA binding domain: in vitro activities and incorporation of a fusion protein into viral particles. *Virology*, **217**, 178-190.

Keckesova, Z., Ylinen, L.M. and Towers, G.J. (2006) Cyclophilin A renders human immunodeficiency virus type 1 sensitive to Old World monkey but not human TRIM5 alpha antiviral activity. *J Virol*, **80**, 4683-4690.

Kessler, M. and Mathews, M.B. (1992) Premature termination and processing of human immunodeficiency virus type 1-promoted transcripts. *J Virol*, **66**, 4488-4496.

Khan, M.A., Akari, H., Kao, S., Aberham, C., Davis, D., Buckler-White, A. and Strebel, K. (2002) Intravirion processing of the human immunodeficiency virus type 1 Vif protein by the viral protease may be correlated with Vif function. *J Virol*, **76**, 9112-9123.

Kim, J., Hake, S.B. and Roeder, R.G. (2005) The human homolog of yeast BRE1 functions as a transcriptional coactivator through direct activator interactions. *Mol Cell*, **20**, 759-770.

Kim, S.H., McQueen, P.G., Lichtman, M.K., Shevach, E.M., Parada, L.A. and Misteli, T. (2004) Spatial genome organization during T-cell differentiation. *Cytogenet Genome Res*, **105**, 292-301.

Kim, S.Y., Byrn, R., Groopman, J. and Baltimore, D. (1989) Temporal aspects of DNA and RNA synthesis during human immunodeficiency virus infection: evidence for differential gene expression. *J Virol*, **63**, 3708-3713.

Kimpton, J. and Emerman, M. (1992) Detection of replication-competent and pseudotyped human immunodeficiency virus with a sensitive cell line on the basis of activation of an integrated beta-galactosidase gene. *J Virol*, **66**, 2232-2239.

Kimura, H. and Cook, P.R. (2001) Kinetics of core histones in living human cells: little exchange of H3 and H4 and some rapid exchange of H2B. *J Cell Biol*, **153**, 1341-1353.

Kootstra, N.A., Munk, C., Tonnu, N., Landau, N.R. and Verma, I.M. (2003) Abrogation of postentry restriction of HIV-1-based lentiviral vector transduction in simian cells. *Proc Natl Acad Sci U S A*, **100**, 1298-1303.

Kootstra, N.A. and Schuitemaker, H. (1999) Phenotype of HIV-1 lacking a functional nuclear localization signal in matrix protein of gag and Vpr is comparable to wild-type HIV-1 in primary macrophages. *Virology*, **253**, 170-180.

Kouzarides, T. (2007) Chromatin modifications and their function. *Cell*, **128**, 693-705.

Kremers, G.J., Goedhart, J., van Munster, E.B. and Gadella, T.W., Jr. (2006) Cyan and yellow super fluorescent proteins with improved brightness, protein folding, and FRET Forster radius. *Biochemistry*, **45**, 6570-6580.

Kupfer, A. and Kupfer, H. (2003) Imaging immune cell interactions and functions: SMACs and the Immunological Synapse. *Semin Immunol*, **15**, 295-300.

Kurdistani, S.K. and Grunstein, M. (2003) Histone acetylation and deacetylation in yeast. *Nat Rev Mol Cell Biol*, **4**, 276-284.

Lai, M.C., Lin, R.I., Huang, S.Y., Tsai, C.W. and Tarn, W.Y. (2000) A human importin-beta family protein, transportin-SR2, interacts with the phosphorylated RS domain of SR proteins. *J Biol Chem*, **275**, 7950-7957.

Lai, M.C., Lin, R.I. and Tarn, W.Y. (2001) Transportin-SR2 mediates nuclear import of phosphorylated SR proteins. *Proc Natl Acad Sci U S A*, **98**, 10154-10159.

Lakadamyali, M., Rust, M.J., Babcock, H.P. and Zhuang, X. (2003) Visualizing infection of individual influenza viruses. *Proc Natl Acad Sci U S A*, **100**, 9280-9285.

Lakadamyali, M., Rust, M.J. and Zhuang, X. (2006) Ligands for clathrin-mediated endocytosis are differentially sorted into distinct populations of early endosomes. *Cell*, **124**, 997-1009.

Lampe, M., Briggs, J.A., Endress, T., Glass, B., Riegelsberger, S., Krausslich, H.G., Lamb, D.C., Brauchle, C. and Muller, B. (2007) Double-labelled HIV-1 particles for study of virus-cell interaction. *Virology*, **360**, 92-104.

Larson, D.R., Johnson, M.C., Webb, W.W. and Vogt, V.M. (2005) Visualization of retrovirus budding with correlated light and electron microscopy. *Proc Natl Acad Sci U S A*, **102**, 15453-15458.

Lee, M.S. and Craigie, R. (1998) A previously unidentified host protein protects retroviral DNA from autointegration. *Proc Natl Acad Sci U S A*, **95**, 1528-1533.

Lehmann, M.J., Sherer, N.M., Marks, C.B., Pypaert, M. and Mothes, W. (2005) Actin- and myosin-driven movement of viruses along filopodia precedes their entry into cells. *J Cell Biol*, **170**, 317-325.

Lehmann-Che, J. and Saib, A. (2004) Early stages of HIV replication: how to hijack cellular functions for a successful infection. *AIDS Rev*, **6**, 199-207.

Lewin, B. (2004) *Genes VIII*. Pearson Prentice Hall, Upper Saddle River, NJ.

Lewinski, M.K., Bisgrove, D., Shinn, P., Chen, H., Hoffmann, C., Hannenhalli, S., Verdin, E., Berry, C.C., Ecker, J.R. and Bushman, F.D. (2005) Genome-wide analysis of chromosomal features repressing human immunodeficiency virus transcription. *J Virol*, **79**, 6610-6619.

Lewinski, M.K., Yamashita, M., Emerman, M., Ciuffi, A., Marshall, H., Crawford, G., Collins, F., Shinn, P., Leipzig, J., Hannenhalli, S., Berry, C.C., Ecker, J.R. and Bushman, F.D. (2006) Retroviral DNA integration: viral and cellular determinants of target-site selection. *PLoS Pathog*, **2**, e60.

Lewis, P., Hensel, M. and Emerman, M. (1992) Human immunodeficiency virus infection of cells arrested in the cell cycle. *Embo J*, **11**, 3053-3058.

Lewis, P.F. and Emerman, M. (1994) Passage through mitosis is required for oncoretroviruses but not for the human immunodeficiency virus. *J Virol*, **68**, 510-516.

Lewis, W., Day, B.J. and Copeland, W.C. (2003) Mitochondrial toxicity of NRTI antiviral drugs: an integrated cellular perspective. *Nat Rev Drug Discov*, **2**, 812-822.

Li, L., Li, H.S., Pauza, C.D., Bukrinsky, M. and Zhao, R.Y. (2005) Roles of HIV-1 auxiliary proteins in viral pathogenesis and host-pathogen interactions. *Cell Res*, **15**, 923-934.

Li, L., Olvera, J.M., Yoder, K.E., Mitchell, R.S., Butler, S.L., Lieber, M., Martin, S.L. and Bushman, F.D. (2001) Role of the non-homologous DNA end joining pathway in the early steps of retroviral infection. *Embo J*, **20**, 3272-3281.

Li, L., Yoder, K., Hansen, M.S., Olvera, J., Miller, M.D. and Bushman, F.D. (2000) Retroviral cDNA integration: stimulation by HMG I family proteins. *J Virol*, **74**, 10965-10974.

Liebl, D., Difato, F., Hornikova, L., Mannova, P., Stokrova, J. and Forstova, J. (2006) Mouse polyomavirus enters early endosomes, requires their acidic pH for productive infection, and meets transferrin cargo in Rab11-positive endosomes. *J Virol*, **80**, 4610-4622.

Limon, A., Devroe, E., Lu, R., Ghory, H.Z., Silver, P.A. and Engelman, A. (2002a) Nuclear localization of human immunodeficiency virus type 1 preintegration complexes (PICs): V165A and R166A are pleiotropic integrase mutants primarily defective for integration, not PIC nuclear import. *J Virol*, **76**, 10598-10607.

Limon, A., Nakajima, N., Lu, R., Ghory, H.Z. and Engelman, A. (2002b) Wild-type levels of nuclear localization and human immunodeficiency virus type 1 replication in the absence of the central DNA flap. *J Virol*, **76**, 12078-12086.

Lin, C.W. and Engelman, A. (2003) The barrier-to-autointegration factor is a component of functional human immunodeficiency virus type 1 preintegration complexes. *J Virol*, **77**, 5030-5036.

Liu, H., Wu, X., Xiao, H., Conway, J.A. and Kappes, J.C. (1997) Incorporation of functional human immunodeficiency virus type 1 integrase into virions independent of the Gag-Pol precursor protein. *J Virol*, **71**, 7704-7710.

Liu, H., Wu, X., Xiao, H. and Kappes, J.C. (1999a) Targeting human immunodeficiency virus (HIV) type 2 integrase protein into HIV type 1. *J Virol*, **73**, 8831-8836.

Liu, J., Xiao, N. and DeFranco, D.B. (1999b) Use of digitonin-permeabilized cells in studies of steroid receptor subnuclear trafficking. *Methods*, **19**, 403-409.

Llano, M., Saenz, D.T., Meehan, A., Wongthida, P., Peretz, M., Walker, W.H., Teo, W. and Poeschla, E.M. (2006) An essential role for LEDGF/p75 in HIV integration. *Science*, **314**, 461-464.

Llano, M., Vanegas, M., Fregoso, O., Saenz, D., Chung, S., Peretz, M. and Poeschla, E.M. (2004) LEDGF/p75 determines cellular trafficking of diverse lentiviral but not murine oncoretroviral integrase proteins and is a component of functional lentiviral preintegration complexes. *J Virol*, **78**, 9524-9537.

Lu, R., Limon, A., Devroe, E., Silver, P.A., Cherepanov, P. and Engelman, A. (2004) Class II integrase mutants with changes in putative nuclear localization signals are primarily blocked at a postnuclear entry step of human immunodeficiency virus type 1 replication. *J Virol*, **78**, 12735-12746.

Luby-Phelps, K. (2000) Cytoarchitecture and physical properties of cytoplasm: volume, viscosity, diffusion, intracellular surface area. *Int Rev Cytol*, **192**, 189-221.

Luo, Y., Yu, H. and Peterlin, B.M. (1994) Cellular protein modulates effects of human immunodeficiency virus type 1 Rev. *J Virol*, **68**, 3850-3856.

Lutzke, R.A., Vink, C. and Plasterk, R.H. (1994) Characterization of the minimal DNA-binding domain of the HIV integrase protein. *Nucleic Acids Res*, **22**, 4125-4131.

Macdonald, N., Welburn, J.P., Noble, M.E., Nguyen, A., Yaffe, M.B., Clynes, D., Moggs, J.G., Orphanides, G., Thomson, S., Edmunds, J.W., Clayton, A.L., Endicott, J.A. and Mahadevan, L.C. (2005) Molecular basis for the recognition of phosphorylated and phosphoacetylated histone h3 by 14-3-3. *Mol Cell*, **20**, 199-211.

Macek, B., Waanders, L.F., Olsen, J.V. and Mann, M. (2006) Top-down protein sequencing and MS3 on a hybrid linear quadrupole ion trap-orbitrap mass spectrometer. *Mol Cell Proteomics*, **5**, 949-958.

Maertens, G., Cherepanov, P., Debyser, Z., Engelborghs, Y. and Engelman, A. (2004) Identification and characterization of a functional nuclear localization signal in the HIV-1 integrase interactor LEDGF/p75. *J Biol Chem*, **279**, 33421-33429.

Maertens, G., Cherepanov, P., Pluymers, W., Busschots, K., De Clercq, E., Debyser, Z. and Engelborghs, Y. (2003) LEDGF/p75 is essential for nuclear and chromosomal targeting of HIV-1 integrase in human cells. *J Biol Chem*, **278**, 33528-33539.

Maertens, G., Vercammen, J., Debyser, Z. and Engelborghs, Y. (2005) Measuring protein-protein interactions inside living cells using single color fluorescence correlation spectroscopy. Application to human immunodeficiency virus type 1 integrase and LEDGF/p75. *Faseb J*, **19**, 1039-1041.

Maeshima, K. and Laemmli, U.K. (2003) A two-step scaffolding model for mitotic chromosome assembly. *Dev Cell*, **4**, 467-480.

Mahadevan, L.C., Willis, A.C. and Barratt, M.J. (1991) Rapid histone H3 phosphorylation in response to growth factors, phorbol esters, okadaic acid, and protein synthesis inhibitors. *Cell*, **65**, 775-783.

Malim, M.H., Hauber, J., Le, S.Y., Maizel, J.V. and Cullen, B.R. (1989) The HIV-1 rev trans-activator acts through a structured target sequence to activate nuclear export of unspliced viral mRNA. *Nature*, **338**, 254-257.

Malim, M.H., Tiley, L.S., McCarn, D.F., Rusche, J.R., Hauber, J. and Cullen, B.R. (1990) HIV-1 structural gene expression requires binding of the Rev trans-activator to its RNA target sequence. *Cell*, **60**, 675-683.

Mammano, F., Kondo, E., Sodroski, J., Bukovsky, A. and Gottlinger, H.G. (1995) Rescue of human immunodeficiency virus type 1 matrix protein mutants by envelope glycoproteins with short cytoplasmic domains. *J Virol*, **69**, 3824-3830.

Manes, S., del Real, G., Lacalle, R.A., Lucas, P., Gomez-Mouton, C., Sanchez-Palomino, S., Delgado, R., Alcami, J., Mira, E. and Martinez, A.C. (2000) Membrane raft microdomains mediate lateral assemblies required for HIV-1 infection. *EMBO Rep*, **1**, 190-196.

Mannioui, A., Nelson, E., Schiffer, C., Felix, N., Le Rouzic, E., Benichou, S., Gluckman, J.C. and Canque, B. (2005) Human immunodeficiency virus type 1 KK26-27 matrix mutants display impaired infectivity, circularization and integration but not nuclear import. *Virology*, **339**, 21-30.

Marcello, A., Zoppe, M. and Giacca, M. (2001) Multiple modes of transcriptional regulation by the HIV-1 Tat transactivator. *IUBMB Life*, **51**, 175-181.

Marchand, C., Neamati, N. and Pommier, Y. (2001) In vitro human immunodeficiency virus type 1 integrase assays. *Methods Enzymol*, **340**, 624-633.

Margottin, F., Bour, S.P., Durand, H., Selig, L., Benichou, S., Richard, V., Thomas, D., Strebel, K. and Benarous, R. (1998) A novel human WD protein, h-beta TrCp, that interacts with HIV-1 Vpu connects CD4 to the ER degradation pathway through an F-box motif. *Mol Cell*, **1**, 565-574.

Margueron, R., Trojer, P. and Reinberg, D. (2005) The key to development: interpreting the histone code? *Curr Opin Genet Dev*, **15**, 163-176.

Markosyan, R.M., Cohen, F.S. and Melikyan, G.B. (2005) Time-resolved imaging of HIV-1 Env-mediated lipid and content mixing between a single virion and cell membrane. *Mol Biol Cell*, **16**, 5502-5513.

Maroun, M., Delelis, O., Coadou, G., Bader, T., Segeral, E., Mbemba, G., Petit, C., Sonigo, P., Rain, J.C., Mouscadet, J.F., Benarous, R. and Emiliani, S. (2006) Inhibition of early steps of HIV-1 replication by SNF5/Ini1. *J Biol Chem*, **281**, 22736-22743.

Marsh, M. and Helenius, A. (2006) Virus entry: open sesame. *Cell*, **124**, 729-740.

Matlin, K.S., Reggio, H., Helenius, A. and Simons, K. (1981) Infectious entry pathway of influenza virus in a canine kidney cell line. *J Cell Biol*, **91**, 601-613.

McDonald, D., Vodicka, M.A., Lucero, G., Svitkina, T.M., Borisy, G.G., Emerman, M. and Hope, T.J. (2002) Visualization of the intracellular behavior of HIV in living cells. *J Cell Biol*, **159**, 441-452.

McDonald, D., Wu, L., Bohks, S.M., KewalRamani, V.N., Unutmaz, D. and Hope, T.J. (2003) Recruitment of HIV and its receptors to dendritic cell-T cell junctions. *Science*, **300**, 1295-1297.

Meaburn, K.J. and Misteli, T. (2007) Cell biology: chromosome territories. *Nature*, **445**, 379-781.

Meier, O., Boucke, K., Hammer, S.V., Keller, S., Stidwill, R.P., Hemmi, S. and Greber, U.F. (2002) Adenovirus triggers macropinocytosis and endosomal leakage together with its clathrin-mediated uptake. *J Cell Biol*, **158**, 1119-1131.

Miesenbock, G., De Angelis, D.A. and Rothman, J.E. (1998) Visualizing secretion and synaptic transmission with pH-sensitive green fluorescent proteins. *Nature*, **394**, 192-195.

Miller, M.D., Farnet, C.M. and Bushman, F.D. (1997) Human immunodeficiency virus type 1 preintegration complexes: studies of organization and composition. *J Virol*, **71**, 5382-5390.

Minsky, M. (1988) Memoir on Inventing the Confocal Scanning Microscope. *Scanning*, **10**, 128-138.

Misteli, T. (2007) Beyond the sequence: cellular organization of genome function. *Cell*, **128**, 787-800.

Mitchell, R., Chiang, C.Y., Berry, C. and Bushman, F. (2003) Global analysis of cellular transcription following infection with an HIV-based vector. *Mol Ther*, **8**, 674-687.

Mitchell, R.S., Beitzel, B.F., Schroder, A.R., Shinn, P., Chen, H., Berry, C.C., Ecker, J.R. and Bushman, F.D. (2004) Retroviral DNA integration: ASLV, HIV, and MLV show distinct target site preferences. *PLoS Biol*, **2**, E234.

Mooslehner, K., Karls, U. and Harbers, K. (1990) Retroviral integration sites in transgenic Mov mice frequently map in the vicinity of transcribed DNA regions. *J Virol*, **64**, 3056-3058.

Morita, E. and Sundquist, W.I. (2004) Retrovirus budding. *Annu Rev Cell Dev Biol*, **20**, 395-425.

Muller, B., Daecke, J., Fackler, O.T., Dittmar, M.T., Zentgraf, H. and Krausslich, H.G. (2004) Construction and characterization of a fluorescently labeled infectious human immunodeficiency virus type 1 derivative. *J Virol*, **78**, 10803-10813.

Muller, H.P. and Varmus, H.E. (1994) DNA bending creates favored sites for retroviral integration: an explanation for preferred insertion sites in nucleosomes. *Embo J*, **13**, 4704-4714.

Nakayama, J., Rice, J.C., Strahl, B.D., Allis, C.D. and Grewal, S.I. (2001) Role of histone H3 lysine 9 methylation in epigenetic control of heterochromatin assembly. *Science*, **292**, 110-113.

Naldini, L., Blomer, U., Gage, F.H., Trono, D. and Verma, I.M. (1996) Efficient transfer, integration, and sustained long-term expression of the transgene in adult rat brains injected with a lentiviral vector. *Proc Natl Acad Sci U S A*, **93**, 11382-11388.

Nicola, A.V. and Straus, S.E. (2004) Cellular and viral requirements for rapid endocytic entry of herpes simplex virus. *J Virol*, **78**, 7508-7517.

Nishigaki, A., Ohshima, S. and Nakayama, K. (2000) Characterization of three forms of light-harvesting chlorophyll a/b-protein complexes of photosystem II isolated from the green alga, Dunaliella salina. *Plant Cell Physiol*, **41**, 591-599.

Nishizawa, Y., Usukura, J., Singh, D.P., Chylack, L.T., Jr. and Shinohara, T. (2001) Spatial and temporal dynamics of two alternatively spliced regulatory factors, lens epithelium-derived growth factor (ledgf/p75) and p52, in the nucleus. *Cell Tissue Res*, **305**, 107-114.

Nowak, S.J. and Corces, V.G. (2004) Phosphorylation of histone H3: a balancing act between chromosome condensation and transcriptional activation. *Trends Genet*, **20**, 214-220.

Ono, A. and Freed, E.O. (2001) Plasma membrane rafts play a critical role in HIV-1 assembly and release. *Proc Natl Acad Sci U S A*, **98**, 13925-13930.

Ormo, M., Cubitt, A.B., Kallio, K., Gross, L.A., Tsien, R.Y. and Remington, S.J. (1996) Crystal structure of the Aequorea victoria green fluorescent protein. *Science*, **273**, 1392-1395.

Panet, A. and Cedar, H. (1977) Selective degradation of integrated murine leukemia proviral DNA by deoxyribonucleases. *Cell*, **11**, 933-940.

Pante, N. and Kann, M. (2002) Nuclear pore complex is able to transport macromolecules with diameters of about 39 nm. *Mol Biol Cell*, **13**, 425-434.

Parissi, V., Calmels, C., De Soultrait, V.R., Caumont, A., Fournier, M., Chaignepain, S. and Litvak, S. (2001) Functional interactions of human immunodeficiency virus type 1 integrase with human and yeast HSP60. *J Virol*, **75**, 11344-11353.

Patterson, G.H. and Lippincott-Schwartz, J. (2002) A photoactivatable GFP for selective photolabeling of proteins and cells. *Science*, **297**, 1873-1877.

Paxton, W., Connor, R.I. and Landau, N.R. (1993) Incorporation of Vpr into human immunodeficiency virus type 1 virions: requirement for the p6 region of gag and mutational analysis. *J Virol*, **67**, 7229-7237.

Pelkmans, L., Burli, T., Zerial, M. and Helenius, A. (2004) Caveolin-stabilized membrane domains as multifunctional transport and sorting devices in endocytic membrane traffic. *Cell*, **118**, 767-780.

Pelkmans, L., Kartenbeck, J. and Helenius, A. (2001) Caveolar endocytosis of simian virus 40 reveals a new two-step vesicular-transport pathway to the ER. *Nat Cell Biol*, **3**, 473-483.

Pelkmans, L., Puntener, D. and Helenius, A. (2002) Local actin polymerization and dynamin recruitment in SV40-induced internalization of caveolae. *Science*, **296**, 535-539.

Perlman, M. and Resh, M.D. (2006) Identification of an intracellular trafficking and assembly pathway for HIV-1 gag. *Traffic*, **7**, 731-745.

Peterlin, B.M. and Trono, D. (2003) Hide, shield and strike back: how HIV-infected cells avoid immune eradication. *Nat Rev Immunol*, **3**, 97-107.

Petit, C., Schwartz, O. and Mammano, F. (2000) The karyophilic properties of human immunodeficiency virus type 1 integrase are not required for nuclear import of proviral DNA. *J Virol*, **74**, 7119-7126.

Piatak, M., Jr., Saag, M.S., Yang, L.C., Clark, S.J., Kappes, J.C., Luk, K.C., Hahn, B.H., Shaw, G.M. and Lifson, J.D. (1993) High levels of HIV-1 in plasma during all stages of infection determined by competitive PCR. *Science*, **259**, 1749-1754.

Pietiainen, V., Marjomaki, V., Upla, P., Pelkmans, L., Helenius, A. and Hyypia, T. (2004) Echovirus 1 endocytosis into caveosomes requires lipid rafts, dynamin II, and signaling events. *Mol Biol Cell*, **15**, 4911-4925.

Pines, J. (1995) GFP in mammalian cells. *Trends Genet*, **11**, 326-327.

Piston, D.W. and Kremers, G.J. (2007) Fluorescent protein FRET: the good, the bad and the ugly. *Trends Biochem Sci*, **32**, 407-414.

Pluymers, W., Cherepanov, P., Schols, D., De Clercq, E. and Debyser, Z. (1999) Nuclear localization of human immunodeficiency virus type 1 integrase expressed as a fusion protein with green fluorescent protein. *Virology*, **258**, 327-332.

Poirier, M.G. and Marko, J.F. (2002) Mitotic chromosomes are chromatin networks without a mechanically contiguous protein scaffold. *Proc Natl Acad Sci U S A*, **99**, 15393-15397.

Pomerantz, R.J., Seshamma, T. and Trono, D. (1992) Efficient replication of human immunodeficiency virus type 1 requires a threshold level of Rev: potential implications for latency. *J Virol*, **66**, 1809-1813.

Pommier, Y., Johnson, A.A. and Marchand, C. (2005) Integrase inhibitors to treat HIV/AIDS. *Nat Rev Drug Discov*, **4**, 236-248.

Popov, S., Rexach, M., Zybarth, G., Reiling, N., Lee, M.A., Ratner, L., Lane, C.M., Moore, M.S., Blobel, G. and Bukrinsky, M. (1998) Viral protein R regulates nuclear import of the HIV-1 pre-integration complex. *Embo J*, **17**, 909-917.

Powell, D.M., Amaral, M.C., Wu, J.Y., Maniatis, T. and Greene, W.C. (1997) HIV Rev-dependent binding of SF2/ASF to the Rev response element: possible role in Rev-mediated inhibition of HIV RNA splicing. *Proc Natl Acad Sci U S A*, **94**, 973-978.

Prasher, D.C. (1995) Using GFP to see the light. *Trends Genet*, **11**, 320-323.

Prasher, D.C., Eckenrode, V.K., Ward, W.W., Prendergast, F.G. and Cormier, M.J. (1992) Primary structure of the Aequorea victoria green-fluorescent protein. *Gene*, **111**, 229-233.

Pruss, D., Bushman, F.D. and Wolffe, A.P. (1994) Human immunodeficiency virus integrase directs integration to sites of severe DNA distortion within the nucleosome core. *Proc Natl Acad Sci U S A*, **91**, 5913-5917.

Pryciak, P.M., Sil, A. and Varmus, H.E. (1992) Retroviral integration into minichromosomes in vitro. *Embo J*, **11**, 291-303.

Pryciak, P.M. and Varmus, H.E. (1992) Nucleosomes, DNA-binding proteins, and DNA sequence modulate retroviral integration target site selection. *Cell*, **69**, 769-780.

Purcell, D.F. and Martin, M.A. (1993) Alternative splicing of human immunodeficiency virus type 1 mRNA modulates viral protein expression, replication, and infectivity. *J Virol*, **67**, 6365-6378.

Ratnasabapathy, R., Sheldon, M., Johal, L. and Hernandez, N. (1990) The HIV-1 long terminal repeat contains an unusual element that induces the synthesis of short RNAs from various mRNA and snRNA promoters. *Genes Dev*, **4**, 2061-2074.

Reid, B.G. and Flynn, G.C. (1997) Chromophore formation in green fluorescent protein. *Biochemistry*, **36**, 6786-6791.

Reil, H., Bukovsky, A.A., Gelderblom, H.R. and Gottlinger, H.G. (1998) Efficient HIV-1 replication can occur in the absence of the viral matrix protein. *Embo J*, **17**, 2699-2708.

Reymond, A., Meroni, G., Fantozzi, A., Merla, G., Cairo, S., Luzi, L., Riganelli, D., Zanaria, E., Messali, S., Cainarca, S., Guffanti, A., Minucci, S., Pelicci, P.G. and Ballabio, A. (2001) The tripartite motif family identifies cell compartments. *Embo J*, **20**, 2140-2151.

Rietdorf, J., Ploubidou, A., Reckmann, I., Holmstrom, A., Frischknecht, F., Zettl, M., Zimmermann, T. and Way, M. (2001) Kinesin-dependent movement on microtubules precedes actin-based motility of vaccinia virus. *Nat Cell Biol*, **3**, 992-1000.

Robinson, H.L. and Gagnon, G.C. (1986) Patterns of proviral insertion and deletion in avian leukosis virus-induced lymphomas. *J Virol*, **57**, 28-36.

Roe, T., Reynolds, T.C., Yu, G. and Brown, P.O. (1993) Integration of murine leukemia virus DNA depends on mitosis. *Embo J*, **12**, 2099-2108.

Rohdewohld, H., Weiher, H., Reik, W., Jaenisch, R. and Breindl, M. (1987) Retrovirus integration and chromatin structure: Moloney murine leukemia proviral integration sites map near DNase I-hypersensitive sites. *J Virol*, **61**, 336-343.

Roth, S.Y., Denu, J.M. and Allis, C.D. (2001) Histone acetyltransferases. *Annu Rev Biochem*, **70**, 81-120.

Rudner, L., Nydegger, S., Coren, L.V., Nagashima, K., Thali, M. and Ott, D.E. (2005) Dynamic fluorescent imaging of human immunodeficiency virus type 1 gag in live cells by biarsenical labeling. *J Virol*, **79**, 4055-4065.

Rust, M.J., Lakadamyali, M., Zhang, F. and Zhuang, X. (2004) Assembly of endocytic machinery around individual influenza viruses during viral entry. *Nat Struct Mol Biol*, **11**, 567-573.

Sampaio, K.L., Cavignac, Y., Stierhof, Y.D. and Sinzger, C. (2005) Human cytomegalovirus labeled with green fluorescent protein for live analysis of intracellular particle movements. *J Virol*, **79**, 2754-2767.

Sandefur, S., Varthakavi, V. and Spearman, P. (1998) The I domain is required for efficient plasma membrane binding of human immunodeficiency virus type 1 Pr55Gag. *J Virol*, **72**, 2723-2732.

Saphire, A.C., Bobardt, M.D. and Gallay, P.A. (2002) trans-Complementation rescue of cyclophilin A-deficient viruses reveals that the requirement for cyclophilin A in human immunodeficiency virus type 1 replication is independent of its isomerase activity. *J Virol*, **76**, 2255-2262.

Sayah, D.M., Sokolskaja, E., Berthoux, L. and Luban, J. (2004) Cyclophilin A retrotransposition into TRIM5 explains owl monkey resistance to HIV-1. *Nature*, **430**, 569-573.

Scarlata, S. and Carter, C. (2003) Role of HIV-1 Gag domains in viral assembly. *Biochim Biophys Acta*, **1614**, 62-72.

Schalch, T., Duda, S., Sargent, D.F. and Richmond, T.J. (2005) X-ray structure of a tetranucleosome and its implications for the chromatin fibre. *Nature*, **436**, 138-141.

Scherdin, U., Rhodes, K. and Breindl, M. (1990) Transcriptionally active genome regions are preferred targets for retrovirus integration. *J Virol*, **64**, 907-912.

Schroder, A.R., Shinn, P., Chen, H., Berry, C., Ecker, J.R. and Bushman, F. (2002) HIV-1 integration in the human genome favors active genes and local hotspots. *Cell*, **110**, 521-529.

Schwartz, O., Marechal, V., Le Gall, S., Lemonnier, F. and Heard, J.M. (1996) Endocytosis of major histocompatibility complex class I molecules is induced by the HIV-1 Nef protein. *Nat Med*, **2**, 338-342.

Seisenberger, G., Ried, M.U., Endress, T., Buning, H., Hallek, M. and Brauchle, C. (2001) Real-time single-molecule imaging of the infection pathway of an adeno-associated virus. *Science*, **294**, 1929-1932.

Semwogerere, D. and Week, E. (2005) Confocal microscopy. In Wnek, G.E. and Bowlin, G.L. (eds.), *Encyclopedia of biomaterials and biomedical engineering*. Marcel Dekker, New York.

Shaner, N.C., Campbell, R.E., Steinbach, P.A., Giepmans, B.N., Palmer, A.E. and Tsien, R.Y. (2004) Improved monomeric red, orange and yellow fluorescent proteins derived from Discosoma sp. red fluorescent protein. *Nat Biotechnol*, **22**, 1567-1572.

Shaner, N.C., Patterson, G.H. and Davidson, M.W. (2007) Advances in fluorescent protein technology. *J Cell Sci*, **120**, 4247-4260.

Shaner, N.C., Steinbach, P.A. and Tsien, R.Y. (2005) A guide to choosing fluorescent proteins. *Nat Methods*, **2**, 905-909.

Sherer, N.M., Lehmann, M.J., Jimenez-Soto, L.F., Horensavitz, C., Pypaert, M. and Mothes, W. (2007) Retroviruses can establish filopodial bridges for efficient cell-to-cell transmission. *Nat Cell Biol*, **9**, 310-315.

Shiio, Y. and Eisenman, R.N. (2003) Histone sumoylation is associated with transcriptional repression. *Proc Natl Acad Sci U S A*, **100**, 13225-13230.

Shilatifard, A., Conaway, R.C. and Conaway, J.W. (2003) The RNA polymerase II elongation complex. *Annu Rev Biochem*, **72**, 693-715.

Shimomura, O., Johnson, F.H. and Saiga, Y. (1962) Extraction, purification and properties of aequorin, a bioluminescent protein from the luminous hydromedusan, Aequorea. *J Cell Comp Physiol*, **59**, 223-239.

Shinohara, T., Singh, D.P. and Fatma, N. (2002) LEDGF, a survival factor, activates stress-related genes. *Prog Retin Eye Res*, **21**, 341-358.

Shumaker, D.K., Lee, K.K., Tanhehco, Y.C., Craigie, R. and Wilson, K.L. (2001) LAP2 binds to BAF.DNA complexes: requirement for the LEM domain and modulation by variable regions. *Embo J*, **20**, 1754-1764.

Shun, M.C., Daigle, J.E., Vandegraaff, N. and Engelman, A. (2007a) Wild-type levels of human immunodeficiency virus type 1 infectivity in the absence of cellular emerin protein. *J Virol*, **81**, 166-172.

Shun, M.C., Raghavendra, N.K., Vandegraaff, N., Daigle, J.E., Hughes, S., Kellam, P., Cherepanov, P. and Engelman, A. (2007b) LEDGF/p75

functions downstream from preintegration complex formation to effect gene-specific HIV-1 integration. *Genes Dev*, **21**, 1767-1778.

Sieczkarski, S.B. and Whittaker, G.R. (2002) Influenza virus can enter and infect cells in the absence of clathrin-mediated endocytosis. *J Virol*, **76**, 10455-10464.

Simon, J.H. and Malim, M.H. (1996) The human immunodeficiency virus type 1 Vif protein modulates the postpenetration stability of viral nucleoprotein complexes. *J Virol*, **70**, 5297-5305.

Singh, D.P., Fatma, N., Kimura, A., Chylack, L.T., Jr. and Shinohara, T. (2001) LEDGF binds to heat shock and stress-related element to activate the expression of stress-related genes. *Biochem Biophys Res Commun*, **283**, 943-955.

Smith, G.A., Pomeranz, L., Gross, S.P. and Enquist, L.W. (2004) Local modulation of plus-end transport targets herpesvirus entry and egress in sensory axons. *Proc Natl Acad Sci U S A*, **101**, 16034-16039.

Smith, G.L., Murphy, B.J. and Law, M. (2003) Vaccinia virus motility. *Annu Rev Microbiol*, **57**, 323-342.

Song, B., Javanbakht, H., Perron, M., Park, D.H., Stremlau, M. and Sodroski, J. (2005) Retrovirus restriction by TRIM5alpha variants from Old World and New World primates. *J Virol*, **79**, 3930-3937.

Sowinski, S., Jolly, C., Berninghausen, O., Purbhoo, M.A., Chauveau, A., Kohler, K., Oddos, S., Eissmann, P., Brodsky, F.M., Hopkins, C., Onfelt, B., Sattentau, Q. and Davis, D.M. (2008) Membrane nanotubes physically connect T cells over long distances presenting a novel route for HIV-1 transmission. *Nat Cell Biol*, **10**, 211-219.

Stephens, D.J. and Allan, V.J. (2003) Light microscopy techniques for live cell imaging. *Science*, **300**, 82-86.

Stevens, S.W. and Griffith, J.D. (1994) Human immunodeficiency virus type 1 may preferentially integrate into chromatin occupied by L1Hs repetitive elements. *Proc Natl Acad Sci U S A*, **91**, 5557-5561.

Stevens, S.W. and Griffith, J.D. (1996) Sequence analysis of the human DNA flanking sites of human immunodeficiency virus type 1 integration. *J Virol*, **70**, 6459-6462.

Strebel, K., Daugherty, D., Clouse, K., Cohen, D., Folks, T. and Martin, M.A. (1987) The HIV 'A' (sor) gene product is essential for virus infectivity. *Nature*, **328**, 728-730.

Stremlau, M., Owens, C.M., Perron, M.J., Kiessling, M., Autissier, P. and Sodroski, J. (2004) The cytoplasmic body component TRIM5alpha restricts HIV-1 infection in Old World monkeys. *Nature*, **427**, 848-853.

Stremlau, M., Song, B., Javanbakht, H., Perron, M. and Sodroski, J. (2006) Cyclophilin A: an auxiliary but not necessary cofactor for TRIM5alpha restriction of HIV-1. *Virology*, **351**, 112-120.

Strukov, Y.G., Wang, Y. and Belmont, A.S. (2003) Engineered chromosome regions with altered sequence composition demonstrate hierarchical large-scale folding within metaphase chromosomes. *J Cell Biol*, **162**, 23-35.

Strunze, S., Trotman, L.C., Boucke, K. and Greber, U.F. (2005) Nuclear targeting of adenovirus type 2 requires CRM1-mediated nuclear export. *Mol Biol Cell*, **16**, 2999-3009.

Suomalainen, M., Nakano, M.Y., Keller, S., Boucke, K., Stidwill, R.P. and Greber, U.F. (1999) Microtubule-dependent plus- and minus end-directed motilities are competing processes for nuclear targeting of adenovirus. *J Cell Biol*, **144**, 657-672.

Suzuki, Y. and Craigie, R. (2002) Regulatory mechanisms by which barrier-to-autointegration factor blocks autointegration and stimulates intermolecular integration of Moloney murine leukemia virus preintegration complexes. *J Virol*, **76**, 12376-12380.

Svarovskaia, E.S., Barr, R., Zhang, X., Pais, G.C., Marchand, C., Pommier, Y., Burke, T.R., Jr. and Pathak, V.K. (2004) Azido-containing diketo acid derivatives inhibit human immunodeficiency virus type 1 integrase in vivo and influence the frequency of deletions at two-long-terminal-repeat-circle junctions. *J Virol*, **78**, 3210-3222.

Swedlow, J.R. and Hirano, T. (2003) The making of the mitotic chromosome: modern insights into classical questions. *Mol Cell*, **11**, 557-569.

Taddei, A., Van Houwe, G., Hediger, F., Kalck, V., Cubizolles, F., Schober, H. and Gasser, S.M. (2006) Nuclear pore association confers optimal expression levels for an inducible yeast gene. *Nature*, **441**, 774-778.

Tagawa, A., Mezzacasa, A., Hayer, A., Longatti, A., Pelkmans, L. and Helenius, A. (2005) Assembly and trafficking of caveolar domains in the cell: caveolae as stable, cargo-triggered, vesicular transporters. *J Cell Biol*, **170**, 769-779.

Tan, W., Dong, Z., Wilkinson, T.A., Barbas, C.F., 3rd and Chow, S.A. (2006) Human immunodeficiency virus type 1 incorporated with fusion proteins consisting of integrase and the designed polydactyl zinc finger protein E2C

can bias integration of viral DNA into a predetermined chromosomal region in human cells. *J Virol*, **80**, 1939-1948.

Tan, W., Zhu, K., Segal, D.J., Barbas, C.F., 3rd and Chow, S.A. (2004) Fusion proteins consisting of human immunodeficiency virus type 1 integrase and the designed polydactyl zinc finger protein E2C direct integration of viral DNA into specific sites. *J Virol*, **78**, 1301-1313.

Terreni, M. (2009).

Thali, M., Bukovsky, A., Kondo, E., Rosenwirth, B., Walsh, C.T., Sodroski, J. and Gottlinger, H.G. (1994) Functional association of cyclophilin A with HIV-1 virions. *Nature*, **372**, 363-365.

Thomas, J.A., Ott, D.E. and Gorelick, R.J. (2007) Efficiency of human immunodeficiency virus type 1 postentry infection processes: evidence against disproportionate numbers of defective virions. *J Virol*, **81**, 4367-4370.

Thomas, J.O. and Travers, A.A. (2001) HMG1 and 2, and related 'architectural' DNA-binding proteins. *Trends Biochem Sci*, **26**, 167-174.

Toomre, D. and Manstein, D.J. (2001) Lighting up the cell surface with evanescent wave microscopy. *Trends Cell Biol*, **11**, 298-303.

Topper, M., Luo, Y., Zhadina, M., Mohammed, K., Smith, L. and Muesing, M.A. (2007) Posttranslational acetylation of the human immunodeficiency virus type 1 integrase carboxyl-terminal domain is dispensable for viral replication. *J Virol*, **81**, 3012-3017.

Towers, G., Collins, M. and Takeuchi, Y. (2002) Abrogation of Ref1 retrovirus restriction in human cells. *J Virol*, **76**, 2548-2550.

Towers, G.J. (2007) The control of viral infection by tripartite motif proteins and cyclophilin A. *Retrovirology*, **4**, 40.

Tsien, R.Y. (1998) The green fluorescent protein. *Annu Rev Biochem*, **67**, 509-544.

Tsurutani, N., Kubo, M., Maeda, Y., Ohashi, T., Yamamoto, N., Kannagi, M. and Masuda, T. (2000) Identification of critical amino acid residues in human immunodeficiency virus type 1 IN required for efficient proviral DNA formation at steps prior to integration in dividing and nondividing cells. *J Virol*, **74**, 4795-4806.

Turelli, P., Doucas, V., Craig, E., Mangeat, B., Klages, N., Evans, R., Kalpana, G. and Trono, D. (2001) Cytoplasmic recruitment of INI1 and PML on

incoming HIV preintegration complexes: interference with early steps of viral replication. *Mol Cell*, **7**, 1245-1254.

Turlure, F., Devroe, E., Silver, P.A. and Engelman, A. (2004) Human cell proteins and human immunodeficiency virus DNA integration. *Front Biosci*, **9**, 3187-3208.

Upla, P., Marjomaki, V., Kankaanpaa, P., Ivaska, J., Hyypia, T., Van Der Goot, F.G. and Heino, J. (2004) Clustering induces a lateral redistribution of alpha 2 beta 1 integrin from membrane rafts to caveolae and subsequent protein kinase C-dependent internalization. *Mol Biol Cell*, **15**, 625-636.

van 't Wout, A.B., Lehrman, G.K., Mikheeva, S.A., O'Keeffe, G.C., Katze, M.G., Bumgarner, R.E., Geiss, G.K. and Mullins, J.I. (2003) Cellular gene expression upon human immunodeficiency virus type 1 infection of CD4(+)-T-cell lines. *J Virol*, **77**, 1392-1402.

Van Maele, B., Busschots, K., Vandekerckhove, L., Christ, F. and Debyser, Z. (2006) Cellular co-factors of HIV-1 integration. *Trends Biochem Sci*, **31**, 98-105.

van Steensel, B., Delrow, J. and Henikoff, S. (2001) Chromatin profiling using targeted DNA adenine methyltransferase. *Nat Genet*, **27**, 304-308.

Vandegraaff, N. and Engelman, A. (2007) Molecular mechanisms of HIV integration and therapeutic intervention. *Expert Rev Mol Med*, **9**, 1-19.

Vandekerckhove, L., Christ, F., Van Maele, B., De Rijck, J., Gijsbers, R., Van den Haute, C., Witvrouw, M. and Debyser, Z. (2006) Transient and stable knockdown of the integrase cofactor LEDGF/p75 reveals its role in the replication cycle of human immunodeficiency virus. *J Virol*, **80**, 1886-1896.

Vanegas, M., Llano, M., Delgado, S., Thompson, D., Peretz, M. and Poeschla, E. (2005) Identification of the LEDGF/p75 HIV-1 integrase-interaction domain and NLS reveals NLS-independent chromatin tethering. *J Cell Sci*, **118**, 1733-1743.

Varthakavi, V., Smith, R.M., Bour, S.P., Strebel, K. and Spearman, P. (2003) Viral protein U counteracts a human host cell restriction that inhibits HIV-1 particle production. *Proc Natl Acad Sci U S A*, **100**, 15154-15159.

Vettese-Dadey, M., Grant, P.A., Hebbes, T.R., Crane- Robinson, C., Allis, C.D. and Workman, J.L. (1996) Acetylation of histone H4 plays a primary role in enhancing transcription factor binding to nucleosomal DNA in vitro. *Embo J*, **15**, 2508-2518.

Vijaya, S., Steffen, D.L. and Robinson, H.L. (1986) Acceptor sites for retroviral integrations map near DNase I-hypersensitive sites in chromatin. *J Virol*, **60**, 683-692.

Vink, C., Oude Groeneger, A.M. and Plasterk, R.H. (1993) Identification of the catalytic and DNA-binding region of the human immunodeficiency virus type I integrase protein. *Nucleic Acids Res*, **21**, 1419-1425.

Violot, S., Hong, S.S., Rakotobe, D., Petit, C., Gay, B., Moreau, K., Billaud, G., Priet, S., Sire, J., Schwartz, O., Mouscadet, J.F. and Boulanger, P. (2003) The human polycomb group EED protein interacts with the integrase of human immunodeficiency virus type 1. *J Virol*, **77**, 12507-12522.

Vodicka, M.A., Koepp, D.M., Silver, P.A. and Emerman, M. (1998) HIV-1 Vpr interacts with the nuclear transport pathway to promote macrophage infection. *Genes Dev*, **12**, 175-185.

Wang, G.P., Ciuffi, A., Leipzig, J., Berry, C.C. and Bushman, F.D. (2007) HIV integration site selection: analysis by massively parallel pyrosequencing reveals association with epigenetic modifications. *Genome Res*, **17**, 1186-1194.

Wang, H., Wang, L., Erdjument-Bromage, H., Vidal, M., Tempst, P., Jones, R.S. and Zhang, Y. (2004) Role of histone H2A ubiquitination in Polycomb silencing. *Nature*, **431**, 873-878.

Wang, W., Cote, J., Xue, Y., Zhou, S., Khavari, P.A., Biggar, S.R., Muchardt, C., Kalpana, G.V., Goff, S.P., Yaniv, M., Workman, J.L. and Crabtree, G.R. (1996) Purification and biochemical heterogeneity of the mammalian SWI-SNF complex. *Embo J*, **15**, 5370-5382.

Ward, B.M. (2005) Visualization and characterization of the intracellular movement of vaccinia virus intracellular mature virions. *J Virol*, **79**, 4755-4763.

Ward, B.M. and Moss, B. (2001a) Vaccinia virus intracellular movement is associated with microtubules and independent of actin tails. *J Virol*, **75**, 11651-11663.

Ward, B.M. and Moss, B. (2001b) Visualization of intracellular movement of vaccinia virus virions containing a green fluorescent protein-B5R membrane protein chimera. *J Virol*, **75**, 4802-4813.

Wei, P., Garber, M.E., Fang, S.M., Fischer, W.H. and Jones, K.A. (1998) A novel CDK9-associated C-type cyclin interacts directly with HIV-1 Tat and mediates its high-affinity, loop-specific binding to TAR RNA. *Cell*, **92**, 451-462.

Wei, S.Q., Mizuuchi, K. and Craigie, R. (1997) A large nucleoprotein assembly at the ends of the viral DNA mediates retroviral DNA integration. *Embo J*, **16**, 7511-7520.

Weidemann, T., Wachsmuth, M., Knoch, T.A., Muller, G., Waldeck, W. and Langowski, J. (2003) Counting nucleosomes in living cells with a combination of fluorescence correlation spectroscopy and confocal imaging. *J Mol Biol*, **334**, 229-240.

Weinberg, J.B., Matthews, T.J., Cullen, B.R. and Malim, M.H. (1991) Productive human immunodeficiency virus type 1 (HIV-1) infection of nonproliferating human monocytes. *J Exp Med*, **174**, 1477-1482.

Weintraub, H. and Groudine, M. (1976) Chromosomal subunits in active genes have an altered conformation. *Science*, **193**, 848-856.

Wensing, A.M. and Boucher, C.A. (2003) Worldwide transmission of drug-resistant HIV. *AIDS Rev*, **5**, 140-155.

West, C.M. (2003) Evolutionary and functional implications of the complex glycosylation of Skp1, a cytoplasmic/nuclear glycoprotein associated with polyubiquitination. *Cell Mol Life Sci*, **60**, 229-240.

Wilk, T., Gross, I., Gowen, B.E., Rutten, T., de Haas, F., Welker, R., Krausslich, H.G., Boulanger, P. and Fuller, S.D. (2001) Organization of immature human immunodeficiency virus type 1. *J Virol*, **75**, 759-771.

Williams, D.A. and Baum, C. (2003) Medicine. Gene therapy--new challenges ahead. *Science*, **302**, 400-401.

Wilson, T. and Carlini, A.R. (1988) Three dimansional imaging in confocal imaging systems with finite-sized detectors. *J. Microsc.*, **141**, 51-66.

Wong, J.K., Hezareh, M., Gunthard, H.F., Havlir, D.V., Ignacio, C.C., Spina, C.A. and Richman, D.D. (1997) Recovery of replication-competent HIV despite prolonged suppression of plasma viremia. *Science*, **278**, 1291-1295.

Wood, A., Krogan, N.J., Dover, J., Schneider, J., Heidt, J., Boateng, M.A., Dean, K., Golshani, A., Zhang, Y., Greenblatt, J.F., Johnston, M. and Shilatifard, A. (2003) Bre1, an E3 ubiquitin ligase required for recruitment and substrate selection of Rad6 at a promoter. *Mol Cell*, **11**, 267-274.

Wu, R., Terry, A.V., Singh, P.B. and Gilbert, D.M. (2005) Differential subnuclear localization and replication timing of histone H3 lysine 9 methylation states. *Mol Biol Cell*, **16**, 2872-2881.

Wu, X., Li, Y., Crise, B. and Burgess, S.M. (2003) Transcription start regions in the human genome are favored targets for MLV integration. *Science*, **300**, 1749-1751.

Wu, X., Liu, H., Xiao, H., Conway, J.A., Hehl, E., Kalpana, G.V., Prasad, V. and Kappes, J.C. (1999) Human immunodeficiency virus type 1 integrase protein promotes reverse transcription through specific interactions with the nucleoprotein reverse transcription complex. *J Virol*, **73**, 2126-2135.

Wu, X., Liu, H., Xiao, H., Conway, J.A., Hunter, E. and Kappes, J.C. (1997) Functional RT and IN incorporated into HIV-1 particles independently of the Gag/Pol precursor protein. *Embo J*, **16**, 5113-5122.

Wu, X., Liu, H., Xiao, H., Kim, J., Seshaiah, P., Natsoulis, G., Boeke, J.D., Hahn, B.H. and Kappes, J.C. (1995) Targeting foreign proteins to human immunodeficiency virus particles via fusion with Vpr and Vpx. *J Virol*, **69**, 3389-3398.

Yamashita, M. and Emerman, M. (2004) Capsid is a dominant determinant of retrovirus infectivity in nondividing cells. *J Virol*, **78**, 5670-5678.

Yamashita, M., Perez, O., Hope, T.J. and Emerman, M. (2007) Evidence for direct involvement of the capsid protein in HIV infection of nondividing cells. *PLoS Pathog*, **3**, 1502-1510.

Yang, F., Moss, L.G. and Phillips, G.N., Jr. (1996) The molecular structure of green fluorescent protein. *Nat Biotechnol*, **14**, 1246-1251.

Yang, X.J. and Seto, E. (2003) Collaborative spirit of histone deacetylases in regulating chromatin structure and gene expression. *Curr Opin Genet Dev*, **13**, 143-153.

Yap, M.W., Nisole, S., Lynch, C. and Stoye, J.P. (2004) Trim5alpha protein restricts both HIV-1 and murine leukemia virus. *Proc Natl Acad Sci U S A*, **101**, 10786-10791.

Yu, H.J., Reuter, M.A. and McDonald, D. (2008) HIV traffics through a specialized, surface-accessible intracellular compartment during trans-infection of T cells by mature dendritic cells. *PLoS Pathog*, **4**, e1000134.

Yu, Q., Konig, R., Pillai, S., Chiles, K., Kearney, M., Palmer, S., Richman, D., Coffin, J.M. and Landau, N.R. (2004) Single-strand specificity of APOBEC3G accounts for minus-strand deamination of the HIV genome. *Nat Struct Mol Biol*, **11**, 435-442.

Yun, C.Y., Velazquez-Dones, A.L., Lyman, S.K. and Fu, X.D. (2003) Phosphorylation-dependent and -independent nuclear import of RS domain-containing splicing factors and regulators. *J Biol Chem*, **278**, 18050-18055.

Yung, E., Sorin, M., Pal, A., Craig, E., Morozov, A., Delattre, O., Kappes, J., Ott, D. and Kalpana, G.V. (2001) Inhibition of HIV-1 virion production by a transdominant mutant of integrase interactor 1. *Nat Med*, **7**, 920-926.

Yuste, R. (2005) Fluorescence microscopy today. *Nat Methods*, **2**, 902-904.

Zack, J.A., Arrigo, S.J., Weitsman, S.R., Go, A.S., Haislip, A. and Chen, I.S. (1990) HIV-1 entry into quiescent primary lymphocytes: molecular analysis reveals a labile, latent viral structure. *Cell*, **61**, 213-222.

Zennou, V., Petit, C., Guetard, D., Nerhbass, U., Montagnier, L. and Charneau, P. (2000) HIV-1 genome nuclear import is mediated by a central DNA flap. *Cell*, **101**, 173-185.

Zhang, H., Dornadula, G. and Pomerantz, R.J. (1996) Endogenous reverse transcription of human immunodeficiency virus type 1 in physiological microenviroments: an important stage for viral infection of nondividing cells. *J Virol*, **70**, 2809-2824.

Zhang, H., Yang, B., Pomerantz, R.J., Zhang, C., Arunachalam, S.C. and Gao, L. (2003) The cytidine deaminase CEM15 induces hypermutation in newly synthesized HIV-1 DNA. *Nature*, **424**, 94-98.

Zheng, R., Ghirlando, R., Lee, M.S., Mizuuchi, K., Krause, M. and Craigie, R. (2000) Barrier-to-autointegration factor (BAF) bridges DNA in a discrete, higher-order nucleoprotein complex. *Proc Natl Acad Sci U S A*, **97**, 8997-9002.

Zhou, Q. and Sharp, P.A. (1995) Novel mechanism and factor for regulation by HIV-1 Tat. *Embo J*, **14**, 321-328.

Zhu, B., Zheng, Y., Pham, A.D., Mandal, S.S., Erdjument-Bromage, H., Tempst, P. and Reinberg, D. (2005) Monoubiquitination of human histone H2B: the factors involved and their roles in HOX gene regulation. *Mol Cell*, **20**, 601-611.

Zuckerman, A.J., E., B.J., R., P.J., D., G.P. and D., S.B. (2004) *Principles and practice of clinical virology*. Wiley, Chichester ; Hoboken, NJ.